Departamento de Física

Development of new biomaterials based on liquid crystalline phases of cellulose derivatives

Cláudio Miguel Dionísio dos Santos

Dissertação apresentada na Faculdade de Ciências e Tecnologia da Universidade Nova de Lisboa para obtenção do Grau de Mestre em Engenharia Biomédica

Orientadores:

Prof. Dr. João Paulo Borges, DCM – FCT/UNL
Dr. Pedro Granja, INEB – Instituto de Engenharia Biomédica, Universidade do Porto

Lisboa
2010

This thesis was supervised by:

→ Prof. Dr. João Paulo Borges (supervisor)

DCM – Departamento de Ciências dos Materiais, Faculdade de Ciências e Tecnologia – Universidade Nova de Lisboa.

→ Dr. Pedro Granja (co-supervisor)

NEWTherapies Group, Biomaterials Division, INEB – Instituto de Engenharia Biomédica, Universidade do Porto.

The research described in this thesis was conducted at:

→ DCM – Departamento de Ciências dos Materiais, Faculdade de Ciências e Tecnologia – Universidade Nova de Lisboa.

→ NEWTherapies Group, Biomaterials Division, INEB – Instituto de Engenharia Biomédica, Universidade do Porto.

Acknowledgements

This is perhaps the hardest section I have to write, but I will, nonetheless, try. I would like to thank to all the ones who have contributed to the accomplishment of this thesis.

First of all I would like to acknowledge to my supervisors Prof. Dr. João Paulo Borges and Dr. Pedro Granja for the help, orientation and transmitted knowledge they gave me. I want to express my gratitude for the opportunity and the privilege of working in a renowned institution, Instituto de Engenharia Biomédica (INEB, Universidade do Porto), that hosted me in an enthusiastic way. I am grateful to several persons who supported and encouraged my research work at Biomaterials Division of INEB and at Departamento de Ciências dos Materiais of Faculdade de Ciências e Tecnologia (DCM, FCT – Universidade Nova de Lisboa). I want to send thanks to all my remarkable friends and colleagues at FCT and INEB with whom I had the privilege of working with. They helped me along these months and were always there to listen and share their experience and knowledge.

At INEB, I would like to give a special thank to Cristina Barrias, who patiently answered all my questions, tracked down papers, guided me during my work and was always there. She was my advisor and taught me numerous things, enabling me to face the hard work with a smile. The scientific discussions and encouragement made by her made the difference to the progress of this work. I also want to thank to the people who worked with me at INEB and FCT for their collaboration and help in several situations at the lab. In particular, the collaboration and advice of Ricardo Vidal Silva and Manuela Brás were fundamental. I can't forget to mention Ana Filipa Lourenço that is the best bench colleague that someone could have. Thank you for all the hours spent with me in that lab. At CEMUP (Centro de Materiais da Universidade do Porto) I would like to thank to all who helped me in Scanning Electron Microscopy and X-ray Photoelectron Spectroscopy. I am sincerely grateful to all. This work would not have been possible without your help and dedication.

I wish to thank my great friends for their support during this last 5 years, in particular to my girlfriend Ana who helped me to get through the difficult situations. As much as I could write here would never be enough to show how grateful I am to her. I am indebted to my student colleagues for providing a stimulating environment to learn and grow.

My final words go to my family. I wish to thank my entire extended family for providing a lovely environment for me, particularly my parents and my brother. I dedicate this thesis to them, for standing by me in difficult hours, trying to enhance my spoiled weekends, dealing with my bad temper, but above all for their effort and motivation during all my entire life.

Thank you!

Abstract

In the present work, new biomaterials based on liquid crystalline phases of cellulose derivatives were prepared and characterized. The possibility to monitor growth and differentiation of stem cells could be an interesting use for the HPC films studied in this thesis. Additionally, the application of HPC films as an anti-adhesive substratum in biomedical applications could also be interesting.

For that purpose, two solutions of hydroxypropylcellulose (HPC) in dimethylacetamide (DMAc) were prepared. An isotropic 30% solution (HPCi) and an anisotropic 60% chiral nematic solution (HPCa) were obtained and submitted to a chemical cross-linking treatment by adding 10% (w/w) of the crosslinking agent (1,6 diisocyanatohexane, 98%). HPC films were then prepared with the help of a calibrated ruler moving at a controlled rate (v = 6 $mm \cdot s^{-1}$). The non-biological characterization of these films included physico-chemical and structural characterization. HPCi and HPCa film characterization was performed by optical microscopy, determination of the gel fraction, mechanical properties, contact angle measurements, infrared spectroscopy (FTIR), x-ray photoelectron spectroscopy (XPS), scanning electron microscopy (SEM) and atomic force microscopy (AFM). The biological experimental characterization included cytotoxicity evaluation, cell adhesion, morphology, proliferation and viability assays. The band texture of HPCa films, formed during the shear, was easily observed using polarized light transmission microscopy. The mechanical anisotropy of HPCa films was also easily identified. FTIR and XPS showed that the surface chemistry of both films is similar, as well as the contact angles measured on both surfaces. SEM results showed a characteristic topography on the HPCa surface, which was verified and quantified by AFM. The interaction of these biomaterials with human mesenchymal stem cells (hMSC) was also investigated. HPC films were also tested for *in vitro* cytotoxicity and were found to be non-cytotoxic. The results showed that the percentage of adherent cells on HPC films was almost zero and that cells were not able to proliferate on these substrates. MSCs became round and aggregated on both HPC films, but remained aggregated and viable. This study has shown that it is possible to prepare sterile and biocompatible HPC films with potential use as coatings for anti-adhesive purposes in medical devices.

Resumo

Neste trabalho procedeu-se à preparação e caracterização de novos biomateriais baseados em fases líquido-cristalinas de derivados da celulose. A possibilidade de monitorizar o crescimento e diferenciação de células estaminais poderia ser uma aplicação interessante para os filmes de HPC estudados nesta tese. O seu uso como substrato anti-adesivo em aplicações biomédicas poderia ser igualmente interessante.

Neste contexto, foram preparadas duas soluções de hydroxypropylcellulose (HPC) em dimetilacetamida (DMAc). Uma solução isotrópica (30 wt% – HPCi) e uma anisotrópica (60 wt% – HPCa) foram obtidas e submetidas a um processo de reticulação adicionando 10% (w/w) do agente reticulante 1,6 diisocyanatohexane 98%. Os filmes de HPC foram posteriormente preparados com a ajuda de uma régua calibrada que se movia a uma velocidade controlada (v = 6 $mm \cdot s^{-1}$). A caracterização não-biológica destes filmes incluiu o estudo das suas propriedades estruturais e físico-químicas. A caracterização dos filmes de HPCi e HPCA incluiu microscopia óptica, determinação da fracção gel, análise das propriedades mecânicas, medida dos ângulos de contacto, espectroscopia de infravermelhos (FTIR), espectroscopia de electrões (XPS), microscopia electrónica de varrimento (SEM) e microscopia de força atómica (AFM). A caracterização biológica incluiu a avaliação da citotoxicidade e ensaios de adesão celular, proliferação, morfologia e viabilidade. A textura em bandas, formada durante o espalhamento, presente no filme de HPCa, foi facilmente observada por microscopia óptica. A anisotropia mecânica do filme de HPCa foi também identificada. As análises de FTIR e XPS mostraram que a química da superfície de ambos os filmes é semelhante, assim como os ângulos de contacto medidos em ambas as superfícies. Os resultados obtidos por SEM identificaram a topografia característica da superfície dos filmes de HPCa, que foi também analisada e quantificada por AFM. A interacção destes filmes com células estaminais mesenquimais humanas (hMSC) foi também alvo de investigação neste trabalho. Os filmes de HPC foram também submetidos a testes de citotoxicidade *in vitro* demonstrando que não são citotóxicos. Os resultados mostraram que a percentagem de células aderentes nos filmes de HPC foi quase nula e que as células não são capazes de proliferar nestes substratos. Quando em contacto com os filmes de HPC, as células estudadas apresentavam um formato redondo, permanecendo no entanto agregadas e viáveis. Este estudo mostrou que é possível preparar filmes de HPC estéreis e biocompatíveis potencialmente aplicáveis em revestimentos de dispositivos médicos onde seja desejado um efeito anti-adesivo.

Aim and structure of the thesis

The aim of this thesis was to develop and characterize cross-linked hydroxypropylcellulose (HPC) films with different properties that can be significant to a variety of potential applications in biology and medicine. The main goal was to explore possible biomedical applications for these biomaterials. It is well known that surface properties influence the adsorption of serum proteins and, hence, cell adhesion. Surface properties such as wettability, charge, topography and chemical composition, among others, play an important role in cell behaviour. The characterization and interaction of these biomaterials with mesenchymal stem cells (MSC) were investigated. The properties of HPCi and HPCa films were compared, as well as the behaviour of MSCs when in contact with them.

It was recently demonstrated that liquid crystals can monitor the growth of embryonic stem cells [1] proving that research in this field could have a bright future. The diversity of biomaterials that reside in living systems and exhibit liquid crystal properties was also demonstrated [2]. It is also known that mesenchymal stem cells are a promising candidate in regenerative medicine and present a huge potential clinical use. Cellulose is the most abundant biopolymer in nature and one of the most commonly used in biomedical applications. Many of its derivatives, like HPC, exhibit chiral nematic liquid crystalline phases. The possibility to monitor growth and differentiation of stem cells could be an interesting use for this biomaterial.

Chapter I gives a general overview of liquid crystals principles and their applications in medicine, describes the current status of regenerative medicine and explains the mechanisms behind cell-material interactions as well the importance of non-fouling biomaterials in biomedical applications.

Currently, the evaluation of biomaterials includes an initial sequence of both non-biological and biological (cell culture) tests. The experimental work is presented along 2 chapters (chapters **II** and **III**).

Chapter II comprises the preparation of HPC films and describes the principles of the experimental methods used during this investigation. The non-biological experimental characterization includes physico-chemical and structural characterization of the materials prepared (optical, electronic and force microscopy, determination of the gel fraction, mechanical properties,

and hydrophilicity). The biological experimental characterization includes cytotoxicity evaluation, cell adhesion, morphology, proliferation and viability assays.

In **Chapter III**, the procedures used in each technique are described and the results are interpreted and discussed.

In the last part of this thesis, a short general discussion (concluding remarks) is presented and possible directions for future research are also given in **Chapter IV** and **Chapter V**, respectively.

List of Symbols

AFM – Atomic Force Microscopy

APC – Acetoxypropylcellulose

ATR – Attenuated total reflectance

BMSC – Bone Marrow Stromal Cells

BPC – n-butyric

CAB – Cellulose Acetate Butyrate

CEL – hydroxypropylmethylcellulose (HPMC)-CMC-coated substratum

CMC – Carboxymethylcellulose

CU – Cuprophan

DMAc – Dimethylacetamide

DMEM – Dulbecco's Modified Eagle Medium

DRS – Diffuse reflectance spectroscopy

E – Young's modulus

EDS – Energy Dispersive Spectrometer

EGC – Embryonic germ cells

EKA – Electro Kinetic Analysis

ESC – Embryonic stem cells

ESCA – Electron Spectroscopy for Chemical Analysis

ESEM – Environmental Scanning Electron Microscopy

EVA – Ethylene Vinyl Acetate

FACS – Fluorescence-activated cell sorting

FBS – Fetal Bovine Serum

FTIR – Fourier Transform Infrared Spectroscopy

HepPc – Heptanionic acid

hESC – human Embryonic Stem Cells

HexPc – Hexanionic

HPC – Hydroxypropylcellulose

HPCa – Anisotropic 60 wt% chiral nematic cross-linked solution

HPCi – Isotropic 30 wt% cross-linked solution

HPMC – Hydroxypropylmethylcellulose

iBPC – Isobutyric

iVPC – Isovaleric

LC – Liquid Crystal

LCD – Liquid crystal display

MC – Methylcellulose

MSC – Mesenchymal stem cells

NFS – Non-Fouling Surfaces

OCA – Optical Contact Angle

PAAm – Polyacrylamide

PBS – Phosphate Buffered Saline

PDMAA – Poly(N,N-dimethyl methacrylamide)

PEG – Poly(Ethylene Glycol)

pHEMA – Poly(2-hydroxyethyl methacrylate)

PPC – Propionic

SEM – Scanning Electron Microscopy

TAC – Cellulose triacetate

vdW – van der Waals

VPC – Valeric

XPS – X-ray Photoelectron Spectroscopy

Contents

Index of Figures

Chapter I

Chapter II

Chapter III

Index of Tables

Chapter I

Chapter II

Chapter III

Chapter I – INTRODUCTION

1. Liquid crystals

1.1. A brief review

The first observation of liquid crystalline behaviour was made by an Austrian botanist named Friedrich Reinitzer who, about a hundred years ago, was investigating a material known as cholesteryl benzoate that had two distinct melting points [3]. Since this discovery, thousands of compounds have been identified to exhibit that new phase of matter — the mesogenic or liquid crystalline phase. The term liquid crystal (LC) describes a state of matter that is intermediate between an isotropic liquid and a crystalline solid state. LCs can be further divided into two main families: thermotropic and lyotropic. These types of LCs are distinguished by the mechanisms that drive their self-organization. Thermotropic LCs exhibit mesophases as function of temperature. On the other hand, lyotropic LCs are obtained when an appropriate concentration of a material is dissolved in some solvent. The most important variable is the amount of solvent (or concentration), under certain conditions of temperature and pressure.

Almost all the thermotropic LCs are composed of rod-like molecules and classified into three subclasses depending on positional and directional arrangements of the molecules: nematic, cholesteric and smectic [4]. Physical parameters such as the long- and short-range orientational order and the long- and short-range translational order characterize these mesophases. The nematic LC is characterized by a high degree of long-range orientational order of the molecules, but no long-range translational order. A dimensionless unit vector *n*, called the *director*, represents the direction of preferred orientation of molecules. The cholesteric mesophase, also known as chiral nematic, are similar to nematic liquid crystals in all physical properties, but in this particular case the molecules tend to adopt a helical configuration. The distance of two layers turned at an angle of 360° corresponds to the pitch P. The spiral arrangement of the molecules in the cholesterics is responsible for their unique optical properties [4]. Cholesterics of low pitch (less than about 5000 Å) exhibit what is known as *blue* phases. These phases exist over a small temperature range $(\sim 1\ °C)$ between the liquid crystal phase and the isotropic liquid. The molecules of the smectic LCs maintain positional order. The most studied subphases of smectics are smectic A and smectic C. In smectic A the molecules are upright in each layer. In smectic C the molecules are inclined with respect to the

normal layer [4-6]. The collective arrangement of the rod-like molecules in the nematic, cholesteric and smectic A phases are schematically represented in the Fig. 1.1.

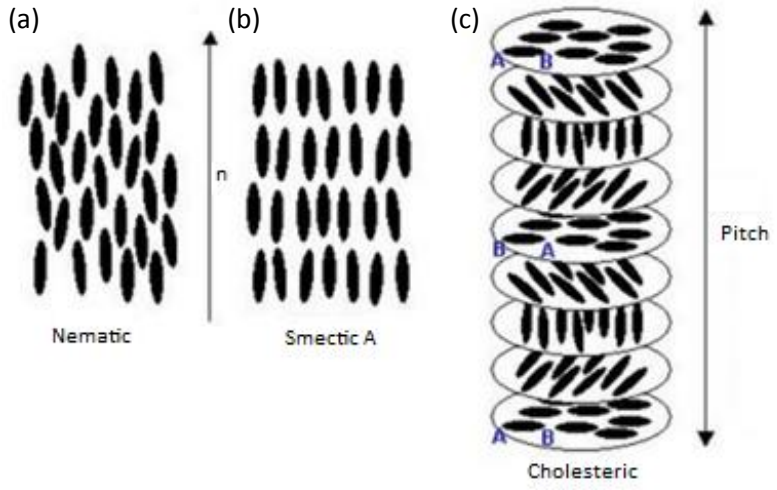

Figure 1.1 – Schematic representation of the collective arrangement of the rod-like molecules in the (a) nematic, (b) smectic A and (c) cholesteric phases. Adapted from [7].

Liquid crystals are found to be birefringent due to their anisotropic nature. It means that they demonstrate double refraction, having two indices of refraction. This effect occurs because the structure of the material is anisotropic and the light polarized parallel to the director has a different index of refraction than the light polarized perpendicularly to the director.

1.2. Liquid crystals in biological systems

Within the biological systems several liquid crystal structures can be found. This idea was firstly proposed by Lehmann [8]. Afterwards, several liquid crystalline materials, which are found in biological systems, have been studied by several researchers. Most liquid crystals are derived from natural sources including cellular membranes [2], hemoglobin [9], chromosomes [9], bile [10], carapace of some insects [9], concentrated solutions of biomolecules, such as proteins, [9, 11-13], and solutions of cellulose and its derivatives [9]. Many liquid crystal biomaterials are found in living systems, which means that several structures have properties that are dependent on the liquid crystallinity for their function. Even materials such as DNA can exhibit mesomorphic behaviour [2].

The structures of cell walls that surround all cells can be described by the fluid mosaic model, where integral proteins float in a two-dimensional lipid sea. Cell membranes contain a variety of

biological molecules, especially lipids and proteins. Each of the membrane lipid classes (phospholipid, glycolipid and cholesterol) and related derivatives has been shown to possess mesomorphic properties and some of them have been widely studied both in their lyotropic, as well as their thermotropic states [2]. For example, aliphatic derivatives of cholesterol were among the first thermotropic liquid crystals to be investigated. Cerebrosides, a class of glycolipids derived from the sphingosine were also found to be potentially thermotropic or lyotropic liquid crystals. J. W. Goodby [2] showed that cells could use liquid crystal technology, typical of materials for display device applications, for modifying their behaviour and/or properties (e.g. modify melting behaviour and to fine tune viscoelastic properties). Goodby [2] also discussed the liquid crystal properties of other bio-materials including aliphatic derivatives of vitamin C and solanin witch exhibit thermotropic smectic A phases in certain conditions. It can be easily concluded that there is a great variety of bio-materials that exhibit mesomorphic behaviour. Some of them are certainly involved in bio-processes and applications (e.g., inter-cellular recognition and surfactants) or could have attractive properties (e.g., pharmaceuticals) [2].

Brown [14] also presented several analogies between the properties of liquid crystals and those of supramolecular arrangements in biology. Brown studies stimulated more probing investigation of liquid crystals in biology over the last 30 years. The importance and the role of liquid crystals properties in and to living systems were demonstrated [14]. Their role in sensory systems, in cellular shape and in the transmission of information were some of the topics discussed.

It is believed that the field of liquid crystals could have a bright future and will play an important role in the understanding of biological process.

1.3. Liquid crystals in medical applications

Several liquid crystal applications are already part of our daily lives and are present in modern technological products such as mobile phones, displays, clocks, thermometers and other materials that change the colour with temperature. The advantage of using liquid crystals in these applications relies in their low power consumption, image resolution, durability and small size. These materials have unique properties and are in a prominent place in materials science. Engineers and scientists have been using liquid crystals in a variety of applications because external perturbations of these materials, like electric and magnetic fields, can induce considerable changes in the macroscopic properties of the liquid crystalline system. It is possible to treat surfaces forcing the

director to point in a specific direction by introducing an outside agent to the system [15]. The most frequent application of liquid crystal technology is the liquid crystal displays (LCD). LCDs are used in several applications like calculators, laptop computer screens, watches and airplanes [9, 16-19].

Temperature changes can influence the colour of a liquid crystal, which makes them useful in medical applications, for instance, to measure body temperature (see Fig. 1.2). Chiral nematic (cholesteric) liquid crystals reflect light with a wavelength equal to the pitch. Since the pitch (distance that the liquid crystals twist over) is temperature dependent, the colour reflected is also temperature dependent, which allows the use of liquid crystals as temperature sensors, just by looking at the colour that indicates different temperatures. When the pitch equals half of the wavelength of red light the liquid crystal will reflect red light. It is possible to build a device for practically any temperature range by mixing diverse compounds. The resolution of liquid crystal sensors is in the 0.1°C range. LC thermometers are economical, simple to install, practically unbreakable and there is no risk of toxic elements being released [19, 20].

Figure 1.2 – Liquid crystal thermometer. Adapted from [21].

Some important and useful liquid crystal applications have been developed in the medicine field. Liquid crystals can be used as a non-invasive, safe and effective tools for healthcare evaluation of complex pain states associated with soft tissue injuries, arthritis and back-pain diseases. It makes the identification of damages easy and could have applications in several areas like respiratory and nervous dysfunctions, locomotor disorders, surgical assistance and skin problems. In the case of nerve injuries, the body temperature will increase and the area of the distribution of the injured nerve could be easily observed. Some physical problems like tumours also have a different temperature than the surrounding tissue. The part of the body under examination is kept in contact with special liquid crystal devices that are allowed to equilibrate with the body temperature for several minutes and the “map” of the skin temperature changes can be seen. This technique is

precise, has high resolution and does not involve ionizing radiation. The thermographic pictures of some affected areas is shown in Fig. 1.3 [18, 22].

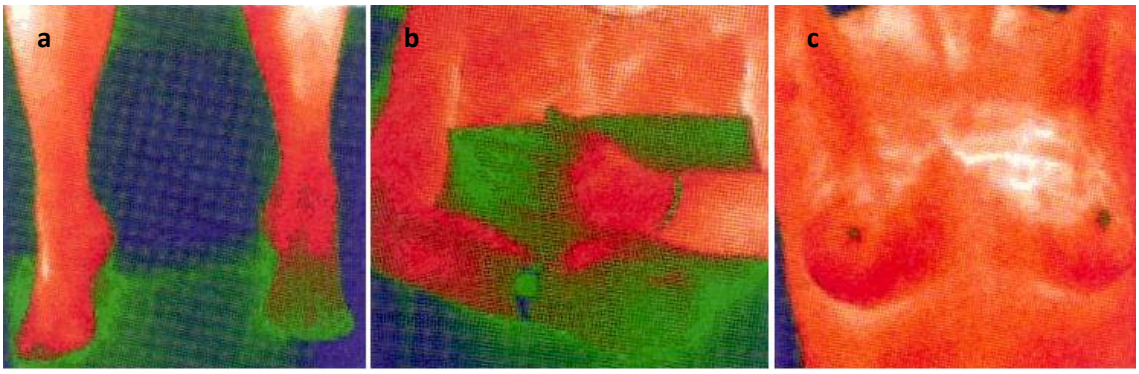

Figure 1.3 – Thermographic pictures of (a) peripheral neuropathy, (b) rheumatoid arthritis and (c) breast cancer. Adapted from [21].

Liquid crystals may also be used in ergonomic applications, for example for detection of occupational joint stress (response inflammation) as a result of physical effort. Other medical application is the measurement of the transient pressure transmitted by a walking foot to the ground. Several techniques have been developed to improve liquid crystal temperature measurements [23, 24].

In 2007, Atyabi and co-workers [25] have studied the utilization of liquid crystal embedded cellulose membranes as a mechanism of thermoresponsive drug permeation. The main objective was to modify the control of permeability and pore variability due to its thermotropic characteristics. As a result, under different temperatures, the permeability can be altered, allowing, for example, the release of drugs only in hyperthermia sites, as desired in the application of chemotherapeutics [25]. Liquid crystals can significantly change the release rate of drugs, increasing solubility, absorption and bioavailability of control. They may also alter the pharmacokinetics, decreasing toxicity and improving clinical effectiveness [26].

Recently, some studies in which synthetic LCs were put in contact with cells have been reported [1, 27, 28]. The main goal of these studies was to investigate the ordering of LCs in contact with cells as a potential tool to infer about the interactions of cells with their environment. Recently, the orientation of the nematic liquid crystal 4'-pentyl-4-cyanobiphenyl (5CB) on fixed (dead) cells attached to surfaces was investigated by Fang and co-workers [28]. A subsequent study showed that this material cause cell death when in contact with live cells [27]. Luk and co-workers [27] found,

during this study, numerous liquid crystals that present no toxicity to live mammalian cells [27]. More recently, Lockwood and co-workers [1] confirmed that it was possible to culture human embryonic stem cells (hESC) on the surface of a film of a nematic LC TL205 (a mixture of cyclohexane-fluorinated biphenyls and fluorinated terphenyls) that were decorated with thin films of the extracellular matrix, Matrigel. This study showed that hESC could survive for approximately two weeks on liquid-crystal substrates without visible signs of toxicity. It was also demonstrated that the ordering of the LC was influenced by the extracellular matrix of the cells and that the reorganization of the extracellular matrix by the stem cells led to ordering transitions in the LCs [1].

It is also known that liquid crystals exhibit electro-optic effects [29], which make them an attractive tool for a variety of applications including fast, compact, and tunable spectral filters, phase modulators, polarization controllers and optical shutters [30]. LCs have been used in a wide range of applications including computer monitors, television, gaming devices, aircraft cockpit displays, instrument panels, video players, calculators and telephones, among others. However, their application in the field of optical imaging just started to emerge. LC devices can also have a great potential in biomedical optical imaging systems and other biomedical applications. According to Abdulhalim *et al.* [30], using a collection of tunable phase retarders one can perform:

- Stokes parameters imaging for skin and eye polarimetric imaging;
- Tunable filtering to be used for hyperspectral imaging, fluorescence microscopy, and frequency domain optical coherence tomography;
- Adaptive optical imaging and eye aberrations correction;
- Phase shift interferometric imaging;
- Variable frequency structured illumination microscopy.

New properties and applications of LCs in medicine are being investigated. These materials have an enormous potential and more industrial and scientific applications involving LCs will certainly be developed in the near future.

1.4. Liquid crystals based on cellulose derivatives

Currently, a large number of cellulose derivatives are known to form lyotropic mesophases [31]. One of the most studied cellulose derivatives for that purpose is hydroxypropylcellulose (HPC), which is an ether of cellulose. In the past decades, Gray, White, Sixou, Navard and co-workers [32-34] performed several investigations on HPC mesophases.

1.4.1. Hydroxypropylcellulose as a biomaterial

HPC is an organic polymer of high solubility in water and alcohols, due to the hydrophilic OH and COC groups as well as hydrophobic organic groups. The chemical structure of HPC can be seen in Fig. 1.4.

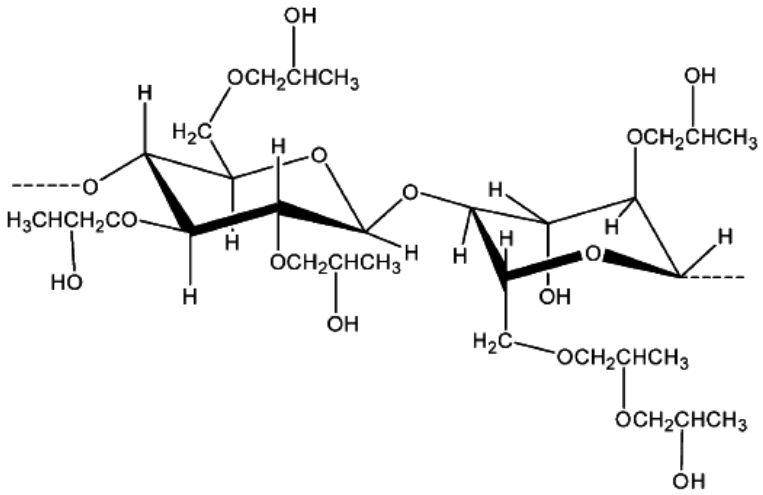

Figure 1.4 – Ideal structure of HPC. DE = 2.5 (Degree of Eterification); ME = 3 (Molar Eterification).

HPC is one of the most studied ether cellulose derivatives. However, it has been poorly studied in the biomedical field.

The first lyotropic cholesteric phase of a cellulose derivative was obtained from this ether, for high concentrations of polymer in water [35]. It has been shown that HPC can originate lyotropic phases when used in some concentrations and can form solid films that can act as barriers to air and moisture. It was also used in coatings, even at high humidity and as a packaging material [36, 37]. Its electro-optical properties have also been the subject of several theoretical and experimental studies [29, 38]. The use of HPC solid films as the matrix of a polymer/liquid crystal composite system, with applications in the production of electro-optical displays, was also investigated [38].

The preparation of various esters of HPC can be found in the literature [35, 39]. The first ester derivative of HPC presented in the literature, as having a liquid crystalline thermotropic phase, was the acetoxypropylcellulose (APC). Subsequently, other esters of HPC, which can generate lyotropic and thermotropic mesophases [40, 41], were prepared and characterized. Propionic (PPC), *n*-butyric (BPC), isobutyric (iBPC), valeric (VPC), isovaleric (iVPC), hexanionic (HexPc), and heptanionic acid (HepPc) esters of HPC are known to form thermotropic cholesteric liquid crystalline phases and

their optical properties were studied [39]. The mesophases of APC, PPC, iBPC, VPC, and iVPC exhibit reflection bands in the visible region, at wavelengths that depend on temperature [42], moisture content, size and number of substituents [42], and degree of polymerization [39]. The pitch of the cholesteric helical structure can be controlled through different processes, including increasing the side chain length and the temperature [29, 39]. Due to the ability of their molecules to spontaneous self-assemble in helicoidal arrangements, light can be reflected selectively, depending on some parameters, like the chain length and the temperature [43-46]. Many research works have been contributing to improve the use of cellulose derivatives for electro-optical applications [39, 47].

Aharoni [48] reported in 1979 that solutions of liquid crystalline polymers could form banded textures in thin-film samples. The film surface features of HPC/water (50–65% w/w) were recently investigated by atomic force microscopy studies [49]. It was demonstrated in this study that the surface of HPC films prepared from liquid crystalline aqueous solutions shows two periodic structures.

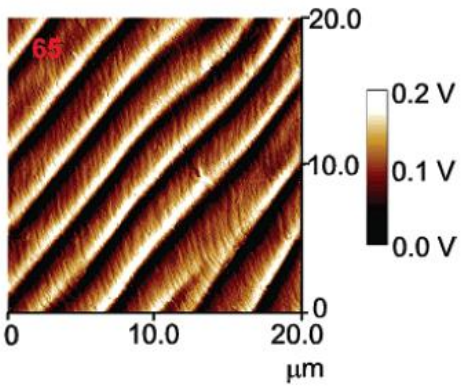

Figure 1.5 – Top view image of the amplitude scan of the free surface of sheared HPC films prepared at a shear rate of v = 5 mm/s from solutions with HPC/water ratio 65% w/w [49].

The results of this study have also shown that a tunable topographical system can be obtained from aqueous HPC liquid crystalline solutions. It was found that the two kinds of periodicities may be locked and adjusted in these systems as a function of the concentration of solutions and depending on the processing conditions, including the shear rate [49].

2. Non-fouling biomaterials

2.1. A brief review

Surfaces that resist to the adsorption of proteins and/or adhesion of cells are usually known as non-fouling surfaces (NFS). It is generally accepted that surfaces that strongly adsorb proteins will probably bind cells and that surfaces that resist protein adsorption will resist cell adhesion [50]. Apart from a few exceptions it was also established that hydrophilic surfaces seem to be more resistant to protein adsorption, while hydrophobic surfaces usually tend to adsorb a monolayer of tightly adsorbed protein [50]. NFSs have several medical and biotechnological applications, including blood compatible materials, biosensors, implantable devices, microchannel flow devices, urinary catheters, diagnostic assays, affinity separators, intravenous syringes and tubing as well as nonmedical applications, including biofouling-resistant heat exchangers and ship bottoms [50]. The use of blood contacting devices, including dialyzers, vascular grafts, oxygenators, blood containers and catheters, requires prevention of protein adsorption and NFSs may resist to fibrinogen adsorption and platelet adhesion [51]. The adsorption of serum proteins is the first event that takes place when a material surface is placed in contact with blood. This will lead to the formation of thrombus or blood clots which could cause serious clinical problems. NFSs have been the subject of many investigations, because they offer important experimental insights into one of the most important phenomenon in biomaterials science, i.e., protein adsorption. Ongoing investigation aims at developing protein-resistant surfaces in order to overcome these issues [51]. The production of anti-fouling films is an important element in the development of biomedical materials, for applications such as medical devices, implants and *in vitro* tests [52]. Such coatings favour the biological integration of these tools by limiting the interactions between the implants and physiological fluids [53, 54]. Until now, various water-soluble polymers have been used for surface grafting. They include nonionic, hydrophilic polymers such as polyacrylamide (PAAm), poly(N,N-dimethyl methacrylamide) (PDMAA), poly(ethylene glycol) (PEG), ethylene vinyl acetate (EVA) and Poly(2-hydroxyethyl methacrylate) (pHEMA) [51].

The protein and cell interactions with biomaterial surfaces have been the subject of several investigations in recent decades and some considerations have been established [50], namely:

- Hydrophobic surfaces have a strong propensity to adsorb proteins irreversibly [55, 56]. It occurs probably due to the unfolding of the protein on the surface, accompanied by the

release of many hydrophobically structured water molecules from the interface, leading to a large entropy gain for the system [57].

- At low ionic strengths cationic proteins bind to anionic surfaces and anionic proteins bind to cationic surfaces [57, 58]. The major thermodynamic driving force for these actions is a combination of ion–ion coulombic interactions, accompanied by an entropy gain due to the release of counter ions along with their waters of hydration [58].

- Proteins tend to adsorb in monolayers, which means that they do not adsorb non-specifically onto their own monolayers [59]. The retention of hydration water by the adsorbed protein molecules, preventing close interactions of the protein molecules in solution with the adsorbed protein molecules is the probable cause for it.

- Studies about surfaces coated with physically or chemically immobilized PEG concluded that its molecular weight should be above a minimum of ca. 2000 in order to provide good protein repulsion [60-62]. The mechanism of protein resistance by the PEG surfaces involves the resistance of the polymer coil to compression due to its ability to retain the volume of a random coil (called “entropic repulsion” or “elastic network” resistance) and involves the resistance of the PEG molecule to release both bound and free water from within the hydrated coil (called “osmotic repulsion”) [62, 63].

The thermodynamic principles governing the adsorption of proteins onto surfaces involve a number of enthalpic and entropic factors favouring adsorption or favouring resistance to protein adsorption (Table 1.1).

Table 1.1 – Thermodynamics of protein adsorption. Adapted from [50].

		Favouring adsorption
$\Delta \boldsymbol{H_{ads}}$	$(-)$	van der Waals (VdW) interactions (short-range)
	$(-)$	ion–ion interactions (long-range)
$\Delta \boldsymbol{S_{ads}}$	$(+)$	desorption of many H_2Os
	$(+)$	unfolding of protein

		Opposing adsorption
$\Delta \boldsymbol{H_{ads}}$	$(+)$	dehydration (interface between surface and protein)
	$(+)$	chain compression (PEO)
	$(+)$	unfolding of protein
$\Delta \boldsymbol{S_{ads}}$	$(-)$	protein hydrophobic exposure
	$(-)$	chain compression (PEO)
	$(-)$	adsorption of protein
	$(-)$	osmotic repulsion (PEO)

The main factors favouring adsorption are the entropic gain of released water and the enthalpy loss due to cation–anion attractive interactions between ionic protein groups and surface groups. The major factors favouring resistance to protein adsorption are the retention of bound water and, in the case of an immobilized hydrophilic polymer, entropic and osmotic repulsion of the polymer coils.

The mechanism behind the action of non-fouling surfaces has been the subject of several studies. Although it seems difficult to ascertain, the principal factor favouring resistance to protein adsorption seems to be the retention of bound water by the surface molecules. In the case of the immobilized hydrophilic polymer, entropic and osmotic repulsion by the polymer coils seems to be also related. Taking these observations into account, one can conclude that the most common approaches used in non-fouling surfaces research, consists in making them more hydrophilic with the aim of reducing protein adsorption and cell binding. The behaviour of non-fouling surfaces *in vivo* is still largely unknown and the stability and longevity of non-fouling biomaterials remains unclear. Biomaterials researchers keep trying to develop non-fouling surfaces. Their specific applications, biological environments and intended life services must be taken into account in their development.

Some of the different biomaterial compositions that have been applied as non-fouling surfaces are summarized in Table 1.2.

Table 1.2 – Non-fouling biomaterial surface compositions. Adapted from [50].

Synthetic Hydrophilic Surfaces	Natural Hydrophilic Surfaces
► **PEG polymers and surfactants** ► **Neutral polymers** - **Poly(2-hydroxyethyl methacrylate)** - **Polyacrylamide** - **Poly(N-vinyl-2-pyrrolidone)** - **Poly(N-isopropyl acrylamide) (below 31◦C)** ► **Anionic polymers** ► **Phosphoryl choline polymers** ► **Gas discharge-deposited coatings (especially from PEG-like monomers)** ► **Self-assembled n-alkyl molecules with oligo-PEG head groups** ► **Self-assembled n-alkyl molecules with other polar head groups**	► **Passivating proteins (e.g., albumin and casein)** ► **Polysaccharides (e.g., hyaluronic acid, cellulose and its derivatives)** ► **Liposaccharides** ► **Phospholipid bilayers** ► **Glycoproteins (e.g., mucin)**

2.2. Surface modulation of biological behaviour

The design and synthesis of biomaterials and devices has been the target of several biomedical investigations to ensure appropriate durability, mechanical properties and *in vivo* functionality depending on the intended medical application [50]. Biocompatibility is one of the most important criteria for selection of a particular biomaterial. It is important to note that biological response to biomaterials and devices is mainly controlled by their surface chemistry and structure. The study of the surface properties and interactions between the biomaterial and the living system interface are important to understand the behaviour of a biomaterial in the biological environment. The surface of a biomaterial can be modified by using mechanical, biological (e.g. proteins and cells) or physicochemical methods. Fig. 1.6 summarizes some surface modifications that can be performed on materials to enhance their properties.

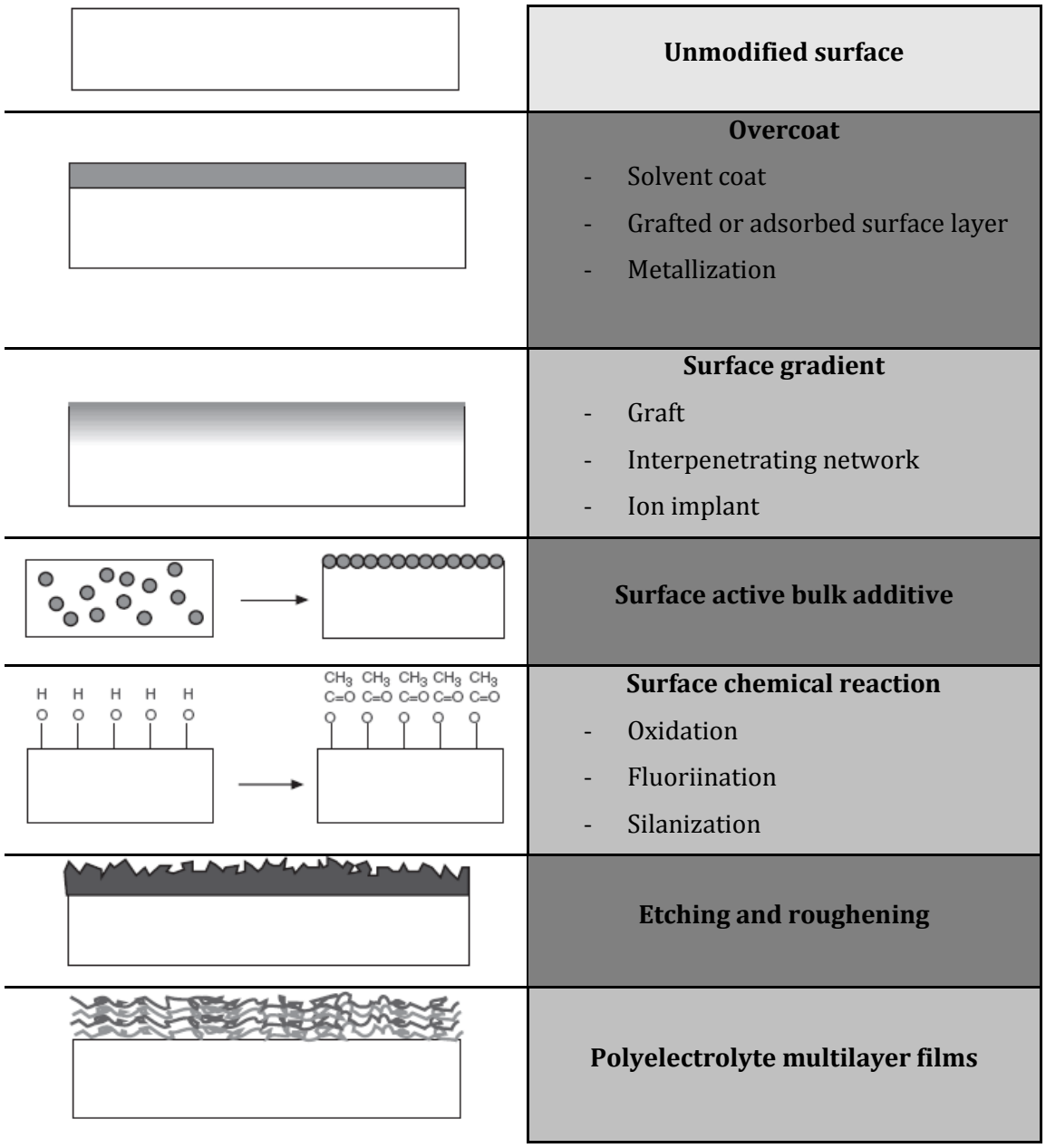

Figure 1.6 – Schematic representation of some methods used to modify surfaces of biomaterials. Adapted from [50].

Surface modifications can be divided into a) chemical or physical modification, etching and mechanically roughening by modify the atoms or molecules composition of the surface and b) coating, grafting and thin film deposition of the surface with a material having a different composition. Such surface modifications can be used to a wide range of applications including the control of protein adsorption, the modification of blood compatibility, the influence of cell adhesion and growth and can yet improve lubricity, wear and corrosion resistance, alter transport properties and modify the electrical characteristics.

2.3. Protein adsorption and cell adhesion on biomaterial surfaces

The body is able to recognize and respond to implanted biomaterials. Clotting of blood and foreign body reaction are typical biological responses. This response starts with the adsorption of adhesion proteins to the surface of the biomaterials. Afterwards, the interaction of cells with foreign surfaces is mediated by integrin receptors with the adsorbed adhesion proteins. Fig. 1.7 is a scheme which demonstrates how this process works. Proteins are represented by circles, squares and triangles, while the cell is represented by the circular space with a bilayer membrane in which the adhesion receptor protein molecules are partly embedded. The cell will only adhere to the surface-bound form of one protein (represented by a solid circle in Fig. 1.7) that is recognized by the receptor proteins.

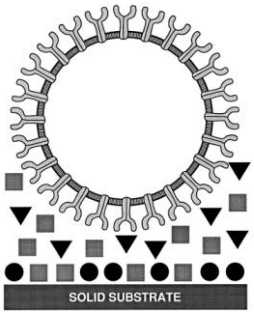

Figure 1.7 – Interaction of cells with foreign surfaces. Adapted from [50].

It is established that adsorbed adhesion proteins influence cellular interactions. An important factor which influences the adhesiveness of cells is the preadsorption of adhesion proteins onto a substrate. It occurs because cell receptors on cell membranes bind specifically to these proteins. It has been proven that albumin preadsorption prevents adhesion of fibroblasts, while fibronectin preadsorption increases it [50]. Several experiments were performed with a variety of cells and adhesion proteins to measure the percentage of adherent cells on different surfaces [50].

Cell attachment to surfaces may be influenced by several factors, including cellular properties, physical and chemical properties of the underlying biomaterial, interfacial chemical conditions and protein adsorption. Depletion studies are an interesting way to inspect the role of an adhesion protein on cell adhesion. By studying the effect of selective depletion from the complex mixture (which means that only one of the proteins is removed from the mixture at a time), the consequences of removal of some proteins (e.g. fibronectin, vitronectin or both) from serum can be quantified. Another remarkable way to inspect the role of adhesion proteins in cell interactions with

biomaterials is to add specific inhibitors of their function. As explained above, the integrin receptors present in cells specifically recognize the adhesion protein binding to it. By adding an antibody that binds to the receptor, the access of a cell to the adhesion protein is blocked and the reaction is inhibited [50].

2.4. Cellulose as anti-adhesive *substratum* in biomedical applications

As described above, cell attachment to surfaces may be influenced by a diverse range of factors, which modulate the cell responses, interfacial chemical conditions and protein adsorption [64-70]. Most cells are anchorage-dependent and adhere to the extracellular matrix in order to grow and survive. Cells unable to spread are deleted by apoptosis, a biochemical cascade that leads to characteristic cell changes and death without triggering an inflammatory response [71, 72]. When adherent cells are cultured onto anti-adhesive surfaces they are not able to find anchorage sites and aggregate [73, 74].

Polysaccharides, like cellulose, are a group of polymers widely used in biomedical applications. Their properties, including nontoxicity, stability to temperature and pH variations, and water solubility or high swelling ability by simple chemical modification are very interesting for applications in therapy [75]. Several cellulose derivatives have been used as anti-adhesive *substrata* and their properties were widely investigated in past years. Currently, the study of anti-adhesive materials with the desired properties, to be used in biomedical applications, remains one of the most difficult challenges. Carboxymethylcellulose (CMC) has been used as anti-adhesive coating in several biomedical applications, such as anti-adhesive meshes [76-79], wound dressings (sutures, gauzes, bandages, compresses) [80-83] and drug delivery matrices [84-87]. Original bi-layered hydroxypropylmethylcellulose (HPMC)-CMC-coated *substratum* (CEL) is another anti-adhesive cellulose coating which adsorbs proteins poorly and does not support cell spreading or the formation of focal contacts, making it a suitable material for studying the molecular mechanisms underlying cell-*substratum* and cell-cell interactions. CEL was designed as an original and sterile bi-layered coating capable of securing an anti-adhesive long-term effect [88]. Cellulose acetate butyrate (CAB), methylcellulose (MC) and hydroxypropylmethylcellulose (HPMC) were also used in ophthalmic products (contact lenses, aqueous eyedrop suspensions) manufacture [75]. Oxidized cellulose was been used as hemostatic agents (gauzes) [75]. Cellulose was the first membrane material used in hemodialysis and, with its derivatives, remains the most used membrane in the field. Cuprophan (CU) is a membrane consisting of natural cellulose that promotes inhibition of cell spreading and is used as

hemodialysis membrane [88, 89]. It was demonstrated that CU promotes poor adsorption of serum adhesive proteins and causes the aggregation of Swiss 3T3 fibroblasts [90]. Cellulose triacetate (TAC) is another membrane frequently used in hemodialysis. Several other ongoing investigations aim at developing non-fouling cellulose-based substrates trying to understand the processes that regulate their behaviour and to assess their efficiency [91, 92].

3. Stem Cells and Regenerative Medicine

The aim of this section is to present scientific knowledge about stem cells and the state of art in regenerative medicine.

3.1. Principles of Regenerative Medicine

Regenerative medicine is a promising branch of medicine whose main goal is to repair, regenerate or replace organs and tissue functions, damaged by chemical or physical injuries or as result of infectious or congenital anomalies, using a biologic approach that involves the delivery of cells, signalling molecules and support structures [93]. Congestive heart failure, osteoporosis, Alzheimer's and Parkinson's diseases, severe burns, spinal cord injuries and birth defects are some areas of critical need that have, currently, few accepted treatments or no cures and kill millions of patients all over the world. The short number of organs available for donation, an aging population and a growing crisis in organ transplantation led to an incredible hope in the therapeutic potential of regenerative medicine in general and stem cells in particular. Perry [94] demonstrated that 128 million people could benefit with the potential of stem cells only in the United States, being the cardiovascular disorders, autoimmune diseases and diabetes on the top of injuries that may be helped by stem cell research [94]. Regenerative medicine covers a wide range of clinical applications. Neural applications in regenerative medicine include trauma (such as spinal cord injuries) and diseases (such as Parkinson's). Cardiovascular applications involve blood vessel substitutes, vascular replacements and myocardial repair [93].

3.2. Stem cells

There are a number of questions that arise when discussing stem cells. What are they? Where do they come from? What classes of stem cells are there? What are the differences between embryonic and adult stem cells? Which are the clinical potential uses of human stem cells? How far

are we from using stem cells as a tool in regenerative medicine? Could stem cells be the solution to some untreated diseases? These are some issues that have aroused the curiosity of the scientific community and society in general [93].

Broadly speaking, a stem cell is an unspecialized cell that can self-renew and differentiate into a wide range of specialized cells of embryonic or adult tissues. Stem cells can originate from embryonic, fetal or adult tissue. Embryonic stem cells (ESC) are commonly derived from the inner mass of a blastocyst, an early (4-5 days) stage of the embryo. Embryonic germ cells (EGC) are isolated from the gonadal ridge of a fetus (5-10 week) and adult stem cells differ from ESCs and EGCs and can also be found in tissues after birth [93]. A schematic picture of the hierarchy of stem cells can be seen in Fig. 1.8.

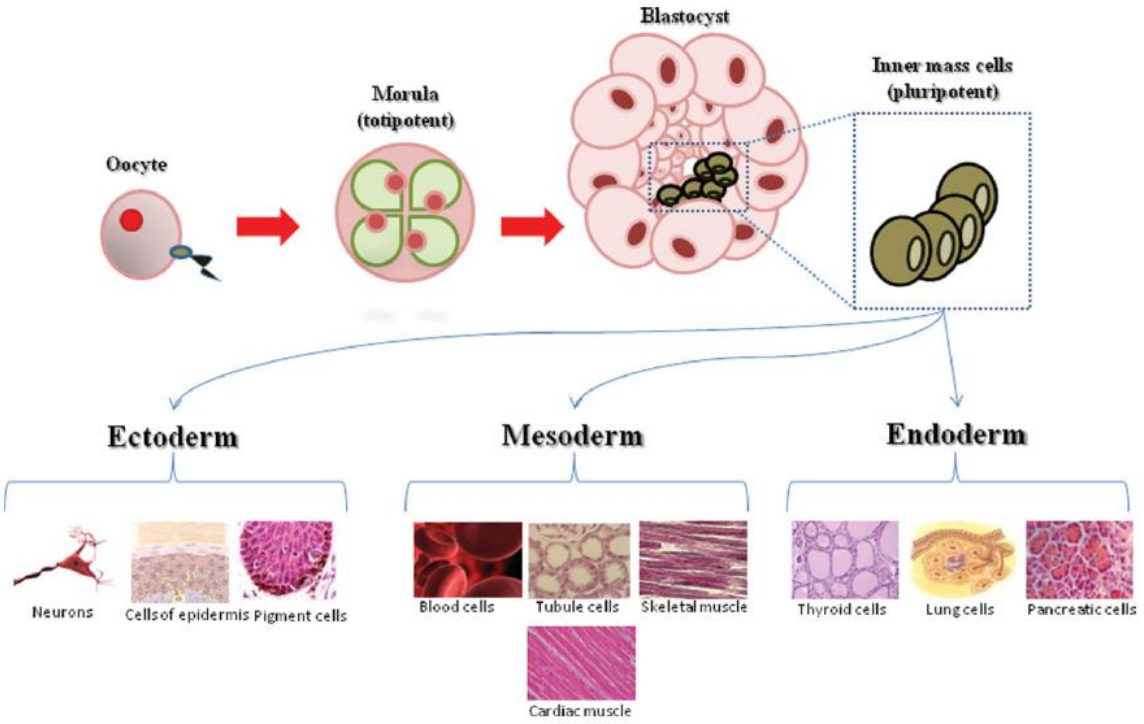

Figure 1.8 – Hierarchy of stem cells. Adapted from [95].

The fertilized oocyte is a totipotent cell capable of differentiating into all three lineages and into extra-embryonic cells that support fetal development. Cells produced by the first few divisions of the fertilized egg are also totipotent. ESCs and EGC are pluripotent cells and can differentiate into all three germ layers. Adult stem cells are considered multipotent which means that they are able to form more than one cell type, but are committed to a specific lineage [93].

ESCs appear to be the most versatile stem cell type for application in regenerative medicine, although their isolation from the inner cell mass of a blastocyst results in the destruction of the pre-implantation embryo. While the use of ESCs in cell-based therapies is under ethical debate and present social, political and legal consequences, adult stem cells are not seen as an ethical problem and allow for the use of autologous cells for individually customized therapeutic applications, avoiding immunological troubles. The ethical issues surrounding the use of ESCs, the lack of understanding about how to specifically regulate ESCs differentiation and the tumorigenicity reported [96] have driven the researchers to use adult stem cells that lack these side effects [93].

Adult stem cells are able to self-renew and yield differentiated cell types. They have been derived from a wide range of adult tissues, including the human bone marrow [97], blood [98], brain [99], fat [100], liver [101], muscle [102], pancreas [103], umbilical cord blood [104], heart, lungs, kidney and spleen [93, 95]. Adult stem cells have been used in some cell-based therapeutical trials. The success in several clinical trials and the progression in the understanding of the mechanisms by which adult stem cells exert their seemingly favourable effects encouraged their use in clinical applications [93].

3.2.1. Mesenchymal stem cells

Mesenchymal stem cells (MSC) are undifferentiated multipotent cells originating from the mesodermal germ layer, which reside in various human tissues and have potential to differentiate. MSCs have been described to give rise to diverse cells including osteoblasts, chondrocytes, adipocytes, myocytes, fibroblasts and other cells from tissues of mesenchymal origin [93, 95]. At the beginning, MSCs were isolated from the bone marrow and from the stroma of spleen and thymus. However, many other tissues in the human body were found to harbor MSC populations and their isolation has been reported from several tissues including cartilage, lung, trabecular bone synovial membrane, adipose tissue, dermis, liver, amniotic fluid, placenta, dental pulp, muscle, periosteum, umbilical cord blood and other skeletal sites, suggesting that MSCs are diversely distributed *in vivo* [93, 95, 105]. MSCs in the body represent reservoirs of reparative cells capable to mobilize, proliferate and differentiate to the appropriate cell type in response to certain signals including injury, inflammation and necrosis. There are still many questions to answer about the true nature and identity of MSCs, including their location, origin and multipotential capacity. In fact, the different methods of isolation and expansion reported and the difference of phenotype, proliferation and

capacity of differentiation showed by MSCs derived from different tissues, make the comparison of the existing data difficult [95, 105].

MSCs represent only between 0.001 and 0.01% of the total nucleated cells within isolated bone marrow aspirates [95]. However, there still remains a great interest in these cells because they can be easily isolated and expanded in a few weeks. The International Society for Cellular Therapy has provided the minimum criteria for defining multipotent human mesenchymal stromal cells [106], namely:

- Plastic-adherent under standard culture conditions;
- Positive for expression of CD105, CD73, and CD90, and absent for expression of the hematopoietic cell surface markers CD34, CD45, CD11a, CD19, and HLA-DR;
- Multipotent differentiation potential: under specific stimulus, MSCs should differentiate into osteocytes, adipocytes, and chondrocytes *in vitro*.

The easy isolation, culture-expansion potential *in vitro*, plasticity, immunosuppressive properties, use in allogeneic transplantation, paracrine-mediated effects, homing and migratory behaviour to sites of tissue injury, inflammation and tumours and absence of ethical considerations are some factors that make MSCs a promising candidate in a wide range of clinical applications.

3.2.1.1. Biological characterization, techniques for isolation and expansion

MSCs have high proliferation potential and can be easily manipulated permitting differentiation before implantation. There are a wide number of procedures for the isolation of MSCs. The simplest method was identified more than 30 years ago by Friedenstein *et al.* [107-109] and involves the adherence properties of MSCs. In this study, Friedenstein put whole bone marrow in plastic culture dishes and the non-adherent cells were washed out after 4 hours. It was observed that cells remained dormant for 2-4 days and then proliferated rapidly.

The density centrifugation of bone marrow is an alternative solution, which involves the use of solutions of high density with low viscosity and low osmotic pressure (e.g., Ficoll, Percoll) to obtain the mononucleated fraction of bone marrow containing MSCs. After that, adherence to plastic occurs, resulting in a MSCs population [93, 110]. However, the techniques mentioned above do not allow the purity of the MSCs sample, because other types of cells, like haematopoietic stem cells, are also present in the preparation. Two new techniques have emerged to solve this issue. One of them

is the magnetic bead sorting technique, which uses epitopes positive for MSCs, which are labeled with antibody-coated magnetic beads. After that, an external magnetic field is applied separating the positive from the negative labelled cells [93, 107]. The second method developed was fluorescence-activated cell sorting (FACS), in which a heterogeneous population of cells (e.g. blood, bone marrow, etc) are characterized and separated based on the intensity of the fluorescence they emit while passing through an illuminated volume. In order to isolate these cells from solid tissues like bone, cartilage or fat, enzymatic treatment with collagenases is required. Collagenases are enzymes that are able to cleave the peptide bonds in the triple helical collagen molecule. Cells are released from the tissue and collected by wash and centrifugation [93, 107].

The step after MSCs isolation is their replication targeting sufficient number for clinical use. The yield of *in vitro* expansion of MSCs depends on various factors such as donor and technique dependent factors. Donor dependence includes age, sex and presence of trauma or systemic disease. The technical issues include the number of passages of MSCs, the method of culture and the media used for expansion [93, 107]. MSCs can be quickly expanded within a relative short period of time and can proliferate for about 19 doublings in culture without losing their property to proliferate and differentiate, despite the fact that expansion gradually reduces their maximal differentiation potential [107]. It was proved that the cardioprotective effect of MSCs is reduced in cells of passage 5 and 10 compared to those of passage 3, a fact that could be explained by the reduced vascular endothelial growth factor release potential [111]. Another important component of successful expansion of MSCs is the media used. Comparative studies between different types of basal media show clear differences in terms of adherence efficacy, growth index and final number of cells obtained. Proliferative growth factors can also be used to increase the time and yield of the cells in culture. The most effective technique for MSCs expansion is the monolayer (2D) culture in glass or polystyrene roller bottles, culture flasks or Petri dishes [107]. Culture conditions include incubation in a maintained temperature of 37°C and a humidified atmosphere with 95% O_2 and 5% CO_2. The culture medium should be changed every 2-3 days and when cells reach confluency they are treated with trypsin solution and seeded into new culture flasks. Several 3D culture environments, including alginate, collagen, fibrin and chitosan have also been developed in the last years in order to encapsulate and support MSCs [107]. An alternative method to their expansion is the use of bioreactors which mimics the *in vivo* conditions of the cells minimizing shear stress, microgravity, efficient nutrient supply and metabolite removal.

3.2.1.2. A promising candidate in regenerative medicine, clinical applications and trials

As previously mentioned, MSCs reside in the connective tissues of most organs, can differentiate into multiple mesenchymal lineages including adipose tissues, bone and cartilage, possess the ability to trans-differentiate into other tissue cells types, can migrate to sites of injury, inflammation and tumours and can alter the tissue microenvironment via secretion of soluble factors. Based on these unique properties, intense research work focus on MSCs has been developed, in recent years, to explore their potential for therapeutic applications. Several phase I/II and III clinical trials have explored the therapeutic potential of MSCs in tissue repair and regeneration. Clinical trials are biomedical or health-related research studies in human beings that follow a pre-defined protocol [112]. Approximately 120 clinical trials were completed or are currently exploring the application of MSCs. At the moment, clinical trials include both interventional and observational studies. Interventional studies are those whose research subjects are assigned by the investigator to a treatment or other intervention and their outcomes are measured. In observational studies, individuals are observed and their outcomes are measured by the investigators. Their beneficial properties were already demonstrated in a diverse range of conditions including renal pathologies, hematologic pathologies, such as graft-versus-host disease [112], osteogenesis imperfect [113], amyotrophic lateral sclerosis [112], Hurler syndrome [114], metachromatic leukodystrophy [114], Crohn's disease [112], fracture [115], ischemic cerebral disease [116, 117], cardiovascular disease [118] and spinal cord injury [119]. After the expansion and *in vivo* administration, MSCs home and engraft to injured tissues and modulate an inflammatory response. Table 1.3 provides a general update on clinical trials involving MSC-based therapies.

Table 1.3 – Clinical trials using mesenchymal stem cells [112].

Clinical Trial	*Disease*	*Cell Type/Source*	*Status*	*Location/Sponsor*
Prochymal™ Adult Human Mesenchymal Stem Cells for Treatment of Moderate-to-severe Crohn's Disease	Crohn's Disease	Bone Marrow derived allogenic MSC (Prochymal)	Completed	Osiris Therapeutics, U.S
Allogeneic Mesenchymal Stem Cells Transplantation for Systemic Sclerosis (SSc)	Systemic Sclerosis	Allogeneic mesenchymal stem cells	Recruiting	Christian Medical College, Vellore, India

The Use of Autologous Bone Marrow Mesenchymal Stem Cells in the Treatment of Articular Cartilage Defects	Degenerative Arthritis; Chondral Defects; Osteochondral Defects	Autologous Bone Marrow Mesenchymal Stem Cells	Recruiting	Cairo University
Autologous Mesenchymal Stem Cell (MSC) Transplantation in Multiple Sclerosis	Relapsing-Remitting Multiple Sclerosis; Secondary Progressive Multiple Sclerosis; Progressive Relapsing Multiple Sclerosis	Autologous mesenchymal stem cell	Not yet recruiting	The Cleveland Clinic
Mesenchymal Stem Cells and Myocardial Ischemia	Chronic Myocardial Ischemia; Left Ventricular Dysfunction	Mesenchymal Stem Cells	Recruiting	University Hospital, Toulouse
Cord Blood Expansion on Mesenchymal Stem Cells	Myelodysplastic Syndrome; Leukemia	Mesenchymal stem cells	Recruiting	M.D. Anderson Cancer Center
Autologous Transplantation of Mesenchymal Stem Cells for Treatment of Patients With Onset of Type 1 Diabetes	Autologous Transplantation; Type 1 Diabetes Mellitus	Autologous bone marrow mesenchymal stem cells	Recruiting	Third Military Medical University
Mesenchymal Stem Cells Transplantation for Refractory Systemic Lupus Erythematosus (SLE)	Refractory Systemic Lupus Erythematosus	Allogeneic MSC	Recruiting	Nanjing Medical University
Mesenchymal Stem Cells Under Basiliximab/Low Dose RATG to Induce Renal Transplant Tolerance	Kidney Transplant	Mesenchymal stem cells	Recruiting	Mario Negri Institute for Pharmacological Research
Transplantation of Bone	Osteoarthritis;	Bone Marrow	Recruiting	University of

Marrow Stem Cells Stimulated by Proteins Scaffold to Heal Defects Articular Cartilage of the Knee	Knee Arthrosis; Osteochondral Defect; Osteochondritis Dissecans; Osteonecrosis	Stem Cells		Marseille
Treatment of Severe Osteogenesis Imperfecta by Allogeneic Bone Marrow Transplantation	Osteogenesis Imperfecta	Allogeneic Bone Marrow	Completed	St. Jude Children's Research Hospital
Bone Mesenchymal Stem Cell (BMSC) Transplantation in Liver Cirrhosis Via Portal Vein	Liver Cirrhosis	Autologous BMSCs	Active, not recruiting	Sun Yat-sen University
Stem Cell Therapy for Vasculogenesis in Patients With Severe Myocardial Ischemia	Myocardial Ischemia; Coronary Heart Disease	Bone Marrow derived MSC	Completed	Rigshospitalet, Denmark
Cell Transplant in Spinal Cord Injury Patients	Chronic Spinal Cord Injury	Autologous Bone Marrow Mesenchymal Stem Cells	Completed	Cairo University
Using Mesenchymal Stem Cells to Fill Bone Void Defects in Patients With Benign Bone Lesions	Bone Neoplasms	Mesenchymal Stem Cells	Not yet recruiting	Emory University
Autologous Mesenchymal Stem Cell Transplant for Parkinson's Disease	Parkinson's Disease	Autologous Bone marrow derived stem cells	Recruiting	Jaslok Hospital and Research Centre
Safety and Efficacy of Prochymal for the Salvage of Treatment-Refractory Acute GVHD Patients	Graft Versus Host Disease	Bone Marrow derived allogenic MSC (Prochymal)	Completed	Osiris Therapeutics
Long-Term Follow-up of Liver Failure Patients	Liver Failure	Mesenchymal Stem Cells	Recruiting	Sun Yat-sen University

Who Received Autologous Mesenchymal Stem Cells (MSCs) Transplantation

3.3. Liquid Crystal-Based Stem Cell Therapies

As shown in the previous section, a large number of investigations and clinical trials have demonstrated the enormous potential of MSCs. The absence of adverse side effects and the seemingly beneficial effects of MSCs have encouraged the field of MSC therapy. Despite this area presents controversial data due to the variation of the techniques followed in each study, several trials employing MSCs as therapeutic agents are still under way. It is believed that MSCs are a promising candidate for regenerative medicine in the near future and the optimization of the techniques will certainly provide a better understanding about MSCs allowing new therapeutic advances.

The study of Lockwood [1] have provided evidence of the potential of liquid crystals in the bioengineering arena by showing that they can monitor the growth of embryonic stem cells.

Chapter II – MATHERIALS AND METHODS

1. Materials Preparation

Hydroxypropylcellulose (M_w ~100,000 $g.mol^{-1}$) and the crosslinking agent 1,6-diisocyanatohexane (98%) were purchased from Aldrich. Dimethylacetamide (DMAc – Aldrich) was used as solvent to prepare the HPC solutions.

1.1. Production of HPC crosslinked films

To produce the solid films, two solutions of HPC (30 and 60 wt%) in DMAc were prepared. The synthesis of HPC solutions was performed by carefully adding HPC to DMAc at room temperature. An isotropic 30 wt% solution (HPCi) and an anisotropic 60 wt% chiral nematic solution (HPCa) were obtained and their content was allowed to homogenize for several weeks. A few days after this procedure the solutions had a similar aspect to that shown in the Fig. 2.1.

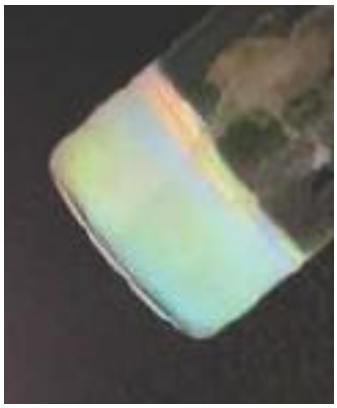

Figure 2.1 – Visual aspect of an HPCa solution in DMAC showing characteristic iridescent colours resultant of the reflection of the light. Kindly provided by Prof. Helena Godinho.

The concentration of HPC used to prepare those solutions was chosen taking into account the studies, performed by Gray [120], on lyotropic phases of HPC in various solvents, including DMAc, in order to have two extreme concentrations.

After homogenization, the solutions were cross-linked to enhance biostability and mechanical properties. Each solution was submitted to a chemical cross-linking treatment by adding 10% (w/w) of the crosslinking agent 1,6 diisocyanatohexane 98% (Aldrich).

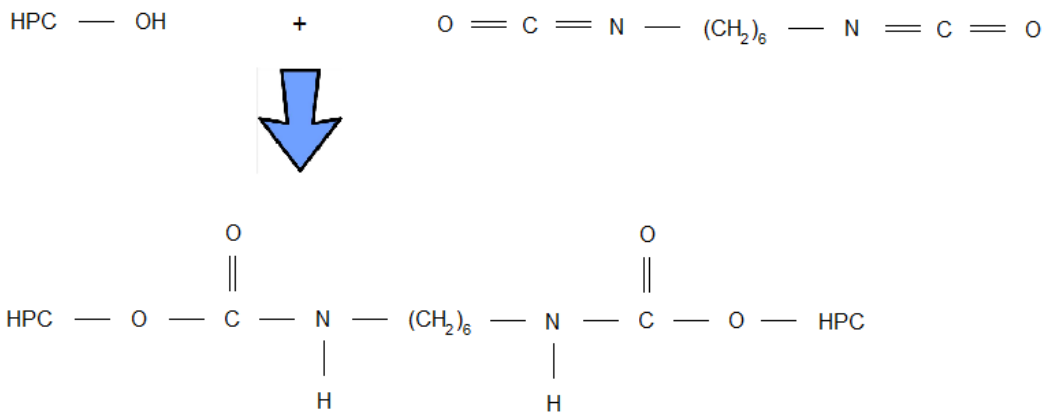

Figure 2.2 – Schematically representation of the cross-linking reaction.

HPC cross-linked solution was then deposited on parafilm, with the help of a calibrated ruler moving at a controlled rate (v = 6 $mm \cdot s^{-1}$), at room temperature, as shown in Fig. 2.3. The solvent was allowed to evaporate in a laboratory atmosphere at room temperature.

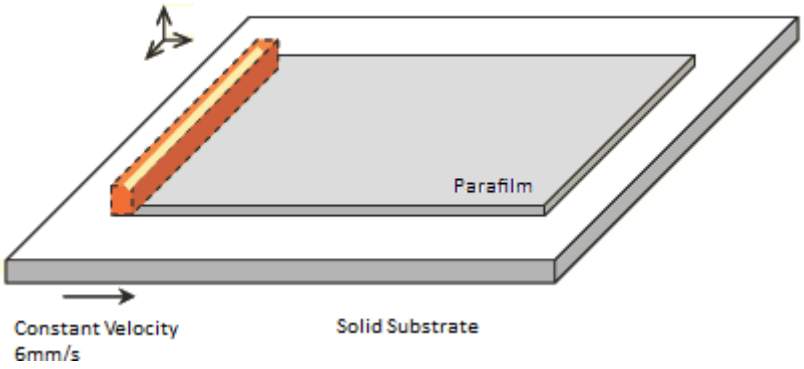

Figure 2.3 – Schematic representation of HPC films preparation. Kindly provided by Prof. Helena Godinho.

The average thickness of the dried films was measured using a digital micrometer (from Mitutoyo, Japan) and was approximately 11 ± 1.00 µm for HPCi films and 19.6 ± 2.00 µm for HPCa films.

2. Structural and Physico-Chemical Characterization

In this section, some properties of solid films and their surfaces were investigated. The principles of the methods used in their characterization are briefly explained.

Surface characterization requires particular techniques and has an important role in biomaterials characterization because the atoms that make up the outermost surface of a biomaterial drive many biological reactions that occur in response to the foreign body, like protein adsorption, cell adhesion, cell growth and blood compatibility, among others. [50] The following table resumes some methods used in this work to characterize film surfaces.

Table 2.1 – Common methods used to characterize biomaterial surfaces. Adapted from Ratner [50].

Method	Principle	Depth analyzed	Spatial resolution
Contact angle	Liquid wetting of surfaces is used to estimate the energy of surfaces	3–20 Å	1 mm
ESCA (XPS) Electron Spectroscopy for Chemical Analysis (X-ray photoelectron spectroscopy)	X-rays induce the emission of electrons of characteristic energy	10–250 Å	10–150 µm
FTIR Fourier transform infrared spectroscopy	IR radiation is adsorbed and excites molecular vibrations	1–5 µm	10 µm
SEM Scanning Electron Microscopy	Secondary electron emission induced by a focused electron beam is spatially imaged	5 Å	40 Å, typically

Table 2.1 presents some characteristics of surface analysis techniques used including their depth of analysis and spatial resolution. The principles of these techniques are described in the next sections.

2.1. Optical polarizing microscopy

It has been previously described [49] that thin solid films prepared from lyotropic solutions of cellulose derivatives develop a characteristic banded texture perpendicular to the shear direction.

The optical anisotropy of the HPC films was inspected by optical polarizing microscopy. The optical properties of thin films were observed using an Olympus (Model BH2) microscope equipped with cross polarizers. Optical microphotographs were taken using a microscope equipped with a camera.

2.2. Determination of the gel fraction

Gel fractions of the HPC films were obtained as a function of HPC concentration used to prepare the solid films and were calculated as the ratio of the weight of the extracted film to that of the non-extracted one. The soluble material of the solid films was extracted in water for 24h using a Soxhlet apparatus. The extracted film was dried in vacuum, at 60ºC.

2.3. Mechanical properties of the dried and wet films

HPC films were submitted to tensile tests performed under dry and wet conditions to determine the influence of HPC composition and of the anisotropy in mechanical properties (measured by the difference in mechanical properties between the direction of the film spreading and the perpendicular to this direction). The mechanical properties of the HPC films are compared. These properties are extremely important to characterize biomaterials and to prevent future failures of materials in biomedical applications.

The measurements of the mechanical properties were performed on a Rheometric Scientific (Minimat, Firmware Vsn 3.1; Fig. 1.12) testing machine at room temperature (25ºC), using the tensile mode. The film samples were cut into pieces with 3 x 0.5 cm. 6 successful determinations were used to obtain average values. The stretching rate was 5 mm/min. For testing in wet state, the samples were soaked in phosphate buffered saline (PBS) solution and then were continuously wetted with this solution when fixed in the device.

Load extension graphs were obtained during this test and converted to stress-strain curves applying the following equations:

$$Stress = \sigma = \frac{F}{A} \qquad \textbf{Equation 1}$$

where F is the applied force and A is the cross sectional area.

$$Strain = \varepsilon = \frac{\Delta l}{L} = \frac{l-L}{L} \qquad \textbf{Equation 2}$$

where l and L are the length at the time of data collection and original length (between clamps), respectively.

The measurements were performed with dry and wet films at room temperature.

Figure 2.4 – Photograph of the (a) tensile tests equipment and (b) detail of the film sample placed between the clamps.

The Young's modulus or elastic modulus (E) is a mechanical parameter that gives information about material stiffness and it is defined as the slope of the stress-strain curve (E=stress/strain) in the elastic deformation region.

2.4. Contact Angle Measurements

While several surface analytical methods require sophisticated equipment and qualified operators, contact angle measurements provide information about surface structure of a biomaterial in a simple and low-cost way [121].

Surface free energy and relative hydrophilicity/hydrophobicity of surfaces constitute information that can be provided by this method.

Contact angle, θ, is a quantitative measure of the wetting of a solid by a liquid. It is defined as the angle formed by a liquid at the three phase boundary where a liquid, vapour and solid meet. In technical terms, the phenomenon behind this technique is based on a balance between the attraction of molecules within the droplet to each other *versus* the attraction or repulsion those droplet molecules experience towards the surface molecules. These are termed "force balances" [50, 122, 123]. This method is believed to be sensitive to the outermost 3 – 20 Å of a surface [50, 121].

The preparation of the materials for contact angle measurement does not usually involve special procedures. The surfaces should be homogeneous, clean, smooth and not swell or dissolve in the test fluid and the measurement should be done in thermodynamic equilibrium [124]. Some factors as the droplet size and time required to obtain readings may affect the contact angle results [121].

The equilibrium value of contact angle is measured according to the Young's equation, which relates θ with γ_{sv}, γ_{lv} and γ_{sl} by the equation $\gamma_{sv} = \gamma_{sl} + \gamma_{lv}cos\theta$, where θ is the contact angle, γ_{sl} is the solid/liquid interfacial tensions, γ_{lv} is the liquid/vapour interfacial tension and γ_{sv} is the solid/vapour interfacial tension [123, 125, 126].

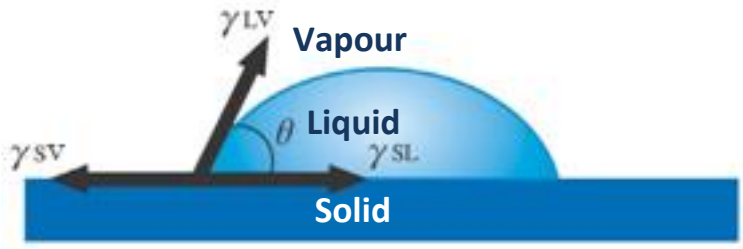

Figure 2.5 – Contact angle with associated forces. Adapted from Kyowa. [127].

Low values of θ indicate that liquid wets well, while high values indicate poor wetting. If the angle θ is less than $90°$, the liquid is said to wet the solid. If it is greater than $90°$ it is said to be non-wetting. A zero contact angle represents complete wetting.

Contact angle analysis on biomaterial surfaces can be carried out by five different techniques, including the sessile drop method, the Wilhemly plate method, the captive air bubble

method, the capillary rise method and the tilted-drop method [50, 121, 128]. The different methods have been summarized in Fig. 2.6. The technique selected depends on the geometry and location of the surface or coating to be studied. In all the methods, the contact angle is the angle of the liquid at the interface relative to the plane of the model surface.

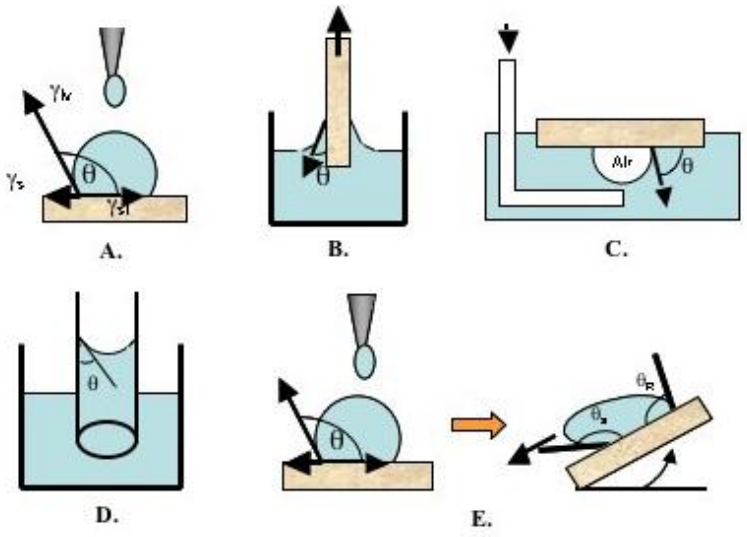

Figure 2.6 – Different contact angle measurements: **A.** Sessile drop method; **B.** Wilhemly plate method; **C.** Captive air bubble method; **D.** Capillary rise method; **E.** Tilted-drop method. Adapted from Stein [122].

Several liquids can be used to measure the contact angle with the sample surface. The most commonly used liquids are water, diiodomethane, ethylene glycol and glycerol. According to the surface tension of the liquid used and the area of sample, it is necessary to optimize the test conditions, in particular the volume and speed of the drop in addition to the diameter of the needle from the syringe in use.

The most commonly used methods are the sessile drop and Wilhelmy balance, with water as the test fluid. [121, 123] In the sessile drop method, a drop of fluid is placed on the surface in study and, after equilibrium, the contact angle can be directly determined using a goniometer. This technique requires small test surfaces and small quantities of test liquid. However, the sessile drop method has poor accuracy and high sensitivity to surface contaminations [123].

In surfaces which present roughness, chemical heterogeneity, contaminations, evaporation and/or molecular movement, liquids do not maintain a constant state when in contact with the material.

The water contact angles, θ, of HPCi and HPCa films were determined using the sessile drop method. Measurements were performed in a DataPhysics (*Optical Contact Angle Device OCA15*) system provided with video camera (CCD) and SCA 20 software for image analysis and contact angles calculation. Samples were placed in a thermostatic environmental chamber (at constant temperature 25ºC) saturated with water to prevent evaporation. Water drops (distilled–deionised with conductivity $\%1\mu S/cm$, $4\mu l$) were applied using a gastight syringe (Hamilton) mounted on an electronic unit. Images were acquired every 2 seconds during 180 seconds. To calculate θ, droplet profiles were fitted using the Young–Laplace (θ >=90º), the ellipse (30º < θ < 90º) or the tangent (θ < 30º) methods and values were obtained by extrapolating the time dependent curve to zero (the line of polynomial regression trend 6th grade: the value of the intersection of the line with the y-axis corresponds to the angle of contact at time zero).

The optical contact angle device used in this experiment is shown in Fig. 2.7.

Figure 2.7 – Optical Contact Angle Device OCA 15.

2.5. Chemical characterization of surfaces

The chemical analysis of HPCi and HPCa films and the investigation of chemical changes after the cross-linking reaction require particular methods. Several techniques have been used to chemically characterize the surfaces of the biomaterials. Fourier transform infrared spectroscopy (FTIR), X-ray photoelectron spectroscopy (XPS), static secondary ion mass spectrometry (SSIMS) and energy dispersive X-ray spectroscopy (EDS) are the usual methods applied in the chemical characterization. These techniques can be used to identify the presence of an element or functional group and to investigate their percentage on a material surface, as well as the chemical states of these elements and their spatial distribution [129, 130].

2.5.1. Fourier Transform Infrared (FTIR) Spectroscopy

FTIR spectroscopy is based on the interaction of infrared (IR) radiation with a material. It provides information on the vibrations of atomic and molecular species. When molecules are exposed to infrared (IR) light, radiation at frequencies matching the fundamental modes of vibration is absorbed. An infrared *spectrum* represents a fingerprint of a sample with absorption peaks that correspond to the frequencies of vibrations between the bonds of the atoms making up the material. Each material has a distinctive *spectrum* because groups of atoms have unique fundamental modes of vibration and the peaks shown in a FTIR *spectrum* represent specific chemical bonds and chemical functional groups [130].

The IR techniques include attenuated total reflectance (ATR) and diffuse reflectance spectroscopy (DRS). The ATR mode has been used most often in biomaterials surface analysis to characterize their chemical composition, physical structure and have also been used in protein adsorption studies [131]. An ATR accessory has to be adapted to IR spectrophotometer to apply this technique.

Modern FTIR instruments are easy and fast to use and are very sensitive. FTIR is a fast, easy and relatively inexpensive technique, which provides rich information. They afford well-defined and consistent *spectra* with great wavelength precision. FTIR presents many advantages and some disadvantages. The first advantage is known as Fellgett advantage. It means that all the spectral elements are measured simultaneously, which makes this technique faster and provides a higher *spectrum* signal to noise (S/N) ratio compared to other techniques. Another important advantage is

known as Jacquinot and it arises because FTIR spectrometers have no slits that attenuate the infrared light, which provides a great optical throughput and a higher signal to noise. The vast majority of molecules in the universe absorb mid-infrared light, making it a highly useful tool. On the other hand, FTIR have some disadvantages, namely it cannot detect atoms and monatomic ions because single atomic entities contain no chemical bonds; it cannot detect molecules comprised of two identical atoms symmetric, such as N_2 or O_2. Aqueous solutions and complex mixtures are very difficult to analyze because water is a strong IR absorber and complex samples give rise to complex *spectra* [129].

A schematic diagram of a FTIR spectrometer is shown in Fig. 2.8. The most important components are the IR source, the beam splitter, the detector and the reference laser. The setup includes reflecting mirrors at various points to direct the path of IR light. The light from the source passes through the aperture wheel and hits a mirror that directs the light onto the beam splitter. The recombined light from the interferometer is finally detected by the detector, after being directed by mirrors into the sample compartment [129, 130].

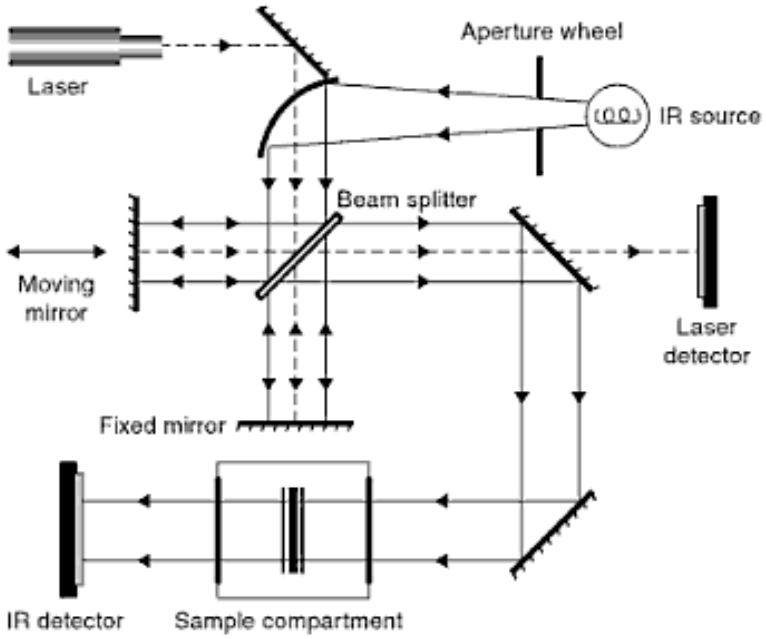

Figure 2.8 – Optical layout of a typical FTIR spectrometer. Image adapted from ref. [129].

FTIR was used to investigate functional groups on the HPCi and HPCa films. FTIR measurements were performed on a Perkin Elmer FTIR spectrophotometer, model 2000. All data were taken at 2 cm^{-1} resolution with a total of 100 scans. Measurements were performed in the mid-IR frequency range (4000–600) and *spectra* were baseline corrected and smoothed.

2.5.2. X-ray Photoelectron Spectroscopy (XPS)

X-ray Photoelectron Spectroscopy (XPS), also known as Electron Spectroscopy for Chemical Analysis (ESCA), is used to determine quantitative atomic composition and chemistry. XPS is more surface sensitive than FTIR and is one of the most popular methods used for surface chemical analysis. It provides information about the type and amount of elements present and also about their oxidation state and chemical surrounding. This method is based upon the photoelectric effect, described by Einstein in 1905. X-rays are focused upon a specimen and their interaction with the atoms of the specimen causes the emission of photoelectrons with energy values characteristic of the elements present at the surface. The energy of this electron is measured and the information about the nature and environment of the atom from which it came can be afforded and presented as a graph of intensity versus electron energy [130, 132].

Equation 3 expresses the basic energy balance that describes this process:

$$E_B = E_K - h\upsilon - \phi \qquad \textbf{Equation 3}$$

where,

E_B is the energy binding the electron to an atom;

E_K is the kinetic energy of the emitted electron that is experimentally measured by the spectrometer;

$h\upsilon$ is the energy of the X-rays;

ϕ is the work function of the analyzer detector.

A schematic diagram illustrating a XPS instrument is shown in Fig. 2.9.

Nowadays, XPS is among the most frequently used techniques because it provides important information of the material surfaces. XPS provides identification of all elements (except H and He) present at concentrations higher than 0.1%, semi-quantitative determination of the approximate elemental surface composition, information about the molecular environment (oxidation state, bonding atoms, etc) and can be used in several applications including identification of stains and discolorations, characterization of cleaning processes, analysis of composition of powders and debris, determination of contaminant sources and examination of polymer functionality before and after processing, to identify and quantify surface changes, among others [132].

XPS has many advantages and few disadvantages. The advantages include the high information provided previously described, the surface localization of the measurement, the speed of analysis, the low damage potential and the ability to analyze most samples with no specimen preparation. The disadvantages include the need for vacuum compatibility, the possibility of sample damage by X-rays if long analysis times are used, the need for experienced operators and the high cost associated [50].

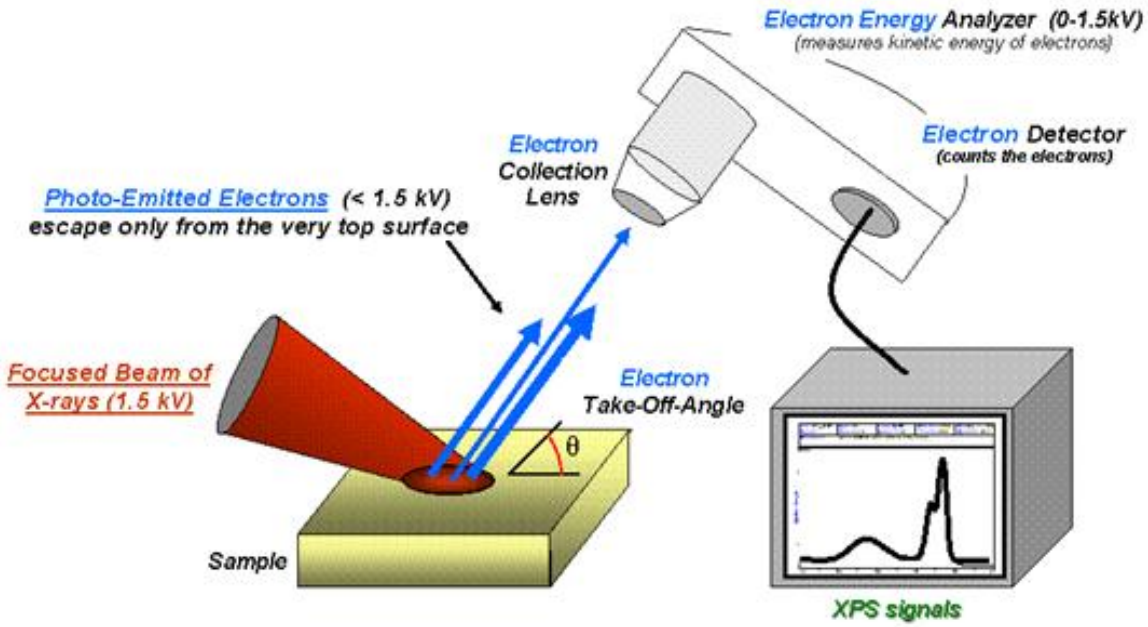

Figure 2.9 – Schematic diagram illustrating basic components of a XPS system. Adapted from [133].

XPS was used to determine the chemical composition of the surface. XPS analyses were performed with a VG Scientific ESCALAB 200A (UK) spectrometer with PISCES software for data acquisition and analyses. An $Al\ k\alpha_{1,2}$ X-ray source operating at 15kV (300 W) was used to stimulate photoemission, and the spectrometer, calibrated with reference to $Ag\ 3d_{5/2}$ (368.27 eV) was operated in CAE mode with 20eV pass energy. All polymer samples were analyzed at a $90°$ takeoff angle relative to surface sample, probing about a few nanometers of the uppermost surface. Survey scans (0–1100 eV binding energy) were run at an analyzer with an X-ray spot size area of 10 mm^2 to determine the elemental composition of each surface. Data acquisition was performed with a pressure lower then $E^{-6}Pa$. High resolution C(1s), O(1s) and N(1s) scans were performed using peak fitting with Gaussian/Lorentzian sum function. The deconvolution of the high resolution *spectra* was made by means of a least-squares peak analysis software, XPSPEAK version 4.1

2.6. Scanning Electron Microscopy (SEM)

Scanning Electron Microscopy (SEM) involves a microscope that uses electrons instead of light to form images of surfaces with great resolution and depth of field and with three dimensional quality. SEM works by focusing a relatively high energy electron beam on a specimen. Low-energy secondary electrons are emitted from each spot where the focused electron beam impacts. The measured intensity of the secondary electron emission is function of atomic composition of the sample and geometry of the features under observation. SEM is a surface analysis method because only secondary electrons generated near the surface can escape from the bulk and be detected [50].

All SEM's consist of an electron gun at the top of the electron column which generates the electron beam, a sample chamber where the electron beam interacts with the sample, detectors to monitor the resultant signals from that interaction and a viewing system that constructs the image from the signal.

Much information can be taken from SEM analysis including: the surface features of a sample (topography); the shape, size and arrangement of the particles on the surface of the sample (morphology); the elements and compounds of the sample and their relative ratios (composition); and finally the arrangement of atoms in the sample and their degree of order (crystallographic information).

As a general imaging and analytical technique SEM has some restrictions, but has several advantages in comparison to other techniques. The principal limitation of SEM is the high vacuum sample environment that is necessary. Nonconductive materials observed have to be coated with a thin, electrically grounded layer of metal to minimize negative charge accumulation from the electron beam. The samples have to be clean, dry and electrically conductive. On the other hand SEM produces high resolution images, which means that closely spaced features can be observed at a high magnification. These advantages, as well as the larger depth of focus and ease of sample observation, make the scanning electron microscope one of the most useful instruments in research today [50, 134].

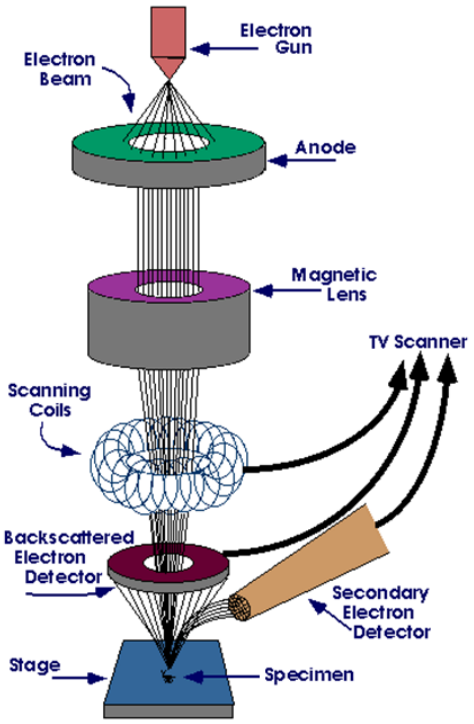

Figure 2.10 – Schematic representation of how does a SEM work. Adapted from [135].

FEI Quanta 400 FEG (resolution 1.2mm) secondary electron images were used to acquire information on the topography of the surfaces. Secondary electron images of the surface were obtained with the sample tilted 50 ° in the transverse direction to the bands, in order to enhance the topographic contrast associated with these. In the acquisition software, the tool "Tilt correction" was activated, that allows to correct the projection effect caused by the tilting of the sample, thereby maintaining the calibration of the images for further measurements. After preliminary tests, it was found that voltages for acceleration of the electron beam promoted degradation of the sample. Therefore, a low accelerating voltage of 5kV was selected for all SEM observations, because it corresponds to a good compromise between resolution and preservation of the surface to be observed. The samples were coated with carbon film obtained by evaporation and with approximately 30 nm thick, to ensure the electrical conductivity of the surface, needed for this type of analysis.

Au-Pd obtained by sputtering was another type of coating tested. However, it was found that this method caused some degradation on the surface, probably caused by the proximity between the sample and the plasma, which occurs in this type of deposition and therefore was not used.

2.7. Atomic Force Microscopy (AFM)

The Atomic Force Microscope was invented in 1986 [136, 137] as a progeny of the Scanning Tunnelling Microscope (STM). The most important difference between them is that AFM allows the investigation of electrically nonconducting samples. AFM can be operated in liquid environments [138] and becomes an important tool for studying biological structures and processes on cellular and molecular scales. This is a unique technique that allows probing true topographic information and permits to study the mechanical properties of cells among other surface properties such as elasticity, adhesion and friction [139].

There are several AFM designs. However, the principal parts are present in almost any AFM. This parts include a sharp tip mounted on a flexible cantilever, a laser diode, a position-sensitive photodiode that detects the laser beam reflected by the cantilever and a piezo device for positioning the sample relative to the tip in three orthogonal dimension, x-y-z. A representative scheme of the principal components of an AFM is shown in Fig. 2.11.

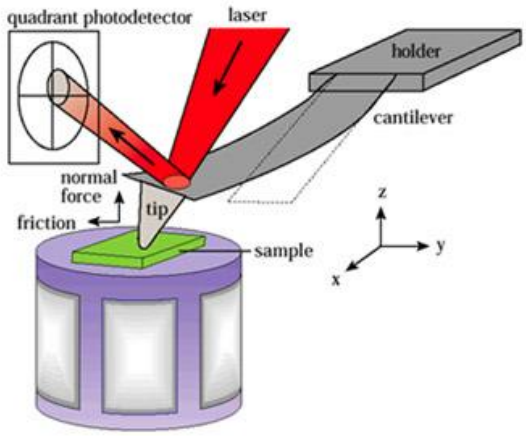

Figure 2.11 – Schematic representation of how does an AFM work. Adapted from [140].

There are three AFM operating modes: imaging mode, force curve mode and force volume mode. In the first mode, the AFM tip is brought into direct physical contact with the sample, while the cantilever deflection is monitored. In the force curve mode, the interaction forces between the AFM tip and the sample is measured and quantified. In this mode, the lateral position of the tip is not changed, while the sample height is ramped such that the tip is brought in and out of contact and the deflection of the cantilever is monitored. Information on adhesion, molecular interactions [141], stiffness [142], hardness [143], electrostatic interaction [144] and other properties of the sample can

be measured in this mode. In force volume mode it is possible to map interaction forces as a function of position, obtaining force curves over different regions of the sample [139].

The topographic features of the surface of HPCa films were quantitatively measured by atomic force microscopy. A PicoPlus Scanning Probe Microscope interfaced with a Picoscan Controller 2500 (both from Agilent Technologies, USA) was used for the atomic force microscopy (AFM) measurements. Each sample was imaged with a $100 \times 100\ \mu m^2$ piezoscanner. Images were obtained in Tapping® mode, in air and at room temperature. A silicon cantilever (AppNANO, USA) was used, with a spring constant 25-75 N/m, in Tapping® mode on solid substrates of HPCa. Three samples of HPCa were analysed at 6 randomly chosen locations. The SPIP™ software was used to measure several parameters.

3. Sterilization

Before cell culture studies the biomaterials were washed and sterilized. For that purpose, after drying the films at room temperature, discs with a diameter of 15 mm were punched out. They were washed with filtered MiliQ water in two steps of 15 and 30 min to remove potential contaminants. Discs were then sterilized by two incubation steps in filtered 70 vol-% ethanol solutions for 15 and 30 min, followed by two rinsing steps of 15 and 30 min with filtered PBS. After this procedure, polymer discs were placed in 24-well tissue culture plates and fixed with sterile silicon o-rings.

The periodic structures observed in HPCa films were preserved after this procedure.

4. Biological characterization

4.1. Cell cultures

Human bone marrow-derived Mesenchymal Stem Cells (hMSC, from Lonza) were expanded and characterized as described previously [145]. All cells were seeded into 150 cm^2 flasks containing Dulbecco's modified essential medium (DMEM, Gibco) supplemented with 10% fetal bovine serum (FBS, Gibco) and 5% Penicillin/Streptomicin. MSC cultures grew at 37°C in a humidified atmosphere of 5% CO_2. The medium was changed subsequently every 3 days. Cells were subcultured when they were approximately 70% confluent. MSCs were recovered using 0.25% Trypsin-EDTA (Gibco) and

replated at a density of 3000 cells per cm^2. The experiments were performed with cells from the 7^{th} or 8^{th} passage that were seeded at $5x10^4$ cells/cm^2 on the various substrates.

4.2. Cytotoxicity

The *in vitro* cytotoxicity test was performed to determine the biological response of cells using appropriate biological parameters in accordance with ISO 10993-12. Sample preparation was in agreement with ISO 10993-12. Liquid extracts were used to simulate the clinical use conditions and to determine the cytotoxicity response. The biocompatibility of the HPCi and HPCa films was evaluated through an *in vitro* indirect cytocompatibility assay on hMSC.

Culture medium with serum was used as extraction vehicle because it allows cellular growth and extracts both polar and non-polar substances. HPCi and HPCa films were extracted in DMEM for 48 h at 37ºC. Cells exposed to fresh medium were used as negative control while cells exposed to methanol 70% were used as positive control in this test. Wells containing only medium (without cells) were used as blank controls.

Cells were pre-incubated and grew to a near-confluent monolayer in 96-well culture dishes for 48 hours at 37ºC. The medium was then removed and replaced by the extracted medium. 1:9, 1:3 and 1:1 dilutions of the extract liquid from HPCi and HPCa films with fresh DMEM were prepared and extracted DMEM was also used, as control. A resazurin test was carried out on cell cultures after 24 and 72 hours of contact with the extracted liquids to investigate cell response. The metabolic activity of hMSCs when in contact with each extract liquid was measured.

4.3. Cell Attachment

One of the simplest methods for examining cell adhesion consists of seeding cells onto substrates of interest, washing off non-adherent cells with a physiological buffer and counting the remaining cells. The percentage of adherent cells on HPC films was assessed by a resazurin-based assay at 24h post-contact. This study was performed on HPCi and HPCa films. Glass coverslips were used as positive control and represent 100% of cell adhesion. Poly(2-hydroxyethylmethacrylate) (pHEMA; from Sigma Aldrich) coated polystyrene plates were used as anti-adhesive controls and represent 0% of cell adhesion. A suspension of hMSCs at a density of 10×10^4 cells/mL was prepared and 500 mL of this solution was seeded on the appropriated *substratum* and incubated 24 h at 37 °C.

24 h post-seeding, a resazurin assay was performed by removing the extracts from each cell culture, washing them with PBS and replacing them with the same medium containing 10% of resazurin. After 3 h of incubation at 37 ºC with the resazurin solution, 100 μl were transferred into a 96-well plate and the fluorescence intensity was measured (λ_{ex}= 530 nm, λ_{em}= 590 nm) using a Synergy Mx (BioTek). For these experiments, a minimum of four replicates for each condition were used for calculating the percentage of adhered cells.

4.4. Cell Morphology

Cell morphology was examined by optical microscopy. hMSCs were cultured on HPCi and HPCa films for 48 h. Glass coverslips were used as positive control for cell adhesion and spreading and pHEMA coated polystyrene plates were used as controls resisting cell adhesion. pHEMA has been commonly used for contact lens and intra-ocular implants and it is known to prevents cell adhesion and spreading [146-152].

0, 4, 12, 24 and 48 h post-seeding photographs were taken on the HPCi and HPCa films, coverslips and pHEMA substrates.

A fluorescent staining of actin micro filaments and DNA were performed to ensure that adherent cells were being observed over the HPCa films. Cells were fixed with 4% formaldehyde in phosphate-buffered saline (PBS) for 15 min and then permeabilized with 0,1% Triton X-100 in PBS for 5 min. The nucleus was visualized using DAPI (4,6 –Diamidina-2-phenylin, Sigma) and F-actin filaments were visualized using Alexafluor 488-phalloidin.

4.5. Cell Proliferation

hMSCs were cultured on HPCi and HPCa films, glass coverslips and pHEMA films for 24 and 48 h. Tissue culture polystyrene dishes were coated with a sterile pHEMA solution and dried for 48 h at 37°. Cells cultured on glass coverslips were removed by incubation with 0.25% trypsin–EDTA (Gibco Invitrogen) for 10 min at 37°C. The trypsin was then neutralised with fresh DMEM containing FBS and the dishes were rinsed two times with DMEM. These cells, as well as the cells cultured on HPCi, HPCa and pHEMA films, were collected to eppendorfs and centrifuged for 5 min at 800 g. Then, the extracts were removed and the pellet was suspended in 500 μL trypsin–EDTA for 5 min at 37°C to

dissociate cell aggregates. DMEM with FBS was added to neutralise trypsin and the viable cells were counted by trypan blue exclusion (Sigma Aldrich).

Cell proliferation corresponds to N/N_0 ratio, where N is the total number of cells at T = 24 h or T =48 h and N_0 is the number at T = 0.

4.6. Cell viability

Cell viability was assessed by trypan blue exclusion (Sigma Aldrich) for cells cultured on HPCi and HPCa films, coverslips and pHEMA films at 24 and 48 h post-seeding. Trypan blue is a stain widely used in dye exclusion procedures for viable cell counting. This method is based on the principle that live (viable) cells do not take up certain dyes, whereas dead (non-viable) cells do. Cell viability was express applying the following equation:

$$\text{Cell viability } (\%) = \frac{\text{Number of live cells}}{\text{Total number of cells}} \times 100 \qquad \textbf{Equation 4}$$

4.7. Environmental Scanning Electron Microscopy

The Environmental Scanning Electron Microscopy (ESEM) retains all of the performance advantages of a conventional SEM but present many advantages toward it. The main advantage is allowing the microscope to adapt the sample environment through a range of temperatures, pressure and gas compositions. The samples do not have to be prepared or modified and can be examined in their natural state [134, 153].

Secondary electron images of the HPCa surface were obtained with an ESEM after the cell cultures. This study was out of the scope of the present work. However, it could be important to understand what happens on the surface of these films after being in contact with cells and culture medium. This test was only performed on HPCa films because it is more interesting to investigate the effect of the bands formed during the preparation of this film.

5. Statistical verification of results

All data present are reported as mean ± the standard deviation and were analysed using the Mann-Whitney U test. Differences between groups were considered statistically different when $p<0.05$. All data was analyzed using SPSS software.

Chapter III – RESULTS AND DISCUTION

1. Characterization

Several techniques were used to study the optical and mechanical properties of HPC films and to investigate their surface properties. The surfaces of HPCi and HPCa films were analyzed by Fourier transform infrared (FTIR) spectroscopy, X-ray photoelectron spectroscopy (XPS), contact angle measurements, scanning electron microscopy (SEM) and atomic force microscopy (AFM). Contact angle measurements were used to measure the surface wettability of the samples. FTIR was used to acquire information on the functional groups and chain order/crystalline structure and XPS was used to investigate the chemical composition of surfaces. SEM and AFM were used to obtain information of the surface morphology and topography.

1.1. Optical polarizing microscopy

HPCi films, prepared from the isotropic (30 wt%) cross-linked solutions, does not present optic birefringence and a dark field could be seen when they were observed on an optical polarizing microscope. A representative image is shown in the Fig. 3.1a.

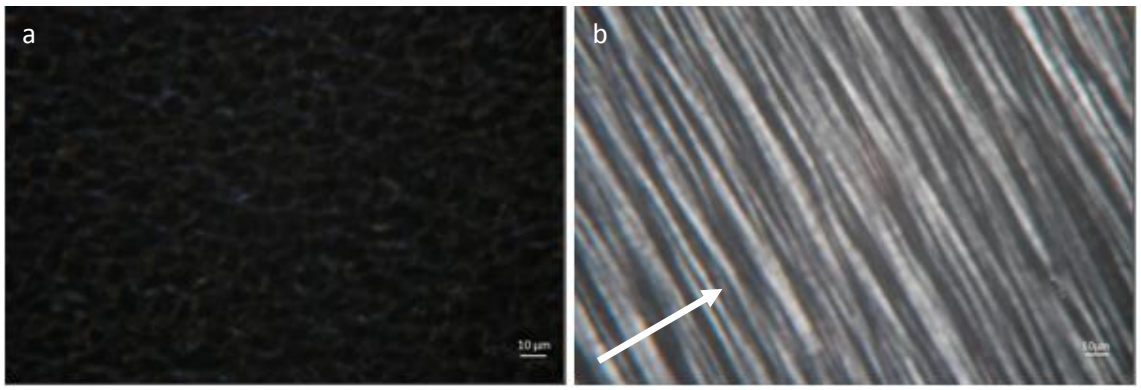

Figure 3.1 – (a) HPCi and (b) HPCa films. Arrow indicates the direction of films spreading.

The optical anisotropy of HPCa films, prepared from the chiral nematic (60 wt%) cross-linked solutions, can be detected by observing the films between cross polarizers. Photographs of the band texture formed during the shear were easily obtained from polarized light transmission microscopy. A representative image is shown in the Fig. 3.1b. All observations were performed at room temperature.

1.2. Determination of the gel fraction

For HPCi and HPCa, the gel fractions are 92% and 89%, respectively. The gel fractions are high and there are no significant differences between the 2 films. These high values show the high reactivity of isocyanate groups and their tendency to bind chemically the hydroxyl groups to form urethane linkages. High gel fractions are indicative of good structural stability, essential for the application in study.

1.3. Mechanical properties of the dried and wet films

The mechanical properties of HPC films were investigated. For each HPC film, the mechanical properties were analysed in the direction of the film spread (λxx‖) and perpendicularly to that direction (λyy⊥). This data allows the comparison of the Young modulus between the films and between both directions examined. The mechanical properties measured are summarized in Table 3.1 and the typical stress-strain curves for HPC films under dry and wet conditions are presented in Figs. 3.3a and 3.3b, respectively.

The tests performed in dry films revealed that the higher stress values were supported by the HPCa film in the direction of the film spreading, reaching 62.5 MPa. The differences between the stress-strain behaviour of dry and wet HPC films are significant. Comparing with dry conditions, HPC films under wet conditions revealed lower break stress values (4.6 – 14.6 MPa) except for HPCa Film λyy⊥ which was similar in dry and wet states and higher elongation values, except for HPCa Film λxx‖.

Fig. 3.2 represents the directions used to measure the mechanical behaviour of HPC films.

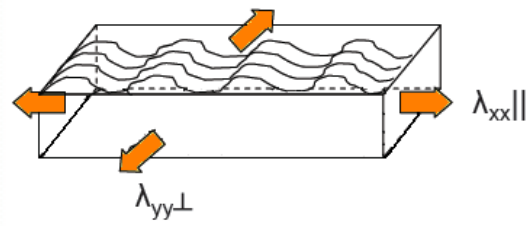

Figure 3.2 – Schematic representation of the directions used to measure the mechanical behaviour of HPC films.

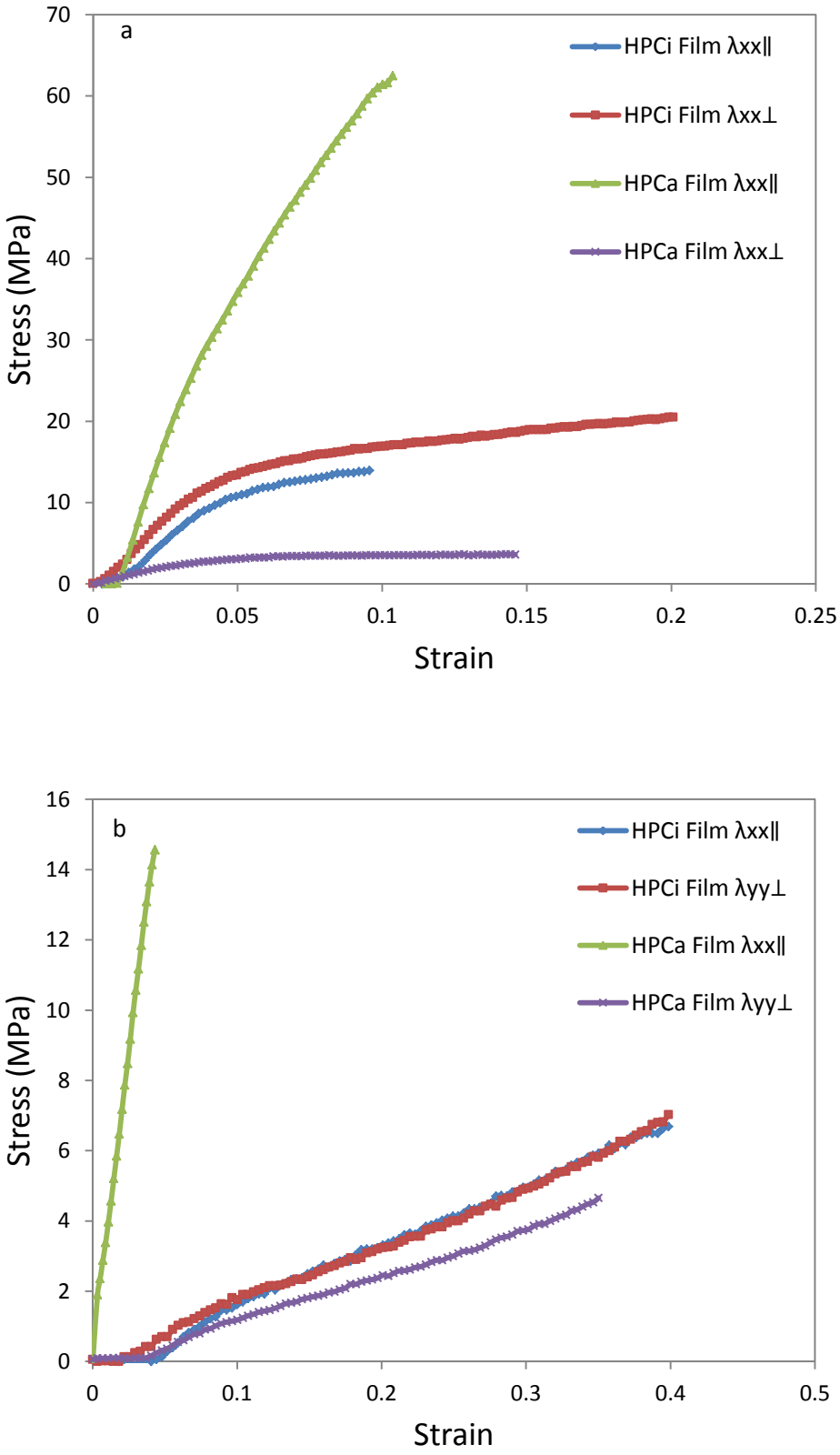

Figure 3.3 – Typical stress-strain curves of HPCi and HPCa solid films recorded at 25ºC. (a) dry conditions; (b) wet conditions.

Table 3.1 – Average values for the Young's modulus obtained for HPC films for various HPC concentration ratios and different directions.

HPC Films	Young's Modulus (MPa)	
	Dry state	**Wet state**
HPCi Film λxx‖	319.8 ± 26.2	27.9 ± 0.3
HPCi Film λyy⊥	339.6 ± 34.2	24.9 ± 1.3
HPCa Film λxx‖	1199.3 ± 136.7	341.2 ± 20.7
HPCa Film λyy⊥	92.7 ± 14.8	15.1 ± 3.9

Statistical analyses (SPSS software) allow to consider that, in dry conditions, there were no statistically significant differences between the Young's modulus of

HPCi films λxx‖ and λyy⊥ was not statistically significant, but there were significant differences between

HPCa films λxx‖ and λyy⊥,

HPCi films λxx‖ and HPCa films λxx‖, and

HPCi films λyy⊥ and HPCa films λyy⊥.

Also, statistical analyses revealed that, in wet conditions, again there were no statistically significant differences between the Young's modulus of

HPCi films λxx‖ and λyy⊥.

However, as in dry conditions, differences were significant between

HPCa films λxx‖ and λyy⊥, between

HPCi films λxx‖ and HPCa films λxx‖, and between

HPCi films λyy⊥ and HPCa films λyy⊥.

The mechanical anisotropy of HPCa films can be easily observed. The Young modulus between HPCa film λxx‖ and HPCa film λyy⊥ was significantly different. On the other hand, the mechanical isotropy of HPCi films was also observed. The Young modulus between HPCi film λxx‖ and HPCi film λyy⊥ was similar. As expected, the Young's modulus values are lower in wet state than in dry state.

1.4. Contact Angle Measurements

Some pictures were taken during the experience to show that surfaces are wetted by water (Fig. 3.4).

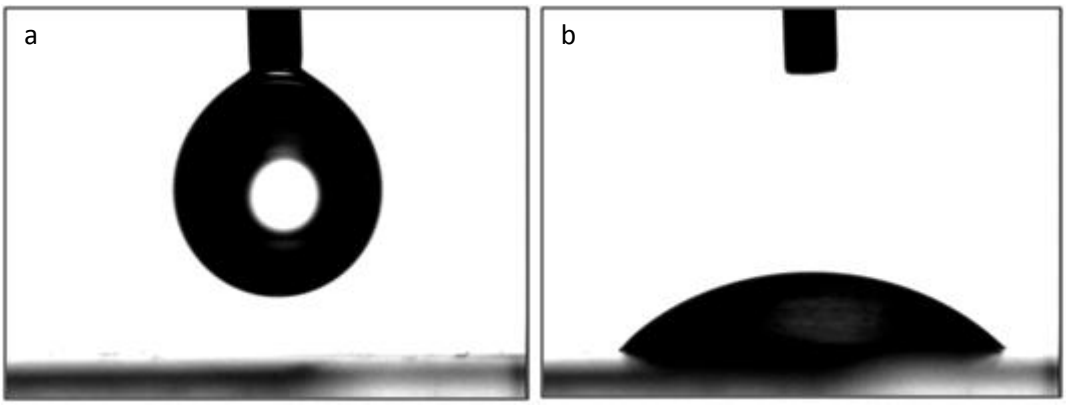

Figure 3.4 – Measurement of the water contact angle on a HPC film: (a) pendant drop, (b) water drop wetting the HPC surface.

The contact angles obtained for HPCi and HPCa films are shown in Fig. 3.5 and in Table 3.2.

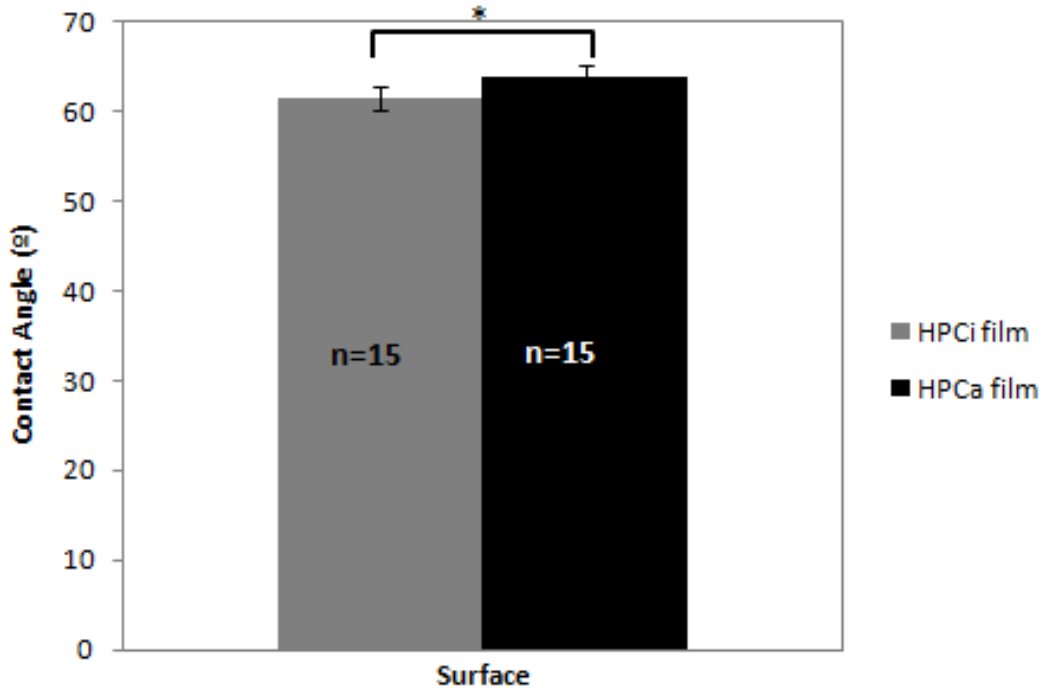

Figure 3.5 – Contact angle measurements on HPCi and HPCa films. (* means statistically significant difference; p<=0.05).

Table 3.2 – Contact angle measurements on HPCi and HPCa films.

	Mean Angle (°)	Standard Deviation (°)
HPCi Film	61.5	1.3
HPCa Film	63.8	1.5

The surface wettability was determined by the water contact angle. This angle was 61.5 ° for HPCi films and 63.8 ° for HPCa films. These differences between contact angles obtained were found to be statistically significant, although values for both films were similar. It can be considered that HPCi film is a little more hydrophilic than the HPCa film.

1.5. Chemical characterization of surfaces

1.5.1. Fourier Transform Infrared (FTIR) Spectroscopy

The IR *spectra* were used to verify if the cross-linking reaction of HPC was successful and to characterize the HPC cross-linked films (HPCi and HPCa). FTIR *spectra* of HPC (provided by the manufacturer), diisocyanatohexane, HPCi and HPCa films are shown in Figs. 3.6 and 3.7. The *spectra* of HPC and cross-linked HPC films were compared.

Fig. 3.6a shows the FTIR *spectrum* of HPC. The *spectrum* of HPC shows a strong absorption band at 3442 cm^{-1} due to the stretching of the -OH group, and another at 2963 and 2877 cm^{-1} from the C-H stretching vibration. The bands around 1457 and 1378 cm^{-1} are assigned to $–CH_2$ scissoring and -OH bending vibration, respectively. The band observed at 1084 cm^{-1} is due to the presence of C-O-C stretching vibrations of the cellulose chain.

The reaction of the hydroxyl groups of hydroxypropylcellulose with the isocyanate group of diisocyanatohexane occurs during the cross-linking process. Fig. 3.6b shows the FTIR *spectrum* of diisocyanatohexane provided by the manufacturer. The peak at 2270 cm^{-1} corresponds to the (–N=C=O–) isocyanate group.

It is possible to identify the characteristic HPC bands in the *spectra* of HPCi and HPCa films (Fig. 3.7). None of these *spectra* presented the characteristic peak from isocyanate group (–N=C=O–) at 2270 cm^{-1}, indicating the absence of unbound isocyanate groups. However, three new bands can be easily identified at 3332 cm^{-1}, 1618 cm^{-1} and 1587 cm^{-1} from the N-H group, which was initially

absent in HPC (Fig. 3.6a), indicating the formation of the urethane (NHCO) group resultant from the reaction of hydroxyl and isocyanate groups. The peak at 3420 cm^{-1} from the stretching of the O-H bond remains in the *spectra* indicating that –OH groups did not react completely with the diisocyanatohexane, as expected.

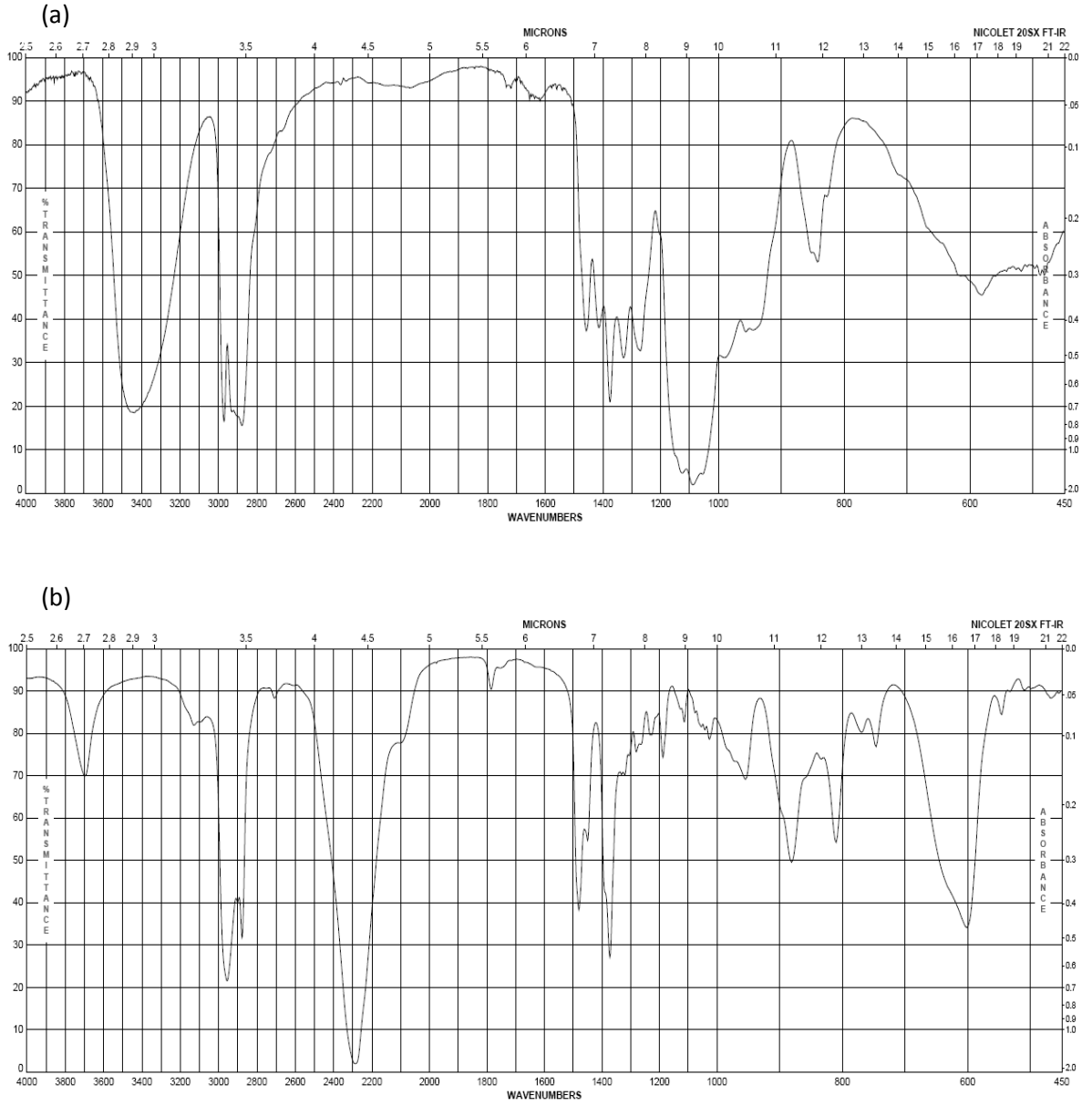

Figure 3.6 – FTIR *spectra* of (a) HPC and (b) diisocyanatohexane provided by the manufacturer [154].

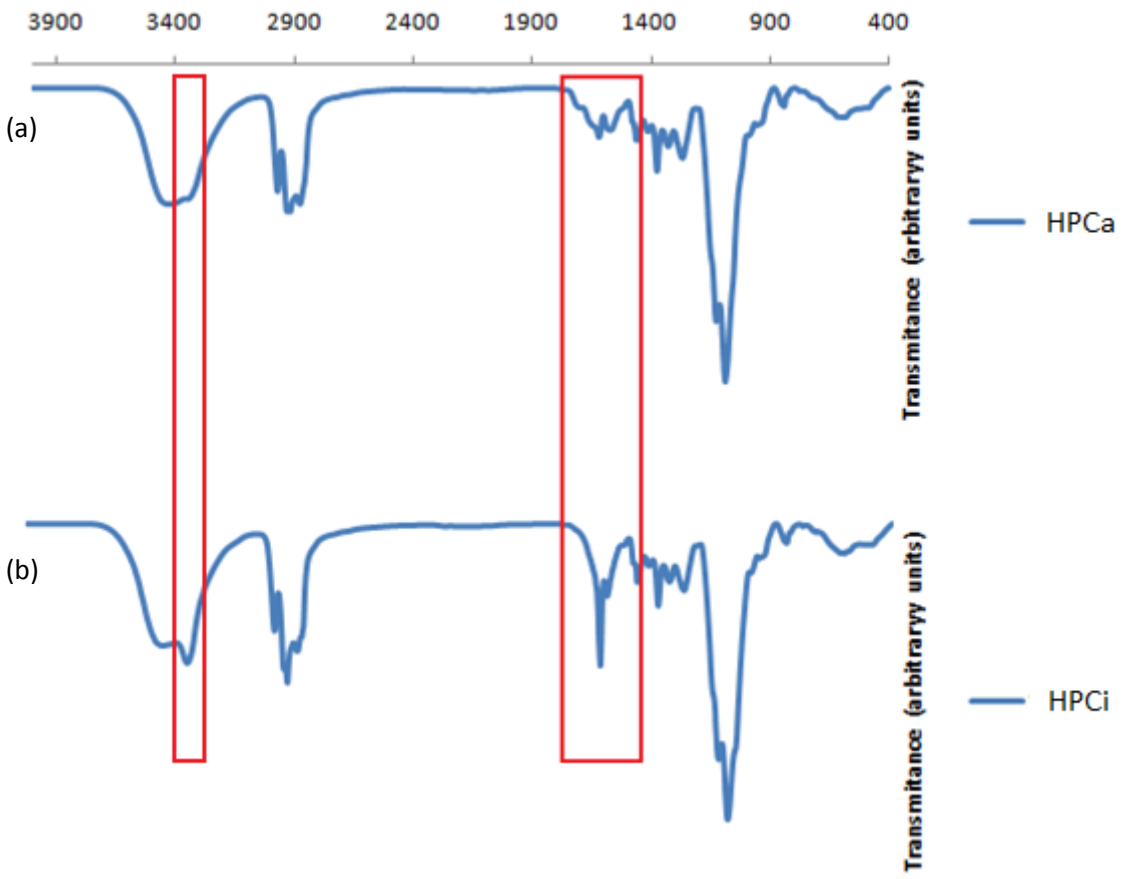

Figure 3.7 – FTIR *spectra* of (a) HPCa and (b) HPCi films, evidencing the presence of the N-H groups resultant from the cross-linking of HPC molecules.

As observed, new peaks appeared on the *spectra* of HPCi and HPCa films, showing that the cross-linking reaction was successful.

1.5.2. X-ray Photoelectron Spectroscopy (XPS)

XPS was used to determine the chemical composition of the films surfaces. Fig. 3.8 shows the *spectra* of the HPCi and HPCa films and Fig. 3.9 and Table 3.3 indicate their elemental compositions. The *spectrum* in Fig. 3.8a corresponds to the HPCi films and the *spectrum* in Fig. 3.8b corresponds to the HPCa films.

All binding energies were referenced by setting the maximum of the resolved C(1s) peak, corresponding to carbon in a hydrocarbon environment (CH_x), to 285.0 eV.

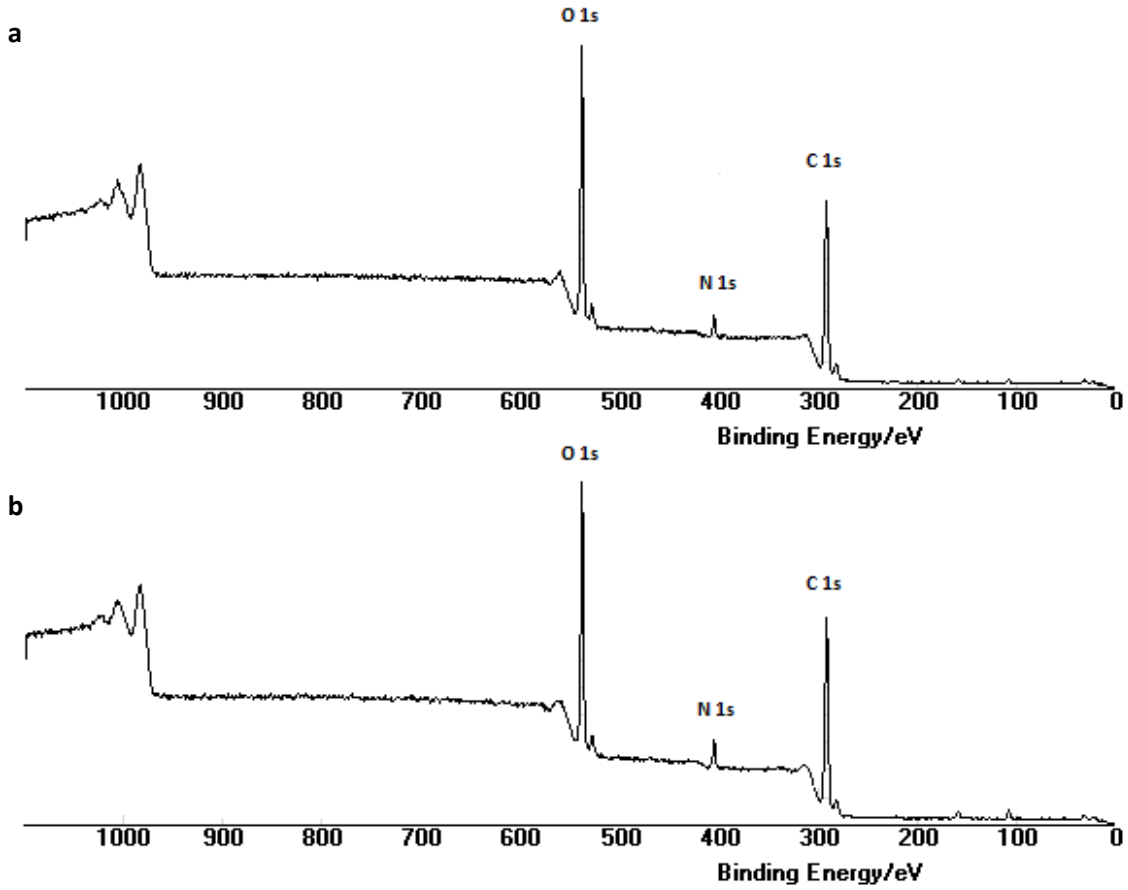

Figure 3.8 – XPS *spectra* of (a) HPCi and (b) HPCa films.

The XPS *spectra* (Fig. 3.8) showed, as expected, that only carbon (C), nitrogen (N) and oxygen (O) were present on the surfaces of HPCi and HPCa films.

Elemental atomic percentages were calculated from the integrated intensities of the XPS peaks, taking into account the atomic sensitivity factors of the instrument data system. Fig. 3.9 shows the elemental compositions of HPC films and their respective atomic concentrations. For the HPCi film, the atomic percentage was 67.8 % C, 3.8 % N and 28.5 % O. For the HPCa film, the atomic percentage was 67.3 % C, 3.4 % N and 29.3 % O.

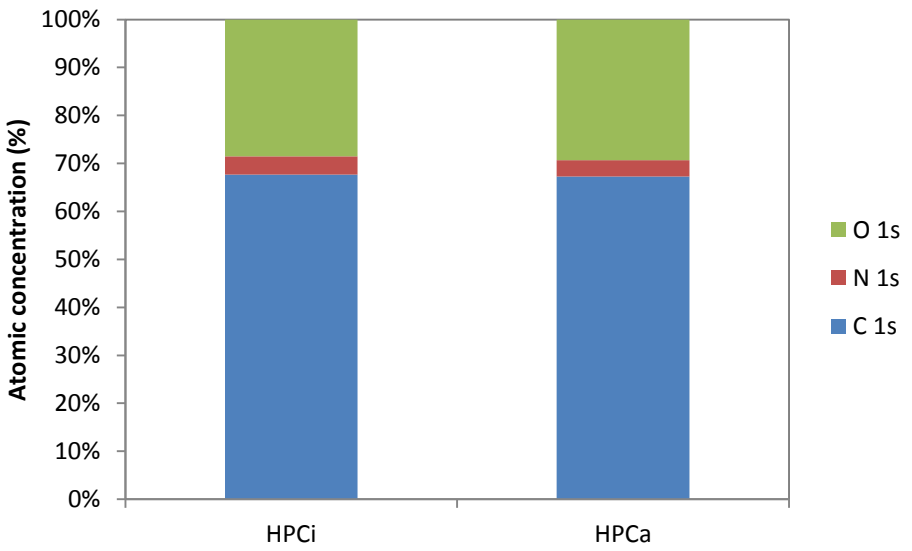

Figure 3.9 – Elemental compositions of HPCi and HPCa films, as determined by XPS.

Table 3.3 – Elemental compositions of HPCi and HPCa films, as determined by XPS.

Element	HPCi	HPCa
C 1s	67.6	67.3
N 1s	3.8	3.4
O 1s	28.5	29.3

The elemental composition of both films was similar, indicating that their chemical surface composition was similar.

The C_{1s}, O_{1s} and N_{1s} core-level *spectra* of the HPCi and HPCa films were also similar and can be compared in Figs. 3.10, 3.11 and 3.12. The resolved C_{1s} *spectrum* of HPCi and HPCa samples revealed three peaks with binding energies of 285.0 eV, 286.2 eV and 288.4 eV. The C_{1s} peak at 285.0 eV was mainly assigned to –CH_2– chemical bindings. The peak at 286.2 eV was assigned to C–O, C–OH and C–N–C=O and the peak at 288.4 eV to O–C–O and N–C=O chemical bindings (Fig. 3.10). [155-158]

a

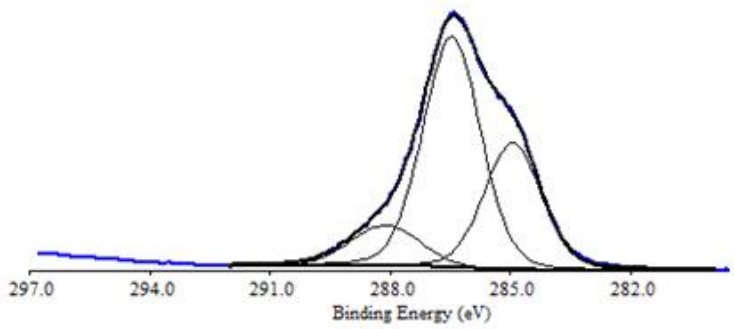

b

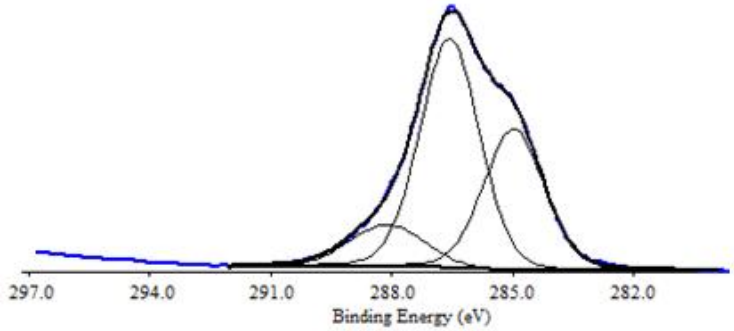

Figure 3.10 – C_{1s} *spectra* of (a) HPCi and (b) HPCa films.

The O_{1s} core-level *spectra* of the HPCi and HPCa samples can be curve-fitted into three peaks (Fig. 3.11) with binding energies of 531.1 eV, 532.8 eV and 534.2 eV, corresponding to N–C=O, C–OH and O–C–O chemical bindings, respectively [156, 158].

a

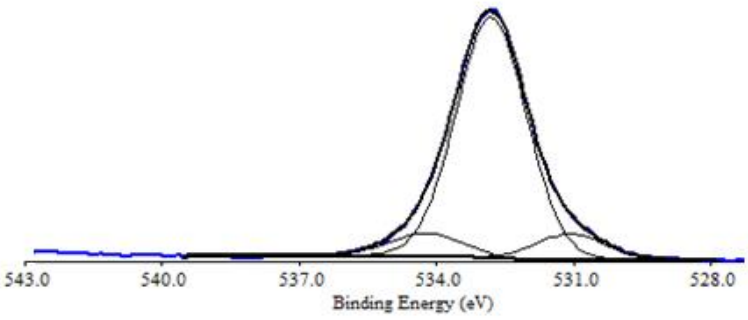

b

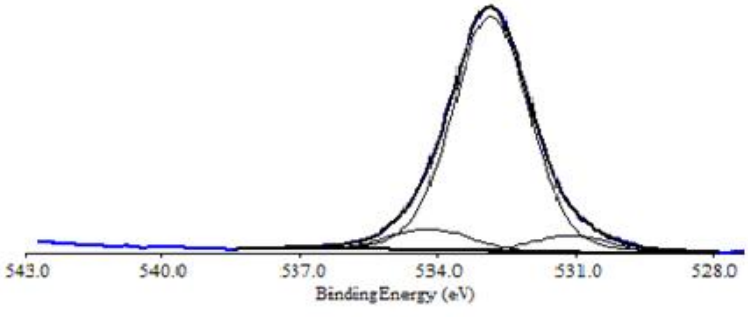

Figure 3.11 – O_{1s} *spectra* of (a) HPCi and (b) HPCa films.

The resolved N 1s core-level *spectra* of the HPCi and HPCa sample can be curve-fitted into one peak (Fig. 3.12) with binding energy of 399.6 eV, corresponding to N–C=O chemical bindings.

a

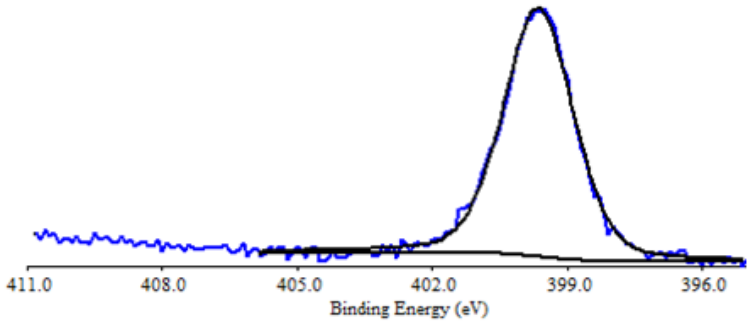

b

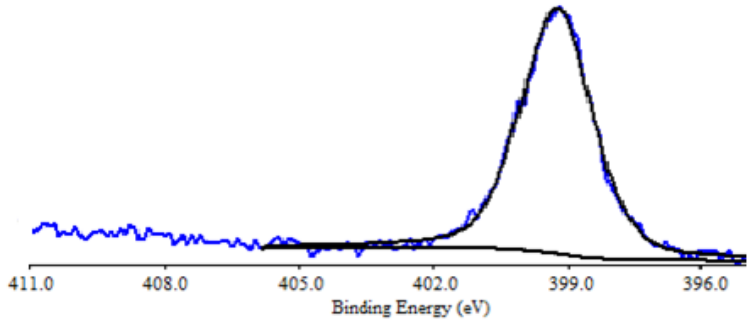

Figure 3.12 – N_{1s} *spectra* of (a) HPCi and (b) HPCa films.

Overall, the XPS *spectra* of HPCi and HPCa films were similar, showing that there is no chemical difference between their surfaces.

1.6. Scanning Electron Microscopy (SEM)

Fig. 3.13 shows SEM images of the HPCi and HPCa samples. The arrow, present in some figures, indicates the direction of the film spreading.

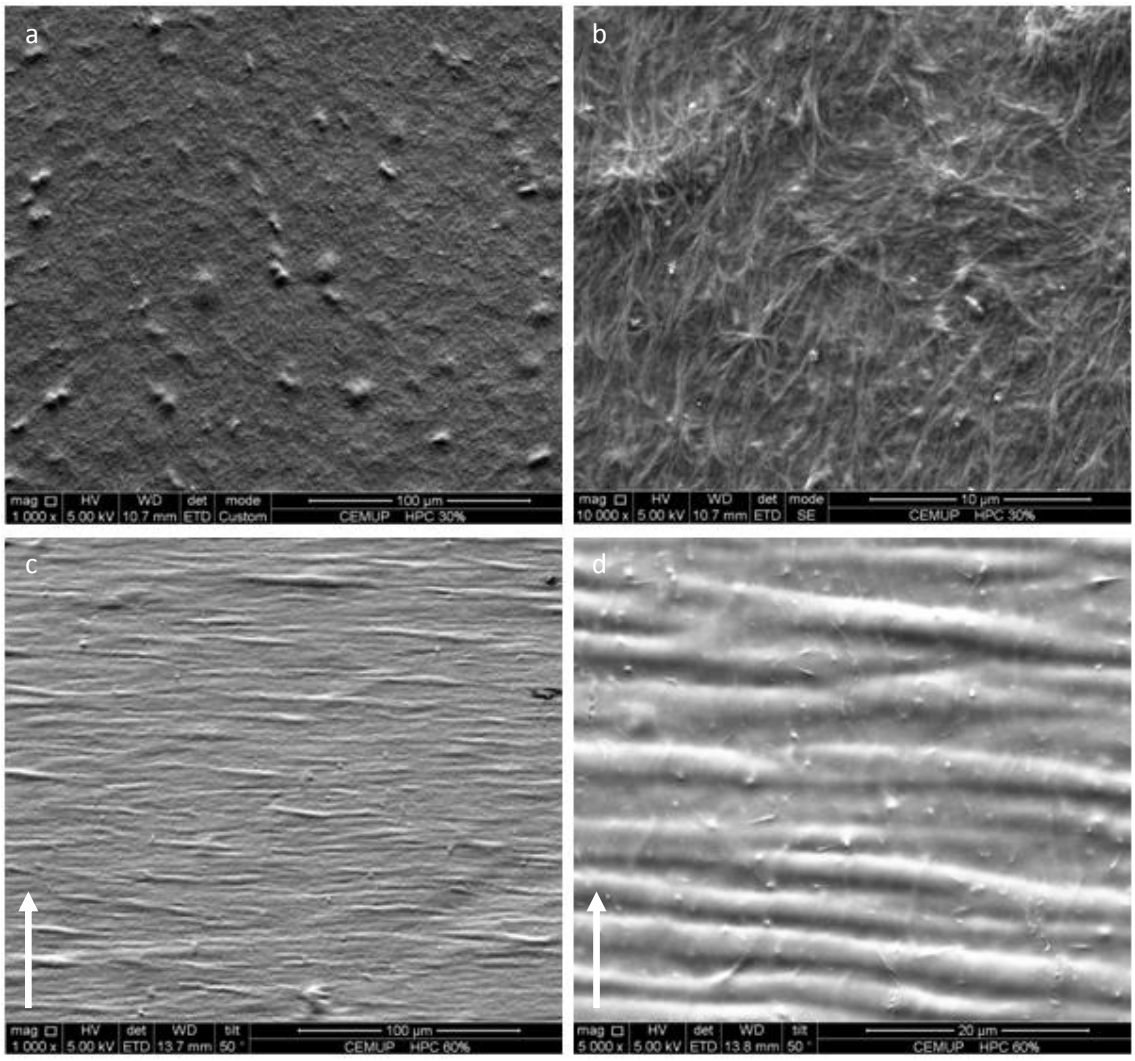

Figure 3.13 – (a) HPCi film (magnification: 1000x); (b) HPCi film (magnification: 10000x); (c) HPCa film (magnification: 1000x; arrow represents shear force direction); HPCa film (magnification: 5000x; arrow represents shear force direction).

It is easy to conclude that the HPCi film did not exhibit any periodicity (Figs. 3.13 a and b). By observing Figs. 3.13 c and d, the formation of banded textures in HPCa film samples obtained from aqueous hydroxypropylcellulose liquid crystalline solutions subjected to shear was confirmed. The periodicity of the "principal" bands is around $3\ \mu m$. The Fig. 3.13 d shows two different periodicities: a primary set of "principal" bands, perpendicular to the shear direction and a smoother texture

characterized by a secondary periodic structure containing “secondary” bands. This behaviour has already been reported in the literature [49].

1.7. Atomic Force Microscopy (AFM)

The surface of the film prepared from HPCi solution did not show any periodicity and was not analysed with AFM.

Fig. 3.14 shows a 3D topography image $(40 \times 40\ \mu m^2\ scan)$ of the surface of the film prepared from an anisotropic solution (HPCa) at a spread rate $v = 6\ mm/s$. Bands perpendicular to the spread direction were found and can be seen in Fig. 3.14.

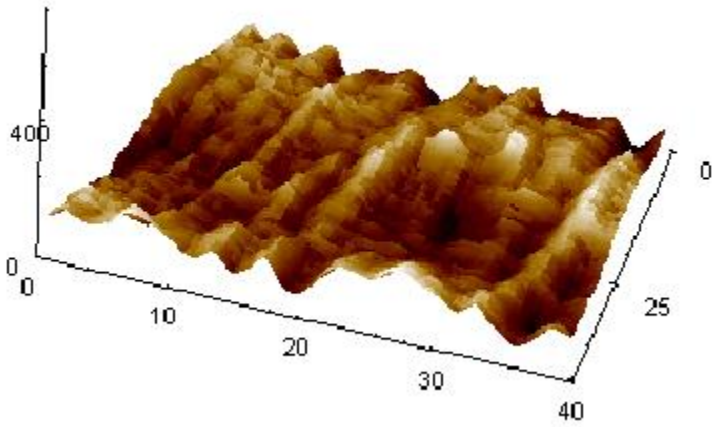

Figure 3.14 – 3D topography image $(40\ \times 40\ \mu m^2\ scan)$ of the HPCa surface.

A top view image of the surface can be seen in the Fig. 3.15. The analysis of the height profile was done by graphic analysis of cross sections: AA’ taken along the spread direction and BB’ taken along the perpendicular direction of the secondary periodic bands.

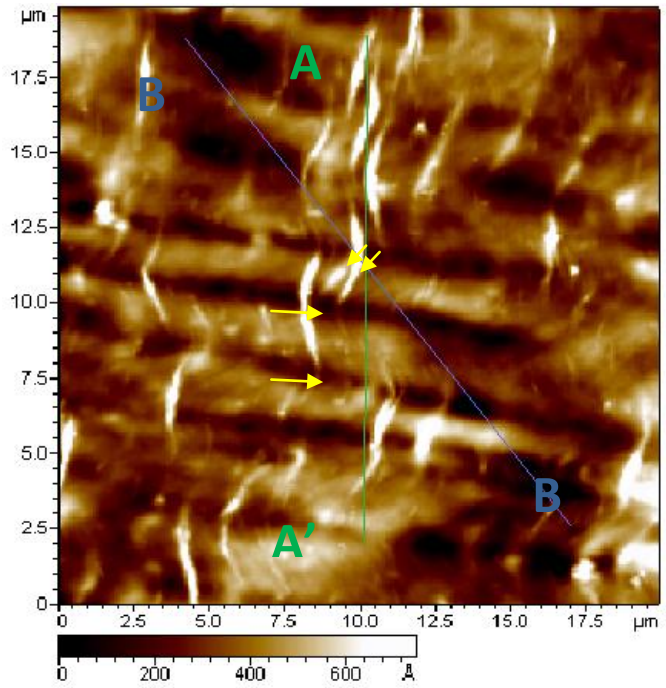

Figure 3.15 – Top view image of the HPCa surface.

The periodicity of the "principal" and "secondary" bands was measured graphically using an image analysis software called Scanning Probe Image Processor. The periodicity Δl_1 and the peak to valley height h_1 of the "principal" bands were determined as shown in Fig. 3.16. The same parameters, Δl_2 and h_2 , were measured for the "secondary" band structures.

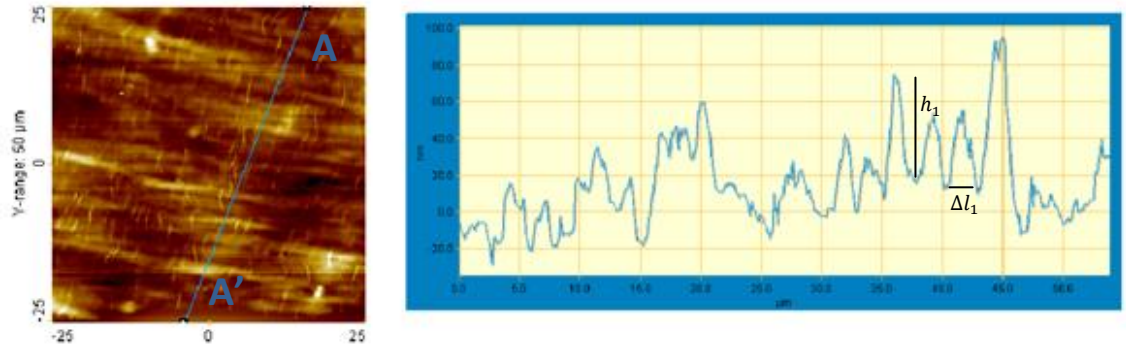

Figure 3.16 – Top view image of HPCa and height profile analysis at the cross sections AA'.

The periodicity of the "principal" bands (perpendicular to the spread direction) was measured and values in the range of $\Delta l_1 = 2.2 - 3.8\ \mu m$ were found. The analysis of the height profile of the same bands showed an average peak to valley height of $h_1 = 63 - 86\ nm$. However, some bands were found outside this range. The "secondary" bands had a periodicity in the range

of $\Delta l_2 = 0.12 – 0.51\ \mu m$. The peak to valley height of these bands was between $h_2 = 2.2 - 4.8\ nm$. The results obtained are summarized in Table 3.4.

Table 3.4 – AFM measurements obtained for HPCa cross-linked films.

solution concentration (% w/w)	60
shear rate (mm/s)	6
$\Delta l_1\ (\mu m)$	2.2–3.8
$h_1\ (nm)$	63–86
$\Delta l_2\ (\mu m)$	0.12–0.51
$h_2\ (nm)$	2.2–4.8
$\Delta \theta_1\ (deg)$	30–33.2

The surface topography of HPCa films was characterized and two periodic set of bands were identified and measured. The values obtained in Table 3.4 are similar to those found in the literature, for the same polymer concentration and a similar shear rate [49].

2. Biological characterization

2.1. Cytotoxicity Assay

The results can be seen in Fig. 3.17.

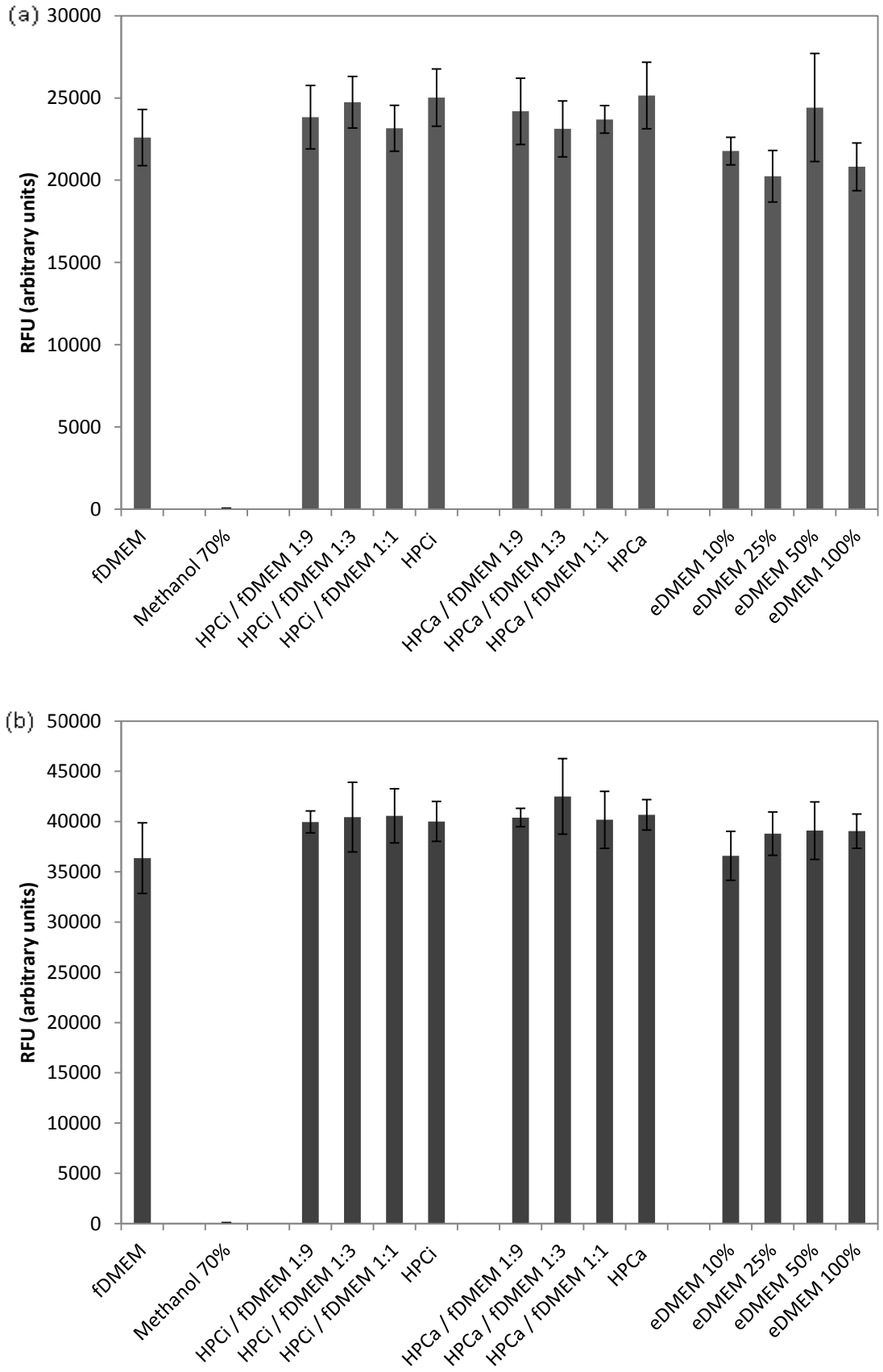

Figure 3.17 – Tests for *in vitro* cytotoxicity after (a) 24h and (b) 72h (where fDMED means fresh DMEM and eDMEM means extracted DMEM).

Statistical analysis of data from Fig. 3.17 indicates that, after 24h and 72h, metabolic activity of hMSCs in contact with:

fDMEM and HPCi extracted liquid was not statistically significant ($p>0.05$);

fDMEM and HPCa extracted liquid was not statistically significant ($p>0.05$);

fDMEM and eDMEM was not statistically significant ($p>0.05$);

fDMEM and methanol 70% was statistically significant ($p<0.05$).

The results showed that HPCi and HPCa films did not induce significant changes in cell viability and metabolic activity. Tests for *in vitro* cytotoxicity after 24h and 72h revealed that no cytotoxic compounds were released from the films. These results are in agreement with the literature [159].

2.2. Cell Attachment

The percentage of cells that attached to HPC films were compared with the 100% positive adhesion control performed on glass coverslips.

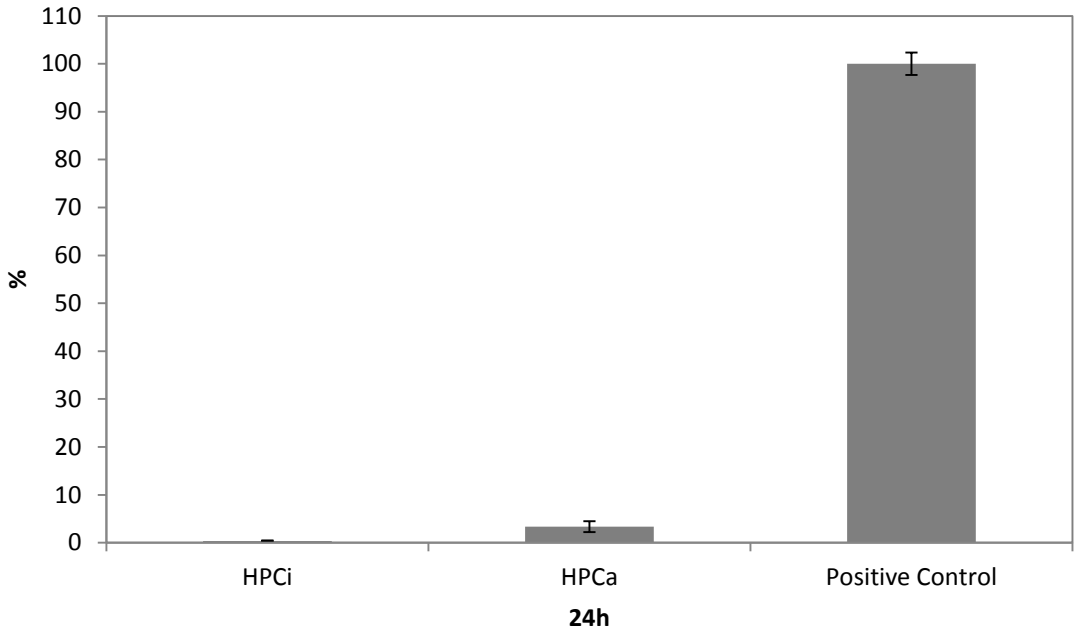

Figure 3.18 – Percentage of cell attachment on HPCi and HPCa films.

While glass coverslips promote cell attachment, cells seeded onto HPCi and HPCa (anti-adhesive surfaces) cannot find anchorage sites and then aggregate. These results are in agreement with the literature. Some studies performed on cellulose and cellulose derivatives *substrata* revealed a similar behaviour [88, 160].

Statistical analyses of cell attachment data shows that, after 24h post-seeding, the percentage of cell attachment between:
HPCi and HPCa films was statistically significant ($p<0.05$);
HPCi films and positive control was statistically significant ($p<0.05$);
HPCa films and positive control was statistically significant ($p<0.05$).

The percentage of cell attachment on HPCi and HPCa films was lower when compared with positive control (100%). However, the percentage of cell attachment on HPCa films was higher than on HPCi films. These results are supported by the images acquired during the first 24 hours post-seeding.

It is well known that the interactions of cells with materials depend on interfacial physico-chemical properties that modulate the responses of cells [65, 66, 68, 70]. As seen previously, the FTIR analysis revealed that there are still many hydroxyl (-OH) groups on the surface of HPCi and HPCa films. It was also discussed before that highly hydrophilic surfaces (with many hydroxyl -OH groups) have a strong propensity to inhibit cell adhesion. Another possible reason to explain the low percentage of cell adhesion on HPCi and HPCa films is the charge of the surface. Electro Kinetic Analysis (EKA) was not performed in this study, but the charge of the surface of HPC films is expected to be negative [161], which also contributes to inhibit cell adhesion.

In fact, adsorbed protein films are, in themselves, reasonable non-fouling surfaces with regard to other proteins. For example, albumin coating has long been considered to passivate polymer surfaces since a preadsorbed layer of albumin inhibits subsequent adhesion of fibrinogen, producing a potentially thromboresistive effect [162, 163]. If a layer of albumin is initially adsorbed by the HPC films, for instance, the absorption of other proteins to the surface could be prevented. This phenomenon appears to minimize adhesion and aggregation of platelets avoiding subsequent thrombus formation. However, this is a speculative hypothesis and could be important to perform an EKA and a protein adsorption assay to better understand this phenomenon and these results.

2.3. Cell Morphology

hMSCs were cultured on HPCi, HPCa and pHEMA films and on glass coverslips. The positive control for cell attachment and spreading was the glass coverslip and the anti-adhesive control was pHEMA. hMSCs spread well on coverslips, while presented rounded aggregated morphology when cultured on HPC films and pHEMA (Fig. 3.19). hMSCs aggregates were mostly merged at 12 h.

Photographs were acquired on HPCi films, HPCa films, glass coverslips and pHEMA films after 0 h, 4 h, 12 h, 24 h and 48 h post-seeding.

Images of hMSC morphology after seeding are shown in Fig. 3.19 and confirm that cells were not aggregated at 0 h.

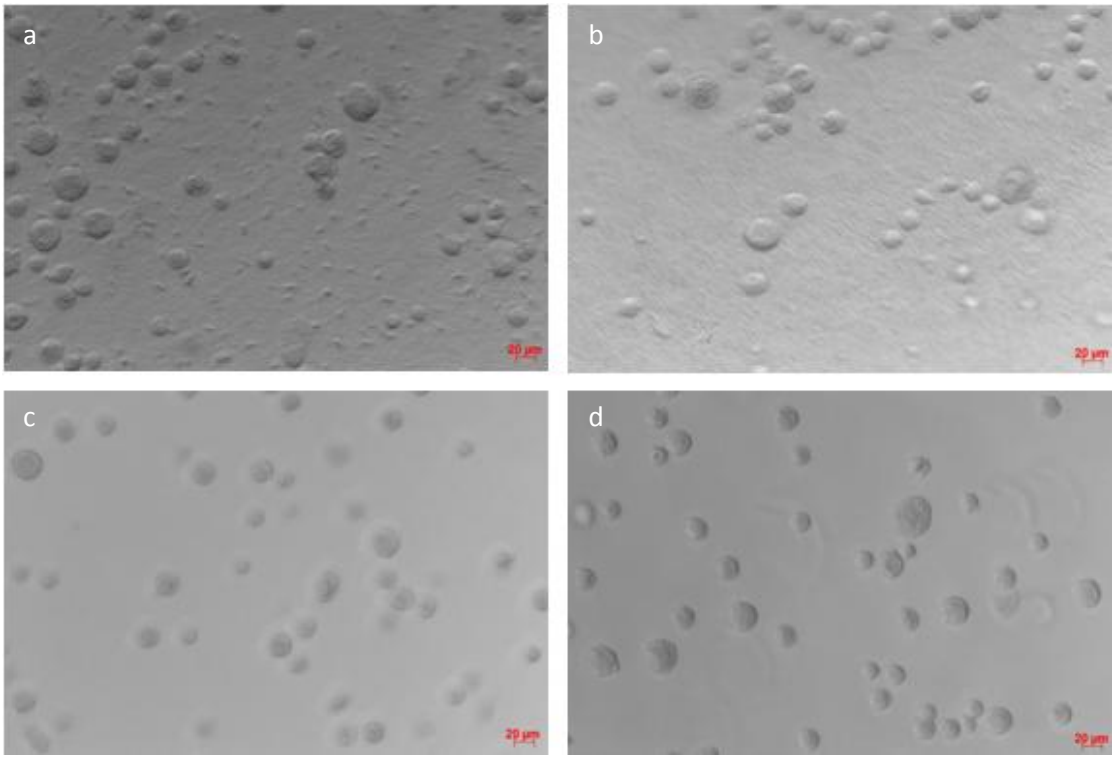

Figure 3.19 – Cell morphology when seeded on (a) HPCi film, (b) HPCa film, (c) coverslip and (d) pHEMA film.

At 4 h, small cell aggregates were formed on HPCi and HPCa films and on the pHEMA film. hMSCs started to spread on the coverslip (Fig. 3.20).

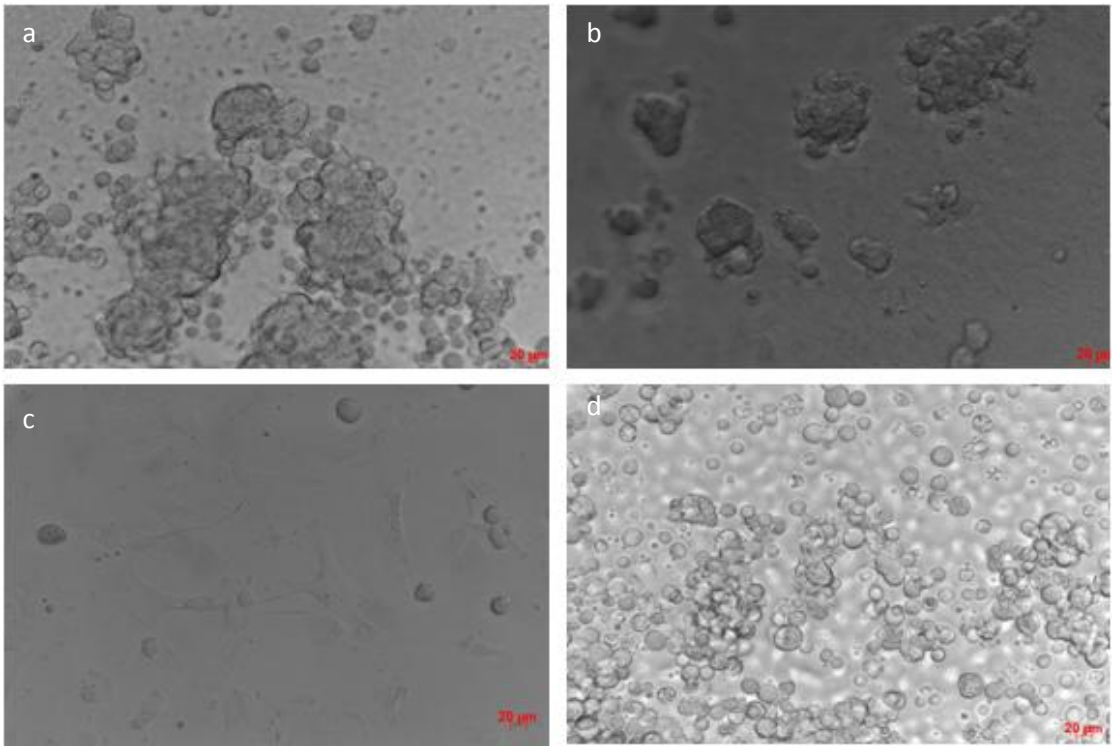

Figure 3.20 – Cell morphology 4 h post-seeding on (a) HPCi film, (b) HPCa film, (c) coverslip and (d) pHEMA film.

12h post-seeding, the aggregates became significantly larger on HPCi and HPCa films and on the pHEMA film. The cells spread well on coverslip, as expected (Fig.3.21).

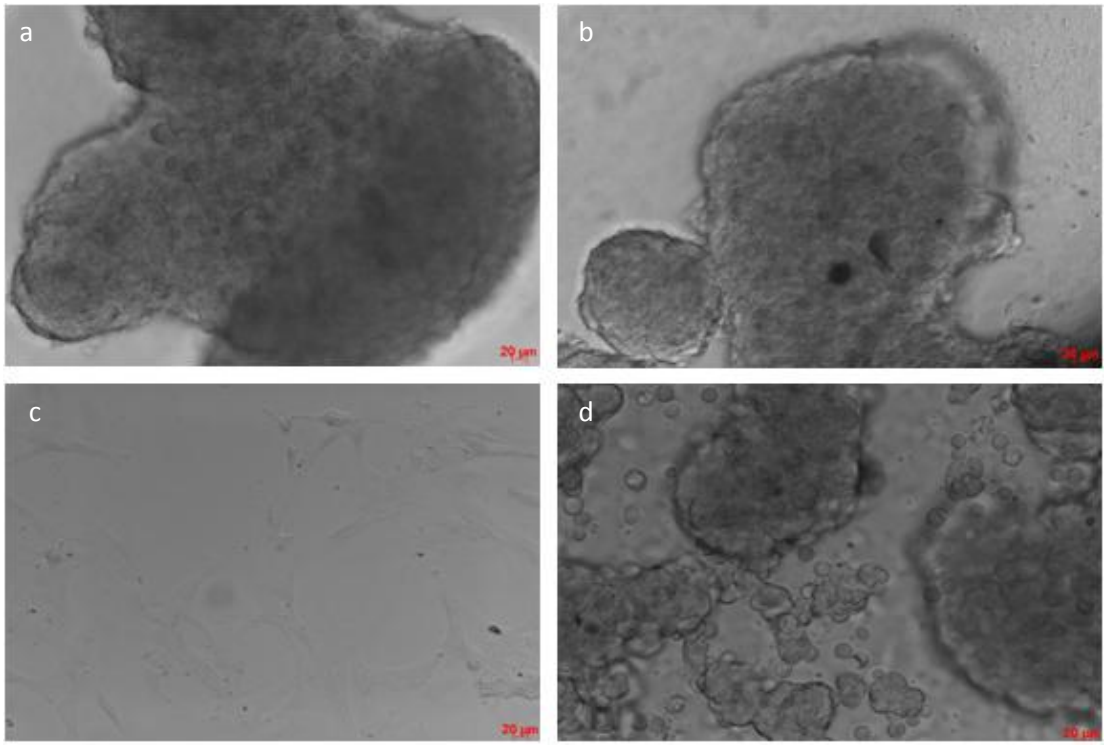

Figure 3.21 – Cell morphology 12 h post-seeding on (a) HPCi film, (b) HPCa film, (c) coverslip and (d) pHEMA film.

After one day (24 h), cells cultured on HPCi and HPCa films and on the pHEMA film formed large aggregates. Cells cultured on coverslip continued to spread and flattened (Fig. 3.22).

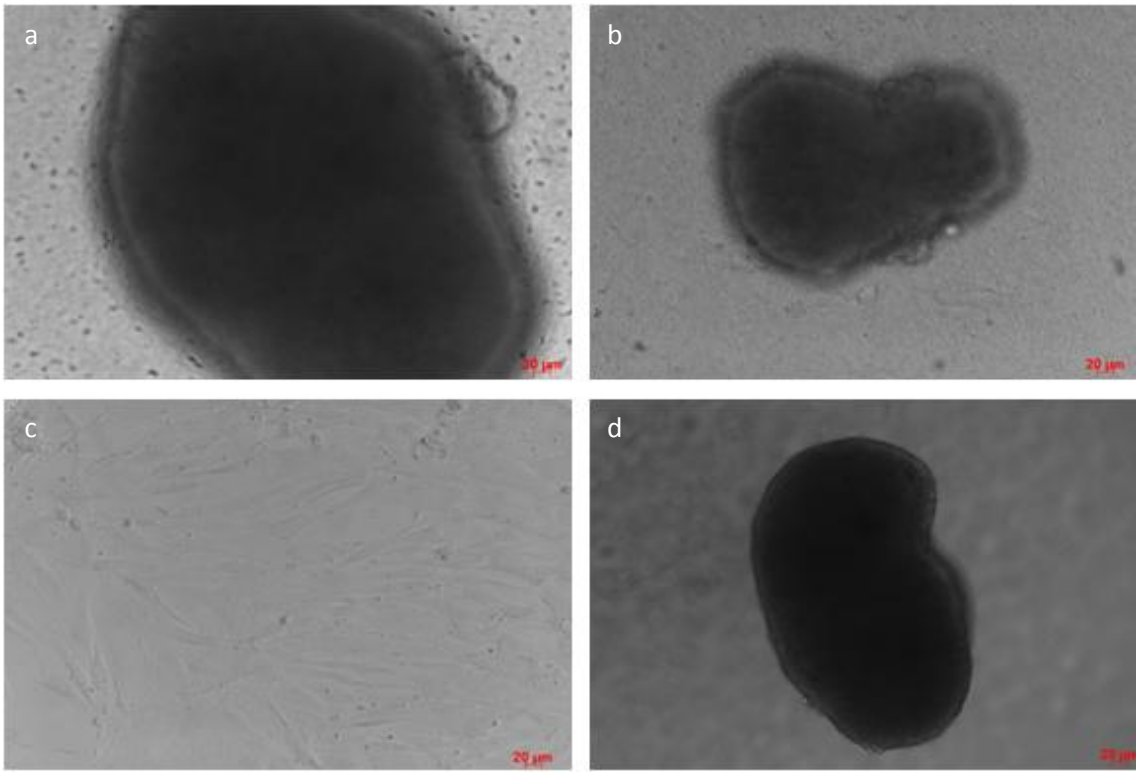

Figure 3.22 – Cell morphology 24 h post-seeding on (a) HPCi film, (b) HPCa film, (c) coverslip and (d) pHEMA film.

Finally, 48h post-seeding the aggregates seemed very similar on HPCi and HPCa films and on the pHEMA film. The number of attached cells on coverslip increased significantly (Fig. 3.23).

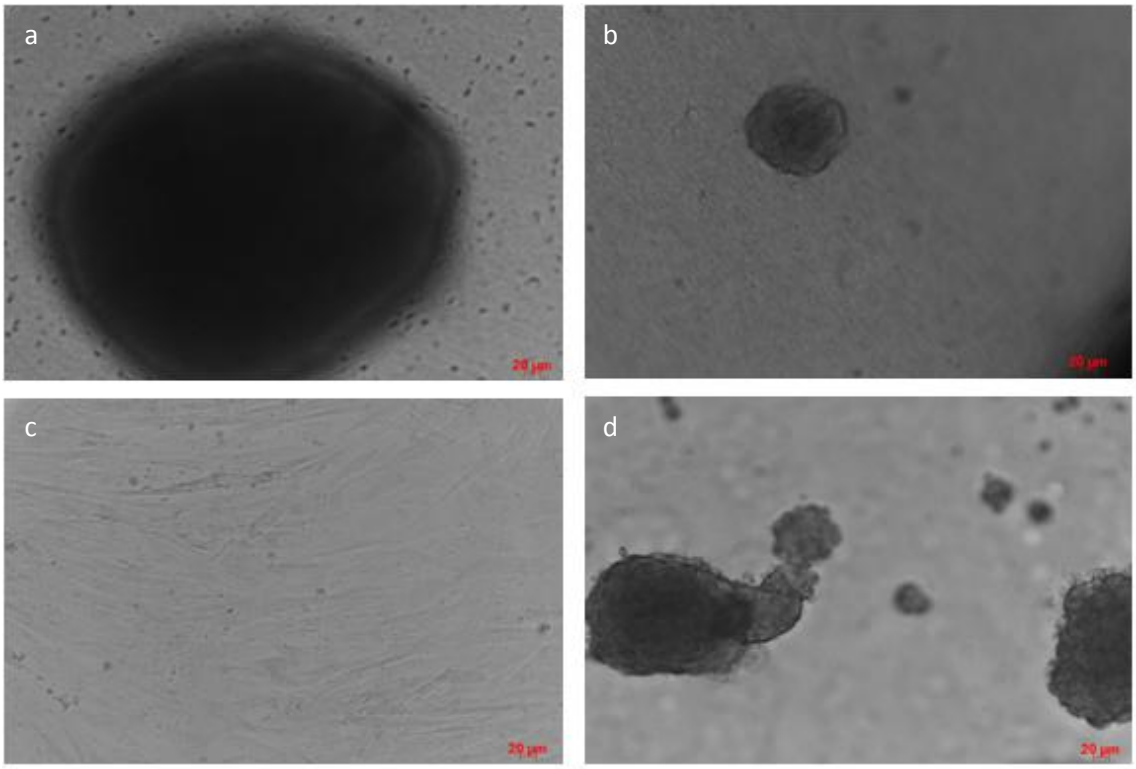

Figure 3.23 – Cell morphology 48 h post-seeding on (a) HPCi film, (b) HPCa film, (c) coverslip and (d) pHEMA film.

The anti-fouling properties of the HPC films were confirmed by direct observation of the cells seeded on surfaces, by optical microscopy. Figs. 3.23 (a) and (b) revealed that cell clusters without any attachment could be observed on HPCi and HPCa film surfaces. The cells have adopted a globular shape, which minimizes the cell/substrate interaction. In contrast, the positive control (glass coverslips) exhibited a strong cell adhesion (Fig. 3.23 (c)). These results are in agreement with the literature. In fact, this behaviour is commonly found on cellulose anti-adhesive *substrata* [88, 160, 164].

After the fluorescent staining of actin micro filaments and DNA some photographs were acquired on HPCa films and on coverslips after 12 h post-seeding (Fig. 3.24).

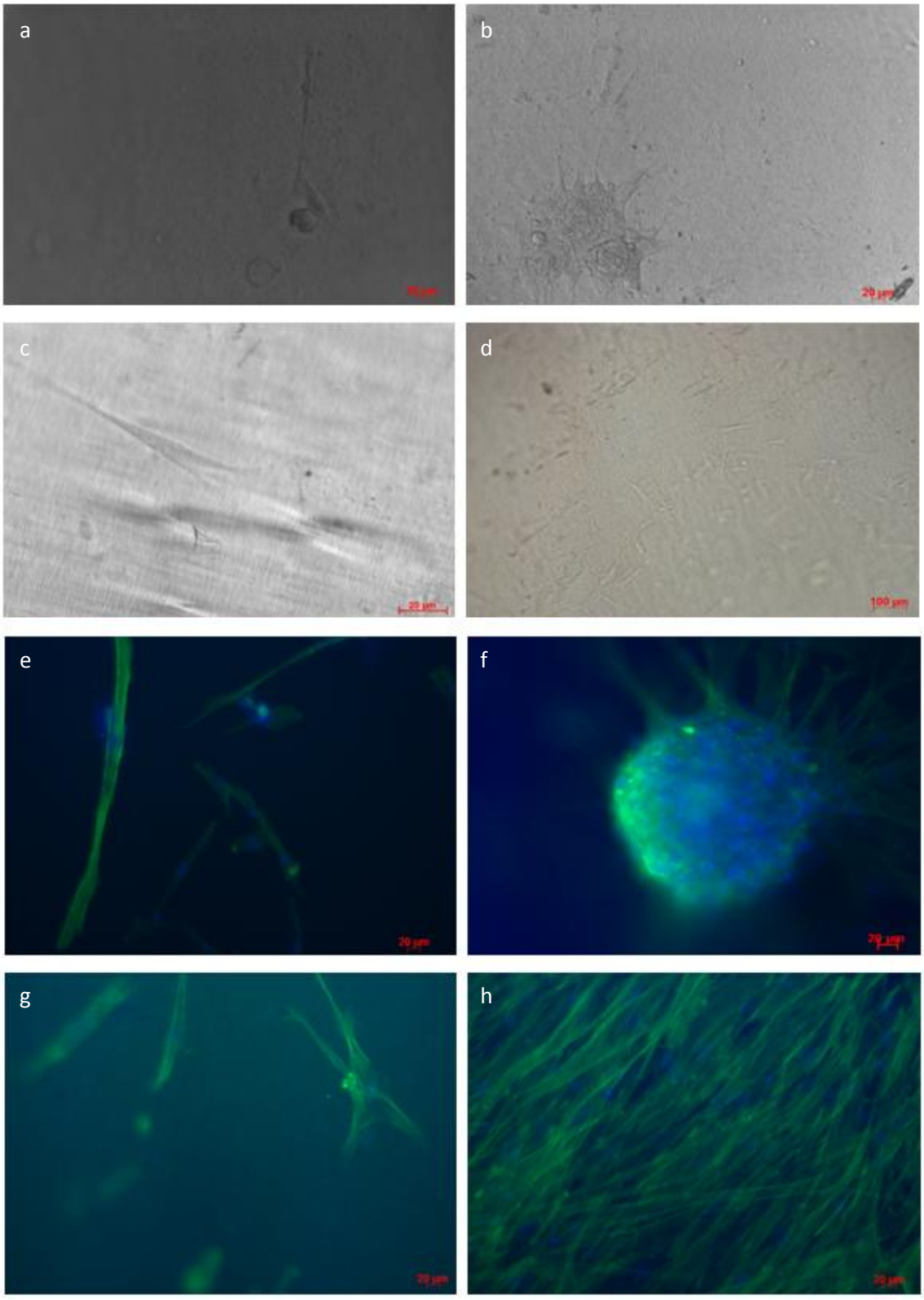

Figure 3.24 – Cell morphology 12 h post-seeding on (a-d) HPCa films; (e-g) HPCa films, after fluorescent staining of actin micro filaments and DNA; (h) coverslips, after fluorescent staining of actin micro filaments and DNA.

Despite the lower percentage of adherent cells to HPC substrates, some cells were able to adhere to HPCa substrates 12 h post-seeding. It can be speculated that some of the additional chemical functionalities provided by the cross-linking agent used in HPCa would provide weak points for cell adhesion. As previously mentioned, surface charge can also play a key role in cell adhesion but unfortunately electro-kinetic experiments carried out in the present work were not conclusive due to technical difficulties in measuring the surface charge of the present films. Additionally, surface roughness can also influence cell adhesion.

2.4. Cell Proliferation

Cell proliferation indexes (N/N_0 ratio) were calculated and differences between the different *substrata* used were found. hMSC proliferation index was similar on HPC films (HPCi and HPCa) compared to polyHEMA (1.01 ± 0.3 for HPCi film, 1 ± 0.25 for HPCa film and 0.96 ± 0.37 for polyHEMA; cell proliferation indexes between these substrates were not statistically significant $p > 0.05$, MW), 24 h post-seeding. The proliferation index on coverslip was considerably higher compared to HPC films or polyHEMA (1.78 ± 0.27; cell proliferation indexes between coverslip and the other substrates were statistically significant, $p < 0.05$, MW).

Cell proliferation indexes of hMCS cultured 48 h on HPCi films (1.28 ± 0.11) and HPCa films (1.20 ± 0.33) was similar (cell proliferation indexes between these substrates were not statistically significant $p > 0.05$, MW). The proliferation index was lower on polyHEMA films (1.04 ± 0.22, cell proliferation indexes between polyHEMA and HPC films were statistically significant $p < 0.05$, MW) and was significantly higher on coverslip when compared with the proliferation index of cells cultured on HPC and polyHEMA films (2.82 ± 0.25, cell proliferation indexes between coverslip and the other substrates were statistically significant, $p < 0.05$, MW). These results are in agreement with the results obtained for cell attachment.

Table 3.5 – Cell proliferation assessed on HPCi and HPCa films, coverslips and polyHEMA films at 24 h and 48 h post-seeding.

	24 h	48 h
HPCi	1.01 ± 0.30	1.28 ± 0.11
HPCa	1.00 ± 0.25	1.20 ± 0.33
polyHEMA	0.96 ± 0.37	1.04 ± 0.22
Coverslip	1.78 ± 0.27	2.82 ± 0.25

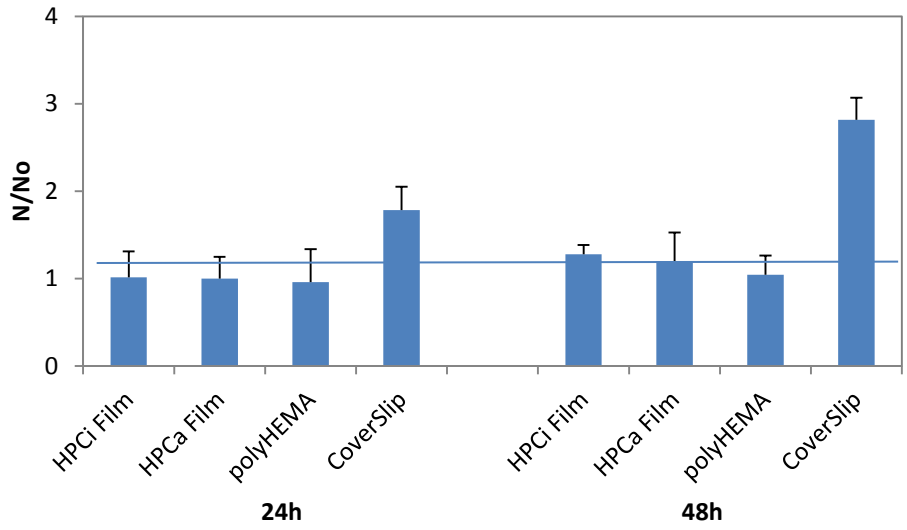

Figure 3.25 – Cell proliferation indexes on HPCi film, HPCa film, polyHEMA film and coverslip after 24 and 48 h. Cell proliferation corresponds to N/N_0 ratio, where N is the total number of cells at T = 24 h or T =48 h and N_0 is the number at T = 0. The blue line corresponds to the ratio of 1 representing the cell number at seeding.

The results demonstrated that hMSCs grew well on coverslips but had a lower proliferation index after 48 h on HPCi, HPCa and polyHEMA films.

2.5. Cell viability

The results of cell viability assessed by trypan blue on HPCi and HPCa films, coverslips and polyHEMA films at 24 h and 48 h post-seeding are present in the Table 3.6.

Table 3.6 – Cell viability assessed by trypan blue on HPCi and HPCa films, polyHEMA films and coverslips at 24 h and 48 h post-seeding.

	24 h	48 h
HPCi	97.8 %	97.2 %
HPCa	96.4 %	97.6 %
polyHEMA	97.9 %	95.1 %
Coverslip	99.3 %	98.9 %

These results confirmed that hMSCs remain viable up to 48 h on all substrates tested. These results are in agreement with the literature. Cellulose is a natural polymer that presents excellent properties for use as a biomedical material, namely its non-toxicity [159]. As expected, hMSCs were kept viable up to the end of the study, which is of great importance for the use of HPCi and HPCa films in biomedical applications.

2.6. Environmental Scanning Electron Microscopy

Figs. 3.26 (a) and (b) represent images of the HPCa films after the cell culture. Locations indicated as A and B in Fig. 3.26 were chemically analysed. After the cell culture, the HPCa film kept its former ordered structure. After chemical analysis using energy dispersive spectroscopy (EDS), it was verified that there is an increase of calcium and phosphate in point B, when compared to point A, indicating a preferential deposition of these elements (Ca and P from the culture medium) in the bands formed, probably in the form of a calcium phosphate mineral. However, it was out of the scope of the present work to further analyze this phenomenon, which should be done in future studies in order to better understand it. Deposition of calcium phosphates is a highly desirable phenomenon in biomaterials for orthopedic applications and several modifications (including using cellulose derivatives) have been investigated to promote it [165]. Hence, the ability of the present materials to induce this behavior should be further analyzed and explored.

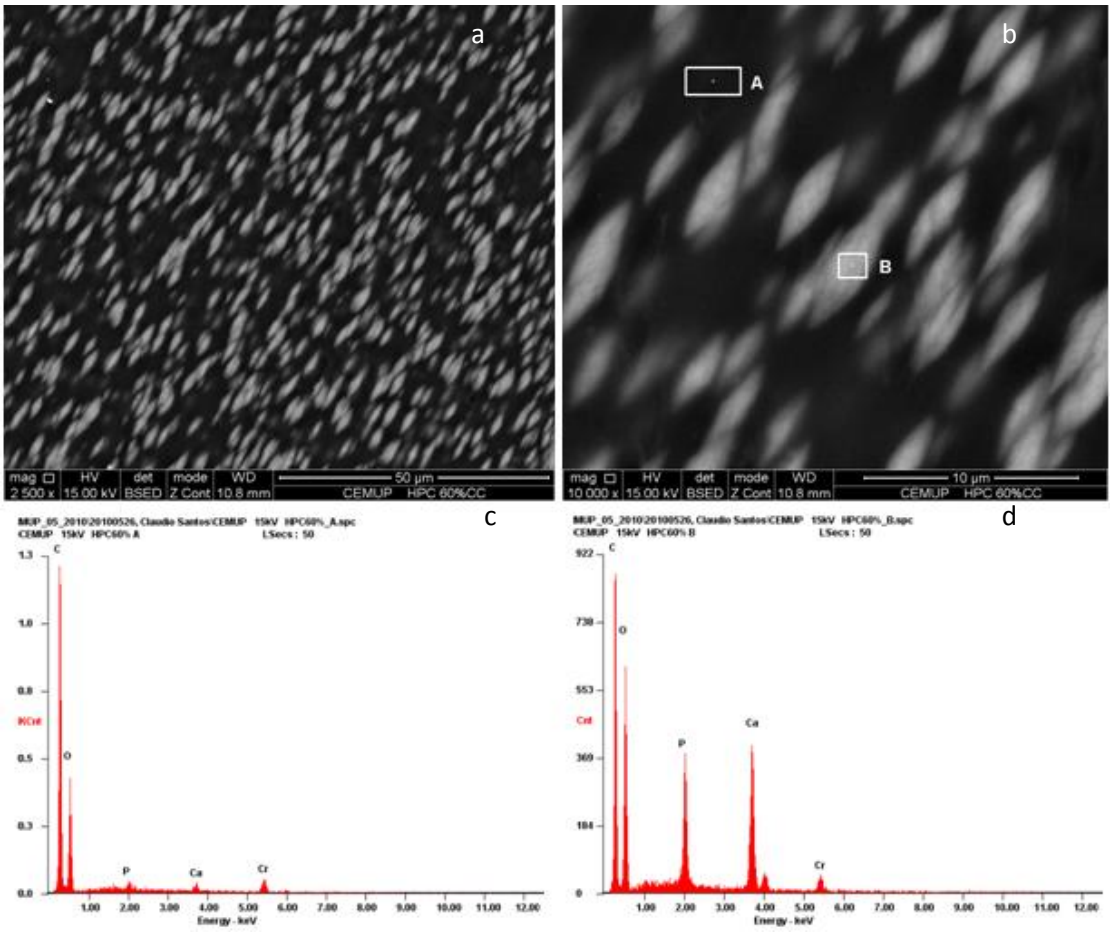

Figure 3.26 – (a) HPCa film (magnification: 2500x) after cell culture; (b) HPCa film (magnification: 10000x) after cell culture; (c) *Spectrum* of point A of image (b); *Spectrum* of point B of image (b).

Chapter IV – CONCLUSION

This study has shown that it is possible to prepare sterile hydroxypropylcellulose (HPC) films, crosslinked with 10% (w/w) of diisocyanatohexane, with potential use as coatings for anti-adhesive purposes in biomedical devices.

The main objective of this study was to investigate the effect of HPCi and HPCa films on the behavior of mesenchymal stem cells (MSCs) and verify if HPCa (films prepared from liquid crystal solutions – 60 wt% crosslinked HPC) induce a different cell response compared to HPCi (films produced from an isotropic solution – 30 wt% crosslinked HPC). HPCi and HPCa films were successfully prepared and characterized.

During the research work several methods were used to investigate the surface properties of HPC films. The first specific objective of this thesis was to prepare and characterize hydroxypropylcellulose films with different properties. The properties of HPCi and HPCa films were compared. The mechanical anisotropy of HPCa films was easily identified. As expected, the Young's modulus values are lower in the wet state than in the dry state. The hydrophobicity of the materials was also assessed. The contact angles obtained for both films were similar. FTIR was initially used for surface characterisation, but also to inspect the success of the cross-linking reaction. New peaks characteristic of the reaction of the cross-linker with cellulose functionalities appeared on the *spectra* of HPCi and HPCa films, showing that the cross-linking reaction was successful. XPS was used to quantitatively determine atomic composition and chemistry of HPCi and HPCa surfaces. No significant shifts occurred in the positions of the peaks of HPCi and HPCa. FTIR and XPS showed that the surface chemistry of both films is similar. The results of SEM showed the formation of banded textures in HPCa film samples obtained from aqueous HPC liquid crystalline solutions subjected to shear. The periodicity of the "principal" bands is around$3\ \mu m$. Two different periodicities were obtained: a primary set of "principal" bands, perpendicular to the shear direction, and a smoother texture, characterized by a secondary periodic structure containing "secondary" bands. The surface topography of HPCa films was also characterized by AFM and the two periodicities were identified and measured.

The biologic characterization started with a cytotoxicity assay. HPCi and HPCa films were tested for *in vitro* cytotoxicity and it was revealed that no cytotoxic compounds were released from the films. The behaviour of hMSC on HPC films was also investigated. Cell attachment, morphology and proliferation were investigated. The results of the cell attachment assay revealed that the percentage of attached cells on HPCi and HPCa was almost zero and that cells were not able to proliferate on these substrates, which make them adequate for anti-fouling applications. While glass

coverslips promote cell attachment, hMSCs seeded onto HPCi and HPCa cannot find anchorage sites and then aggregate of the HPC films. This study indicates that both HPC films are effective anti-adhesive biomaterials that give reproducible and consistent results. HPC films seem to be an interesting tool to analyse the early biochemical events that govern intercellular communications and could be a suitable substrate to analyse cell-cell communication and cell-*substratum* interactions. The cell morphology assay confirmed the results of cell attachment assay. The anti-fouling properties of the HPC films were confirmed by direct observation of the cells seeded on surfaces, using an optical microscope. Figures revealed cell clusters without any attachment on HPCi and HPCa film surfaces. The cells have adopted a globular shape, which minimizes the cell/substrate interaction. In contrast, the positive control (glass coverslips) exhibited a strong cell adhesion and spreading. Therefore, an examination of the cell growth of hMSCs on HPCi and HPCa films was performed. It was concluded that hMSCs grew well on coverslips but had a lower proliferation index after 48 h on HPCi, HPCa and polyHEMA films. A cell viability assay assessed by trypan blue confirmed that hMSCs remain viable up to 48 h on HPCi and HPCa films.

HPC films, studied in this work, seem to be a great candidate for biomedical applications requiring adhesion-resistant *substrata*, including bioreactors and other biomedical devices. Furthermore, HPCa smart materials (prepared from a liquid crystal solution), able to respond to external stimuli, can be interesting candidates for a number of biomedical applications since it is possible to adjust the surface topography of these systems as function of the concentration of HPC used to prepare the solutions and depending on the processing conditions, including the shear rate.

Chapter V – FUTURE DIRECTIONS

The continuation of the present work can follow two different ways. The non-fouling properties of HPC films can be explored performing protein adsorption assays, for example, by real time monitoring of protein adsorption using a quartz crystal microbalance. Protein adsorption can be performed using a single protein to study its biological reactions or from multiprotein solutions (such as blood plasma that contains hundreds of proteins) to infer about the reaction observed for implanted biomaterials. Other important test that could be done is an annexin-V binding assay to study the percentage of apoptotic cells. It could be also performed an Electro Kinetic Analysis (EKA) to infer about the charge and adsorption properties of HPCi and HPCa surfaces.

The behaviour of HPC films as anticoagulative materials could also be studied. The development of nonthrombogenic biomaterials remains one of the great challenges nowadays in this field [166]. The development of blood contacting artificial organs has been delayed because a universal nonthrombogenic material has not yet been developed [167]. It has recently been discovered that biomembranes possess the morphosis of a liquid crystal. It was also demonstrated that surfaces of cell membranes contacting with blood frequently are all in the mobile lipid liquid crystal state [168]. So it is expected that membrane materials whose surfaces are in the state of an ordinal and mobile liquid crystal, especially with the conformation of cholesteryl liquid crystals, could have excellent anticoagulative properties [167].

This material could also be used to study the effects of cell-cell contact between stem cells *per se* on the lineage differentiation of stem cells, without other interferences (soluble factors, etc). Recently, a similar study was performed and revealed that isolated cells exhibited less significant differentiation than paired or aggregated cells [169]. Rat BMSCs were used in this study and it was proved that cell differentiation could be influenced by cell-cell contact.

It would also be interesting to analyse cell–cell communication and cell–*substratum* interactions on HPC surfaces. It has been shown that cells aggregated on a cellulose *substratum* are able to rapidly establish gap junctions for communication [170, 171]. This phenomenon is very important for the fields of tissue engineering and the preparation of biomaterials for hybrid artificial organs.

HPC films could be also a useful culture support for research on the anoikis, studying signalling mechanisms involved in this process.

The other possibility relies in turning the surface of HPC films adhesive to cells, for instance by grafting of RGD peptides. Since identification of the RGD (Arg- Gly-Asp) sequence as mediating the attachment of cells to several plasma and ECM proteins (fibronectin, vitronectin, collagen, laminin, etc), several research works have been investigating the grafting of RGD-containing peptides on biomaterial surfaces to promote cell attachment [172]. RGD ability to bind a variety of cells through ligand–receptor interactions makes it a useful sequence for incorporating onto HPC surfaces to promote cell adhesion and proliferation. This would allow to investigate the possibility of HPCa films (prepared from liquid crystal solutions) to influence or monitor the differentiation of stem cells, studying the importance of these microenvironments in stem cell lineage specification [172]. It would be interesting to adjust the surface topography of these smart materials to compare the behaviour of hMSCs on their surfaces.

References

1. Lockwood, N.A., et al., *Thermotropic Liquid Crystals as Substrates for Imaging the Reorganization of Matrigel by Human Embryonic Stem Cells.* Advanced Functional Materials, 2006. **16**: p. 618–624.
2. Goodby, J.W., *Liquid crystals and life.* Liquid Crystals, 1998. **24**(1): p. 25-38.
3. Bahadur, B., *Liquid crystals: applications and uses*. Vol. 1. 1990, Singapore: World Scientific.
4. Chandrasekhar, S., *Liquid Crystals*. 1992: Cambridge University Press.
5. H. Stegemeyer, G.E., *Liquid crystals*. Vol. 3. 1994, New York: Springer.
6. Khoo, I.-C., *Liquid crystal*. Second ed. 2007: John Wiley & Sons. Inc.
7. 24-07-2010]; Available from: http://amaze-lcdtv.blogspot.com/2008/09/lcd-vocab-liquid-crystal-lc.html.
8. Lehmann, O., Z. Physik. Chem., 1889. **4**: p. 462
9. Godinho, M.H., A.F. Martins, and J.L. Figueirinhas, *Composite systems for display applications from cellulose elastomers and nematic liquid crystals.* January 1998. **9**(1-4): p. 226-229.
10. Yang, H.M., et al., *Optic properties of bile liquid crystals in human body.* World Journal of Gastroenterology, 2000. **6**(2): p. 248-251.
11. Caffrey, M., *Membrane protein crystallization.* Journal of Structural Biology, 2003. **142**(1): p. 108-132.
12. Bouligand, Y. and V. Norris, *Chromosome separation and segregation in dinoflagellates andbacteria may depend on liquid crystalline states.* Biochimie, 2001. **83**(2): p. 187-192.
13. Smeller, L., *Pressure-temperature phase diagrams of biomolecules.* Biochimica et Biophysica Acta (BBA) - Protein Structure and Molecular Enzymology, 2002. **1595**(1-2): p. 11-29.
14. Brown, G.H. and J.J. Wolken, Liquid Crystals and Biological Structures New York: Academic Press, 1979.
15. Collings, P.J., *Liquid crystals: nature's delicate phase of matter*. 2002, Princeton University Press: New Jersey.
16. Kosc, T.Z., et al., *Progress in the development of polymer cholesteric liquid crystal flakes for display applications.* December 2004. **25**(5): p. 171-176.
17. Leenhouts, F., S.M. Kelly, and A. Villiger, *Novel ferroelectric smectic C liquid crystal mixtures for display applications.* January 1990. **11**(1): p. 41-45.
18. Collings, P.J. and M. Hird, *Introduction to Liquid Crystals: Chemistry and Physics*. 1997, London: Taylor and Francis.
19. Demus, D., J. Goodby, and G.W. Gray, *Handbook of Liquid Crystals*. Vol. 1-3. 1998, Weinheim, Germany: Wiley-VCH.
20. Glogowski, W., *Liquid Crystal Lab Notes*. 2003, Yerkes Winter Institute, Center for Cosmological Physics, University of Chicago.
21. Panigrahi, P.K. 2000 19-07-2010]; Available from: http://www.iitk.ac.in/infocell/Archive/dirmar2/techno_crystals.html.
22. Panigrahi, P.K., *Colourful World of Liquid Crystals* 2000, Indian Institute of Technology Kanpur: Kanpur.
23. Praisner, T.J., D.R. Sabatino, and C.R. Smith, *Simultaneously combined liquid crystal surface heat transfer and PIV flow-field measurements.* Experiments in Fluids, 2001. **30**(1): p. 1-10.
24. Sabatino, D.R., T.J. Praisner, and C.R. Smith, *A high-accuracy calibration technique for thermochromic liquid crystal temperature measurements.* Experiments in Fluids, 2000. **28**(6): p. 497-505.
25. Atyabi, F., E. Khodaverdi, and R. Dinarvand, *Temperature modulated drug permeation through liquid crystal embedded cellulose membranes.* International Journal of Pharmaceutics, 2007. **339**(1-2): p. 213-221.

26. Formariz, T.P., et al., *Relationship between structural features and in vitro release of doxorubicin from biocompatible anionic microemulsion.* Colloids and Surfaces B: Biointerfaces, 2007. **60**(1): p. 28-35.
27. Luk, Y.-Y., et al., *Liq. Cryst.* 2004: p. 611
28. Fang, J., et al., Langmuir, 2003. **19**: p. 2865.
29. Costa, I., et al., *New cellulose derivatives composites for electro-optical sensors.* Carbohydrate Polymers, 2007. **68**: p. 159-165.
30. Abdulhalim, I., R. Moses, and R. Sharon, *Biomedical Optical Applications of Liquid Crystal Devices.* Optical Materials, 2007. **112**(5).
31. Salamone, J.C., *Polymeric materials encyclopedia.* **2**.
32. Werbowyj, R.S. and D.G. Gray, *Ordered Phase Formation in Concentrated Hydroxpropylcellulose Solutions.* Macromolecules, 1980. **13**: p. 69-73.
33. Sakellariou, P., R.C. Rowe, and E.F.T. White, *The thermomechanical properties and glass transition temperatures of some cellulose derivatives used in film coating.* International Journal of Pharmaceutics, 1985. **27**(2-3): p. 267-277.
34. Noël, P.C. and P. Navard, *Liquid crystal polymers.* Progress in Polymer Science, 1991. **16**(1): p. 55-110.
35. Godinho, M.H.F., *CONTRIBUIÇÃO PARA O ESTUDOO DOS POLÍMEROS LÍQUIDOS CRISTALINOS DERIVADOS DA CELULOSE*, in *Materiais*. 1991, Universidade Nova de Lisboa, Faculdade de Ciências e Tecnologia: Lisboa.
36. Klug, E.D., *Food Technol.* Hercules Chem, 1970. **24** p. 51.
37. Rossman, J. and A.J. Desmarais, *J. Rossman, A.J. Desmarais, Hercules Chem. 61 (1970) 9.* 1970. **61**: p. 9.
38. Godinho, M.H., C. Costa, and J.L. Figueirinhas, *Liquid Crystal and Cellulose Derivatives Composites Used in Electro-Optical Applications* Molecular Crystals and Liquid Crystals, 1999. **331**: p. 173 - 179.
39. Rusig, I., et al., *Optical properties of cholesteric (2-hydroxypropyl) cellulose (HPC) esters.* Journal of Polymer Science Part B: Polymer Physics, 1994. **32**(11): p. 1907-1914.
40. Bianchi, E., et al., *Polymeric liquid crystals: cholesteric superstructure from blends of hydroxypropylcellulose esters.* Polymers for Advanced Technologies, 2003. **14**: p. 529-536.
41. Gray, D.G., *Chiral nematic ordering of polysaccharides.* Carbohydrate Polymers, 1994. **25**(4): p. 277-284.
42. Bhadani, S.N. and D.G. Gray, *Cellulose-based liquid crystalline polymers – esters of (hydroxypropyl)cellulose.* Molecular Crystals and Liquid Crystals, 1983. **99**(1-4): p. 29-38.
43. Giasson, J., et al., *Preparation of chiral nematic gels by radiation cross-linking.* Macromolecules, 1991. **24**(7): p. 1694-1696.
44. Hou, H., et al., *Tuning of the pitch height of thermotropic cellulose esters.* Macromolecular Chemistry and Physics, 2000. **201**: p. 2050-2054.
45. Sato, T., A.N. Teramoto, and M.M. Green, *Cholesteric pitch of lyotropic polymer liquid crystals.* Macromolecules, 1998. **31**(4): p. 1398-1405.
46. Tseng, S.L., A. Valente, and D.G. Gray, *Cholesteric liquid crystalline based on (acetoxypropyl) cellulose.* Macromolecules, 1981. **14**(3): p. 715-719.
47. Costa, I., et al., *New cellulose derivatives composites for electro-optical sensors.* Carbohydrate Polymers, 2007. **68**(1): p. 159-165.
48. Aharoni, S.M., Macromolecules, 1979. **12**: p. 271-280.
49. Godinho, M.H., et al., *Atomic Force Microscopy Study of Hydroxypropylcellulose Films Prepared from Liquid Crystalline Aqueous Solutions.* Macromolecules, 2002. **35**: p. 5932-5936.
50. Ratner, B.D., et al., *Biomaterials Science*. 2nd ed. 2004: Elsevier Academic Press.
51. Grest, G.S., et al., *Grafting, characterization techniques, kinetic modeling*, ed. Springer. 1998.
52. Anderson, J.M., *BIOLOGICAL RESPONSES TOMATERIALS.* Annu. Rev. Mater. Res, 2001. **31**: p. 81–110.

53. Andrade, J., *Surface and interfacial aspects of biomedical polymers*. 1985, New York: Plenum Press.
54. Brash, J., *Exploiting the current paradigm of blood-material interactions for the rational design of blood-compatible materials.* J Biomater Sci Polym, 2000. **11**(11): p. 1135-46.
55. Horbett, T.A. and J.L. Brash, *Proteins at interfaces: current issues and future prospects.* Proteins at Interfaces, Physicochemical and Biochemical Studies, ACS Symposium Series, 1987. **343**: p. 1–33.
56. Hoffman, A.S., *A general classification scheme for hydrophilic and hydrophobic biomaterial surfaces.* J. Biomed. Mater. Res., 1986. **20**.
57. Hoffman, A.S., *Non-fouling surface technologies.* Journal of Biomaterials Science, Polymer Edition, 1999. **10**: p. 1011–1014.
58. Horbett, T.A. and A.S. Hoffman, *Bovine plasma protein adsorption to radiation grafted hydrogels based on hydroxyethylmethacrylate and N-vinylpyrrolidone.* Advances in Chemistry Series, 1975. **145**: p. 230–254.
59. Horbett, T.A., *Principles underlying the role of adsorbed plasma proteins in blood interactions with foreign materials.* Cardiovasc. Pathol, 1993. **2**: p. 137S–148S.
60. Mori, Y., *Interactions between hydrogels containing PEO chains and platelets.* Biomaterials 1983. **4**: p. 825-830.
61. Merrill, E.W., *Poly(ethylene oxide) and blood contact: a chronicle of one laboratory.* Polyethylene Glycol Chemistry: Biotechnical and Biomedical Applications, 1992: p. 199-220.
62. Gombotz, W.R., et al., *Protein adsorption to PEO surfaces.* J. Biomed. Mater. Res., 1991. **25**: p. 1547–1562.
63. Antonsen, K.P. and A.S. Hoffman, *Water structure of PEG solutions by DSC measurements.* Polyethylene Glycol Chemistry: Biotechnical and Biomedical Applications, 1992: p. 15–28.
64. Reyes, C.D. and G. AJ., *A centrifugation cell adhesion assay for high-throughput screening of biomaterial surfaces.* J Biomed Mater Res, 2003 **67**(1): p. 328-33.
65. Bottaro, D., A. Liebmann-Vinson, and M. Heidaran, *Molecular signaling in bioengineered tissue microenvironments.* Ann N Y Acad Sci, 2002. **961**: p. 143–153.
66. Datta, N., et al., *Effect of bone extracellular matrix synthesized in vitro on the osteoblastic differentiation of marrow stromal cells.* Biomaterials 2005. **26**(9): p. 971–977.
67. Lutolf, M. and J. Hubbell, *Synthetic biomaterials as instructive extracellular microenvironments for morphogenesis in tissue engineering.* Nat Biotechnol, 2005. **23**(1): p. 47–55.
68. Rosso, F., et al., *From cell-ECM interactions to tissue engineering.* J Cell Physiol, 2004. **199**(2): p. 174–180.
69. Rosso, F., et al., *Smart materials as scaffolds for tissue engineering.* J Cell Physiol, 2005. **203**(3): p. 465–470.
70. Shin, H., S. Jo, and A. Mikos, *Biomimetic materials for tissue engineering.* Biomaterials 2003. **24**(24): p. 4353–4364.
71. Frisch, S. and H. Francis, *Disruption of epithelial cellmatrix interactions induces apoptosis.* J Cell Biol, 1994. **124**(4): p. 619–626.
72. Meredith, J.J., B. Fazeli, and M. Schwartz, *The extracellular matrix as a cell survival factor.* Mol Biol Cell, 1993. **4**(9): p. 953–961.
73. Faucheux, N., et al., *Behavior of cells cultured on cuprophan.* Modified fibers with medical and specialty applications, 2006: p. 35–47.
74. Faucheux, N., et al., *Gap junction communication between cells aggregated on a cellulose-coated polystyrene: influence of connexin 43 phosphorylation.* Biomaterials 2004. **25**(13): p. 2501-2506.
75. Granja, P., *Biomimetic Natural Materials for Bone Regeneration*, in *Faculdade de Engenharia*. 2000, Universidade do Porto: Porto.

76. Beck, D., *The role of Seprafilm bioresorbable membrane in adhesion prevention.* Eur J Surg Suppl, 1997. **577**: p. 49–55.
77. Buckenmaier, C., M. Summers, and S. Hetz, *Effect of the antiadhesive treatments, carboxymethylcellulose combined with recombinant tissue plasminogen activator and Seprafilm, on bowel anastomosis in the rat.* Am Surg, 2000. **66**(11): p. 1041–1045.
78. Szabo, A., et al., *Evaluation of seprafilm and amniotic membrane as adhesion prophylaxis in mesh repair of abdominal wall hernia in rats.* Eur Surg Res, 2000. **32**(2): p. 125–128.
79. Riet, M.v.t., et al., *Prevention of adhesion to prosthetic mesh: comparison of different barriers using an incisional hernia model.* Ann Surg 2003. **237**(1): p. 123–128.
80. Caruso, D., et al., *Randomized clinical study of Hydrofiber dressing with silver or silver sulfadiazine in the management of partial-thickness burns.* J Burn Care Res, 2006. **27**(3): p. 298–309.
81. Guest, J. and F. Ruiz, *Modelling the cost implications of using carboxymethylcellulose dressing compared with gauze in the management of surgical wounds healing by secondary intention in the US and UK.* Curr Med Res Opin 2005. **21**(2): p. 281–290.
82. Guest, J., et al., *Cost effectiveness of using carboxymethylcellulose dressing compared with gauze in the management of exuding venous leg ulcers in Germany and the USA.* Curr Med Res Opin, 2005. **21**(1): p. 81–92.
83. Ravenscroft, M., J. Harker, and K. Buch, *A prospective, randomised, controlled trial comparing wound dressings used in hip and knee surgery: Aquacel and Tegaderm versus Cutiplast.* Ann R Coll Surg Engl, 2006. **88**(1): p. 18–22.
84. Barbucci, R., G. Leone, and A. Vecchiullo, *Novel carboxymethylcellulose-based microporous hydrogels suitable for drug delivery.* J Biomater Sci Polym Ed, 2004. **15**(5): p. 607–19.
85. Chiumiento, A., et al., *Anti-inflammatory properties of superoxide dismutase modified with carboxymetil-cellulose polymer and hydrogel.* J Mater Sci Mater Med, 2006. **17**(5): p. 427–435.
86. Liu, L., M. Fishman, and K. Hicks, *Pectin in controlled drug delivery a review.* Cellulose, 2007. **14**: p. 15–24.
87. Wu, P., et al., *Percutaneous absorption of captopril from hydrophilic cellulose derivatives through excised rabbit skin and human skin.* Drug Dev Ind Pharm, 1998. **24**(2): p. 179–182.
88. Hindié, M., et al., *Culture of melanoma cells as aggregates on cellulose substratum.* Biomolecular Engineering, 2005. **22**(5-6): p. 205-208.
89. Gekas, J., et al., *The inhibition of cell spreading on a cellulose substrate (cuprophan) induces an apoptotic process via a mitochondria-dependent pathway.* FEBS Letters, 2004. **563**: p. 103-107.
90. Faucheux, et al., *cAMP levels in cells attached to AN69 and Cuprophan: cAMP dependence of cell aggregation and the influence of serum.* Biomaterials, 1999 **20**(2): p. 159-65.
91. Cases, A., et al., *In Vivo Evaluation of Platelet Activation by Different Cellulosic Membranes.* Artificial Organs, 1997. **21**(4): p. 330-334.
92. Fontanellas, A., et al., *Efficiency of three different hemodialysis membranes for plasma porphyrin removal.* American Journal of Kidney Diseases, 1995. **25**(1): p. 30-33.
93. Atala, A., *Principles of regenerative medicine*. 2008: Elsevier.
94. Perry, 2000.
95. Husein K. Salem, C.T., *Mesenchymal Stromal Cells: Current Understanding and Clinical Status.* Stem Cells, 2010. **28**: p. 585-596.
96. Blum and Benvenisty, *The tumorigenicity of human embryonic stem cells.* Adv Cancer, 133-158. **100**: p. 133-158.
97. Edwards, R.G., *Stem cells today: B1. Bone marrow stem cells.* Reproductive BioMedicine Online, 2004. **9**(5): p. 541-583.
98. Ogawa, M., *Differentiation and proliferation of hematopoietic stem cells.* Blood 1993. **81**(11): p. 2844–2853.

99. Steindler, D.A. and D.W. Pincus, *Stem cells and neuropoiesis in the adult human brain.* The Lancet, 2002. **359**(9311): p. 1047-1054.
100. Dragoo, J.L., et al., *Bone induction by BMP-2 transduced stem cells derived from human fat.* Journal of Orthopaedic Research, 2003. **21**(4): p. 622-629.
101. Tosh, D. and A. Strain, *Liver stem cells--prospects for clinical use.* Journal of Hepatology, 2005. **42**(1, Supplement 1): p. S75-S84.
102. Alessandri, G., et al., *Isolation and culture of human muscle-derived stem cells able to differentiate into myogenic and neurogenic cell lineages.* The Lancet, 2004. **364**(9448): p. 1872-1883.
103. Eberhardt, M., et al., *Multipotential nestin and Isl-1 positive mesenchymal stem cells isolated from human pancreatic islets.* Biochemical and Biophysical Research Communications, 2006. **345**(3): p. 1167-1176.
104. Erices, A., P. Conget, and J.J. Minguell, *Mesenchymal progenitor cells in human umbilical cord blood.* British Journal of Haematology, 2000. **109**(1): p. 235-242.
105. Chen, Y., et al., *Mesenchymal stem cells: A promising candidate in regenerative medicine.* The International Journal of Biochemistry & Cell Biology, 2008. **40** p. 815-820.
106. Dominici, M., et al., *Minimal criteria for defining multipotent mesenchymal stromal cells. The International Society for Cellular Therapy position statement.* Cytotherapy, 2006. **8**: p. 315 317.
107. Pountos, I., *Mesenchymal stem cell tissue engineering: Techniques for isolation, expansion and application.* 2007. **38**: p. S23-S33.
108. Alhadlaq, A. and J.J. Mao, *Mesenchymal Stem Cells: Isolation and Therapeutics.* Stem Cells and Development, 2004. **13**: p. 436-448.
109. Friedenstein, A., R. Chailakhjan, and K. Lalykina, *The development of fibroblast colonies in monolayer cultures of guinea-pig bone marrow and spleen cells.* Cell Tissue Kinet 1970. **3**: p. 393-403.
110. Baksh, D., L. Song, and R.S. Tuan, *Adult mesenchymal stem cells: characterization, differentiation, and application in cell and gene therapy.* J. Cell. Mol. Med., 2004 **8**(3): p. 301-316.
111. Crisostomo, P., et al., *High Passage Number of Stem Cells Adversely Affects Stem Cell Activation and Myocardial Protection.* 2006 **26**(6): p. 575-580.
112. 15-08-2010]; Available from: http://clinicaltrials.gov.
113. Horwitz, E., D. Prockop, and L. Fitzpatrick, *Transplantability and therapeutic effects of bone marrow-derived mesenchymal cells in children with osteogenesis imperfecta.* Nat Med, 1999. **5**: p. 309-313.
114. Koc, O., J. Day, and M. Nieder, *Allogeneic mesenchymal stem cell infusion for treatment of metachromatic leukodystrophy (MLD) and Hurler syndrome (MPS-IH).* Bone Marrow Transplant, 2002. **30**: p. 215-222.
115. Devine, S. and ;:. *Mesenchymal stem cells: will they have a role in the clinic?* J Cell Biochem Suppl., 2002. **38**: p. 73-79.
116. Li, Y., J. Chen, and X. Chen, *Human marrow stromal cell therapy for stroke in rat: neurotrophins and functional recovery.* Neurology, 2002. **59**: p. 514-523.
117. Wang, L., Y. Li, and J. Chen, *Ischemic cerebral tissue and MCP-1 enhance rat bone marrow stromal cell migration in interface culture.* Exp Hematol, 2002. **30**: p. 831-836.
118. Barbash, I., P. Chouraqui, and J. Baron, *Systemic delivery of bone marrow-derived mesenchymal stem cells to the infarcted myocardium: feasibility, cell migration, and body distribution.* Circulation, 2003. **108**: p. 863-868.
119. Urdzikova, L., P. Jendelova, and K. Glogarova, *Transplantation of bone marrow stem cells as well as mobilization by granulocyte-colony stimulating factor promotes recovery after spinal cord injury in rats.* J. Neurotrauma, 2006. **23**: p. 1379-1391.
120. Gray, G., J. Appl. Polym. Sci.:Appl. Polym. Symp., 1983. **37**: p. 179

121. Merrett, K., *Surface analysis methods for characterizing polymeric biomaterials.* J. Biomater. Sci. Polymer Edn, 2002. **13**(6): p. 593-621.
122. Stein. *Contact Angle*. J. Biomaterials tutorial 2010 02-08-2010]; Available from: http://www.uweb.engr.washington.edu/research/tutorials/contact.html.
123. Restagno, F., et al., *Contact Angle and Contact Angle Hysteresis Measurements Using the Capillary Bridge Technique.* American Chemical Society, 2009.
124. Werner, C. and H.J. Jacobasch, International Journal of Artificial Organs, 1999. **22**: p. 160.
125. Butt, H., K. Graf, and M. Kappl, *Physics and Chemistry of Interfaces*. 2003: Wiley-VCH. 373.
126. Restagno, F., et al., *Contact Angle and Contact Angle Hysteresis Measurements Using the Capillary Bridge Technique.* Langmuir, 2009. **25**(18): p. 11188-11196.
127. Kyowa. *LCD and FPD*. 2010.
128. Neumann, A. and R. Godd, *Techniques of measuring contact angles.* Surface and colloid science-Experimental methods, 1979. **11**: p. 31-61.
129. Sun, D.-W., *Infrared spectroscopy for food quality analysis and control*. 2009: Elsevier.
130. Xu, Z., X. Huang, and L. Wan, *Surface engineering of polymer membranes*. 2009: Springer.
131. Chan, R. and V. Chen, *Characterization of protein fouling on membranes: opportunities and challenges.* Journal of Membrane Science, 2004. **242**(1-2): p. 169-188.
132. Niemantsverdriet, J.W., *Spectroscopy in catalysis: an introduction*. 2007: WILEY-VCH.
133. 07-06-2010]; Available from: http://en.wikipedia.org/wiki/X-ray_photoelectron_spectroscopy.
134. Kimseng, K. and M. Meissel, *Environmental Scanning Electron Microscope.* 2001.
135. [cited 26-05-2010; Available from: http://www.purdue.edu/rem/rs/sem.htm.
136. Binning and e. al., 1986.
137. Parot, P., et al., *Past, present and future of atomic force microscopy in life sciences and medicine.* JOURNAL OF MOLECULAR RECOGNITION, 2007. **20**: p. 418-431.
138. Drake and e. al, 1989.
139. Radmacher, M., *Methods in Cell Biology*. Studying the Mechanics of Cellular Process by Atomic Force Microscopy. Vol. 83. 2007: Elsevier.
140. 28-03-2010]; Available from: http://mrsec.wisc.edu/Edetc/technologist/thumbnails/Matt/AFM_schematic.jpg.
141. Florin, E., V. Moy, and H. Gaub, *Adhesion forces between individual ligand-receptor pairs.* Science 1994. **264**: p. 415-417.
142. Radmacher, M., M. Fritz, and P.K. Hansma, *Imaging soft samples with the atomic force microscope: Gelatin in water and propanol.* Biophys. J., 1995. **69**(7): p. 264-270.
143. Almqvist, N., et al., *Micromechanical and structural properties of a pennate diatom investigated by atomic force microscopy.* Journal of Microscopy, 2001. **202**(3): p. 518-532.
144. Rotsch, C. and M. Radmacher, *Measuring electrostatic interactions with the atomic force microscope.* Langmuir, 1997. **13**(10): p. 2825-2832.
145. OSWALD, J., et al., *Mesenchymal Stem Cells Can Be Differentiated Into Endothelial Cells In Vitro.* Stem Cells, 2004. **22**: p. 377-384.
146. Bretland, A., J. Lawry, and R. Sharrard, *A study of death by anoikis in cultured epithelial cells.* Cell Proliferation, 2001. **34**(4): p. 199-210.
147. Diaz-Montero, C. and B. McIntyre, *Acquisition of anoikis resistance in human osteosarcoma cells does not alter sensitivity to chemotherapeutic agents.* BMC Cancer, 2005. **5**(1): p. 39.
148. Feder-Mengus, C., et al., *Multiple mechanisms underlie defective recognition of melanoma cells cultured in threedimensional architectures by antigen-specific cytotoxic T lymphocytes.* British Journal of Cancer, 2007. **96**(7): p. 1072-1082.
149. Folkman, J. and A. Moscona, *Role of cell shape in growth control.* Nature, 1978. **273**: p. 345–349.

150. Ghosh, et al., *Culture of melanoma cells in 3-dimensional architectures results in impaired immunorecognition by cytotoxic T lymphocytes specific for Melan-A/MART-1 tumor-associated antigen.* Ann Surg, 2005. **242**: p. 851–857.
151. Gilmore, A., et al., *Integrin-mediated survival signals regulate the apoptotic function of Bax through its conformation and subcellular localization.* Cell Biology, 2000. **149**(2): p. 431–446.
152. Krylov, S. and N. Dovichi, *Single-cell analysis using capillary electrophoresis: influence of surface support properties on cell injection into the capillary.* Electrophoresis, 2000. **21**(4): p. 767–773.
153. 26-05-2010]; Available from: http://www.purdue.edu/rem/rs/sem.htm.
154. 02-06-2010]; Available from: http://www.sigmaaldrich.com/catalog/ProductDetail.do?D7=0&N5=SEARCH_CONCAT_PNO|BRAND_KEY&N4=D124702|ALDRICH&N25=0&QS=ON&F=SPEC.
155. Briggs, D. and M.P. Seah, *Practical Surface Analysis*. Vol. 1. 1990. 437.
156. Beamson, G.D.B., *High Resolution XPS of Organic Polymers.* 1992.
157. Ratner, B.D. and D.G. Caster, *Surface Analysis—The Principal Techniques.* 1997.
158. Amaral, I.F., P.L. Granja, and M.A. Barbosa, *Chemical modification of chitosan by phosphorylation: an XPS, FT-IR and SEM study.* Biomaterials Science, Polymer Edition, 2005. **16**: p. 1575-1593.
159. Granja, P., et al., *Cellulose-based biomaterials for bone regeneration: hemi-synthesis and characterisation.* Proceedings of polymers in medicine and surgery—PIMS'96, 1996: p. 73-80.
160. Velzenberger, E., et al., *Study of cell behaviour on a cellulose anti-adhesive substratum.* Cellulose, 2008. **15**: p. 347-357.
161. Nigmatullin, R., et al., *Atomic force microscopy study of cellulose surface interaction controlled by cellulose binding domains.* Colloids and Surfaces B: Biointerfaces, 2004. **35**(2): p. 125-135.
162. Gonçalves, I.C., et al., *Protein adsorption on 18-alkyl chains immobilized on hydroxyl-terminated self-assembled monolayers.* Biomaterials, 2005. **26**: p. 3891-3899.
163. Gonçalves, I.C., et al., *Protein adsorption and clotting time of pHEMA hydrogels modified with C18 ligands to adsorb albumin selectively and reversibly.* Biomaterials, 2009. **30** p. 5541-5551.
164. Extremina, C.I., et al., *Anti-adhesion and antiproliferative cellulose triacetate membrane for prevention of biomaterial-centred infections associated with Staphylococcus epidermidis.* International Journal of Antimicrobial Agents, 2010. **35**: p. 164-168.
165. Granja, P., et al., *Cellulose phosphates as biomaterials. Mineralization of chemically modified regenerated cellulose hydrogels.* J Mater Sci, 2001. **36**: p. 2163-2172.
166. Kwon, O.H., et al., *Surface modification of polypropylene film by radiation-induced grafting and its blood compatibility.* J. Appl. Polym. Sci.:Appl. Polym. Symp., 2003 **88**: p. 1726-1736.
167. Tu, M., et al., *Synthesis of novel liquid crystal compounds and their blood compatibility as anticoagulative materials.* Biomedical Materials, 2006. **1**(4): p. 202-205.
168. Fromherz, P., *Liquid Crystals and Biological Structures. Von G. H. Brown und J. J. Wolken. Academic Press, New York 1979. 187 S., geb. $ 19.00.* Angewandte Chemie, 1980. **92**(4): p. 329-330.
169. Tang, J., R. Peng, and J. Ding, *The regulation of stem cell differentiation by cell-cell contact on micropatterned material surfaces.* Biomaterials, 2010. **31**: p. 2470–2476.
170. Kobayashi, N., et al., *A new approach to develop a biohybrid artificial liver using a tightly regulated human hepatocyte cell line.* Hum Cell, 2000. **13**: p. 229-235.
171. Kobayashi, N., et al., *Rapidly functional immobilization of immortalized human hepatocytes using cell adhesive GRGDS peptide-carrying cellulose microspheres.* Cell Transplant, 2001. **10**: p. 387-392.

172. Taillaca, L.B.d., et al., *Grafting of RGD peptides to cellulose to enhance human osteoprogenitor cells adhesion and proliferation.* Composites Science and Technology, 2004. **64** p. 827-837.

Annexes

Trypsinization (MSC cells)

1. Warm DMEM medium, PBS and Trypsin at 37º bath (the optimum temperature for trypsin activity is 37ºC).
2. Remove from the CO_2 incubator the flask containing the cell culture.
3. View cultures using a microscope to assess the degree of confluence and confirm the absence of bacterial and fungal contaminations.
4. In sterile conditions, remove spent culture medium with a Pasteur Pipette connected to a suction device.
5. Wash the cell monolayer with 10ml PBS (sterile). Repeat this wash step.
6. Remove PBS with a Pasteur Pipette connected to a suction device.
7. Pipette 4ml of trypsin solution onto the washed cell monolayer. Rotate the flask to cover the monolayer with trypsin solution.
8. Return flask to incubator and leave 10 min. Observe the cells using a microscope to ensure that they are detached and floating.
9. Add culture medium (with serum) to inactivate the trypsin. The volume of culture medium (with serum) added to stop the reaction should be at least equivalent or superior to the volume of trypsin added before.
10. Resuspend the cells from the flask and wash the walls with the suspension to make sure that cells are not left.
11. Transfer the suspension to a centrifuge tube and centrifuge for 5 min at 1200rpm, 25ºC and brake velocity 9.
12. Discard the supernatant and add 2ml of fresh culture medium. Resuspend the cells.
13. Remove 10µl of the suspension and perform a cell count.
14. Transfer the required number of cells (depending on the required seeding density) to a new labeled flask containing pre-warmed medium.
15. Incubate at 37ºC, in a 5% CO_2:95% air temperature.
16. Check cells every day for growth towards confluence and problems such as nutrient depletion and infection.
17. Repeat this process as demanded by the growth characteristics of the cell line.

Resazurin Assay

MATERIALS

Reagents & Materials	Reference	FW	INEB-ref (Storage T)
Resazurin	Sigma, R7017	251.17	
Phosphate-buffered saline (PBS)			
0.01M solution (1 pouch/L)	Sigma, P3813	na	P004 (RT)
DMEM without phenol red			
96-well plates	Greiner, 655096	na	na
(black side, clear bottom)			

RATIONALE

Resazurin assay is a simple and rapid test in which a 0.01 mg/ml (40μM) solution is added to the culture medium, metabolized by cells, and measured either by colorimetry or fluorometry. Greater sensitivity is achieved by fluorimetry. The bioreduction of the dye reduces the amount of the oxidized form (resazurin, blue) and concomitantly increases the fluorescent intermediate (resorufin, red). Measurements can be done either as an endpoint reading or in kinetic mode, providing an excellent estimation of cells metabolic activity. Resazurin is non-toxic to cells, which can then be put back in culture and re-used for further investigations.

EXPERIMENTAL

1. Preparation of 10x resazurin stock solution (0.1 mg/mL): dissolve 10 mg resazurin in 100 mL PBS and sterilize by filtration (0.2 μm). Store at -20ºC, protected from light.

2. Preparation of 1x working solution (0.01 mg/mL, 40μM): dilute the resazurin stock solution 1:10 in culture medium (ideally without phenol red).

3. Remove the cell culture supernatants and carefully wash the monolayers with pre-warmed PBS (500 μL/well for 24-well plates).

4. Add the resazurin working solution (500 μL/well for 24-well plates).

5. Incubate cells for 3 to 4 hrs at 37ºC.

6. Transfer 200µL of the supernatants into 96-well plates and read resorufin fluorescence using a microplate spectrofluorometer (Ex = 530 nm, Em = 590 nm).

7. Add fresh media to the cells incubate at 37ºC.

Fluorescent staining of F-actin filaments and DNA

Reagents

- Alexafluor 488-phalloidin (Molecular Probes, A12379) stock: 200 U/ml solution in methanol (-20ºC)
- DAPI: 4,6 –Diamidina-2-phenylin (Sigma, D-9542)
- Vectashield anti-fade mountant (Vector Laboratories H-1000)
- 10 mg/mL BSA in PBS

Procedure:

1 – Remove the medium.

2 – Wash 2 times with PBS.

3 – Fix the cells with 2ml of 4 % of formaldehyde for 15 min at room temperature.

4 – Wash with PBS 4 times, 5 min each wash.

5 – Permeabilize with 2ml of 0,1% Triton X-100 in PBS for 5 min.

6 – Incubate the samples in 2ml of BSA 10mg/ml (in PBS) for 30 min at 37 ºC.

7 – Incubate in Alexafluor 488-phalloidin at 1:40 in 1% BSA/PBS for 20 min at 37 ºC in the dark.

8 – Wash 2 times with PBS

9 – Incubate with DAPI (20 ug/ml in deionised water) for 10 min at room temperature

10 – Wash with deionised water, 4 times.

11- Remove the water.

12 – Mount the cells with Vectashield anti-fade mountant placing 4 drops of Entellan in the corners of the lamella and overlap with another lamella.

13 – Store at 4 ºC (covered with foil).